Development of a plant-made immunoassay for the detection of *Porcine circovirus* infections in South African swine herds

By

Aune Tuyoleni Angobe

Dissertation presented for the degree of Master of Science

Department of Molecular and Cell Biology

Faculty of Science

University of Cape Town

November 2019

Supervisor: Associate Professor Inga Hitzeroth

Co-supervisor: Dr Albertha van Zyl

Acknowledgments

First and foremost, I would like to humble myself and give thanks to my Heavenly Father for His steadfast care throughout my studies.

I would sincerely like to express my deepest appreciation to Associate professor Inga Hitzeroth and Dr Alta van Zyl for supervising my research from the very beginning until the end. Thank you for your time and helpful suggestions during my time in the lab and when I was writing up. You have greatly contributed to the success of this research and I appreciate you.

I would like to give my special appreciation to Cornelius Gunter, you were always there when I needed you. Thank you for guiding me through.

My greatest acknowledgement goes to Professor Ed Rybicki. During my research, your expertise was incredibly valuable, and I thank you very much.

The Biopharming Research Unit (BRU) team, especially, Francisco, Scott, Paulina, Megan, Asanda, Jennifer and others, I thank you all for the teamwork. Your concerns and contributions towards my research are extremely appreciated. Thank you very much Mohamed Jaffer at the transmission electron microscopy unit for your help.

I would like to thank the Poliomyelitis Research Foundation, the Sam Cohen scholarship trust, The departmental funding and Aunt Vivien for the financial support. You have surely made my stay in Cape Town smooth. Thank you BRU for funding my project, I truly appreciate.

To my precious family, especially my mother, Leena Nangula Nambala, thank you for your prayer’s meme. You are truly a pillar, inspiration and strength that keeps me going Gwatweepa gwandje. My amazing siblings, Foibe Angombe, Sem Angombe, Hofni Angombe, Efraim Angombe and Gottlieb Naftal you have all contributed to the success of my studies and I appreciate you.

To my amazing boyfriend, Florrian Uusiku, thank you for holding my hand through the entire journey of my studies. Whenever I felt like giving up, you were always there to encourage me. Thank you for listening to my complains and for offering me your shoulder to lean on every single moment of this journey. You truly made this whole thing easy for me to handle and for that, I deeply appreciate you my love.

Lastly, to my extended family and friends, thank you for checking up on me always, for encouraging me and making sure that I was managing. Paulina Naupu, Alina Hitewa, Lovisa Nghishe, Ntandokayise Mbuyane, Elizabeth Ipangelwa, Johanna Kapalanga and Josephina Uupindi. My appreciation for all of you goes beyond words.

In loving memory of Kuku Emilia Mpingana Amunyela and Tatekulu Johannes Oleeshiti Nambala

Declaration

I **Aune T. Angobe** understand that plagiarism is using someone’s work and pretend it is one’s own, which is not acceptable.

I confirm that this Dissertation presented for the degree of Master of Science in the Department of Molecular and Cell Biology is my own work and has not been copied from anyone’s work (published or unpublished).

For citation and referencing, I used Harvard's referencing style. Every contribution to and quotation from the work(s) of other individuals in this dissertation has been attributed and cited and referenced.

I also confirm that, where necessary, permission was obtained for all images and figures used in this dissertation and is stated as such, and the original author was cited where permission was not required.

I have not allowed and will not allow anyone to copy my work with the intention of passing it off as his or her own work.

Aune T. Angobe

Signed by candidate

03 November 2020

ABSTRACT

Porcine circovirus type 2 (PCV-2) is considered the major cause of porcine circovirus-associated diseases and is one of the major pathogens in swine producing countries. PCV-2 is a non-enveloped virus with a single stranded circular DNA genome of about 1.8 kb. This encodes the single capsid protein (CP) which is highly immunogenic, as well as a replication-associated protein. Recombinantly expressed CP can self-assemble into virus-like particles (VLPs) that are structurally and immunogenically very similar to native virions. Current commercially available diagnostic kits are VLP-based and are effective at detecting PCV-2 antibodies in sera. However, these diagnostic assays are expensive, therefore limiting their use in developing countries. Plant-based transient expression systems have recently been investigated to express PCV-2 CP for a cheaper diagnostic reagent.

The aim of this study was to develop an inexpensive lateral flow device to be able to test for PCV infection in pig herds. Production of PCV-2 CP in *Nicotiana benthamiana* via transient *Agrobacterium*-mediated expression was optimised by comparing two expression vectors, pEAQ-*HT* and pCBP2, and VLPs were also expressed in *Escherichia coli*. VLPs produced in plants and in *E. coli* were used to set up a lateral flow device. In addition, various purification methods of VLPs such as ion exchange chromatography (IEC) and sucrose gradient ultracentrifugation were explored to obtain pure VLPs free of bacterial contamination.

The VLPs were successfully expressed in *N. benthamiana* with both pEAQ-*HT* and pCBP2, and VLPs were subsequently purified on discontinuous sucrose gradients by ultracentrifugation. The assembly of the CP was assessed by transmission electron microscopy, which showed the presence of assembled VLPs. To further purify the VLPs IEC was used, and fully assembled VLPs which were free of contamination were prepared. Purified VLPs expressed in plants and *E. coli* were successfully used as coating antigen in lateral flow devices, which were able to detect PCV-2 CP antibodies in CP-immunised rabbit sera. *E. coli*-made VLPs showed higher affinity to PCV-2 antibodies compared to plant-made VLPs.

In conclusion, this study has successfully demonstrated the potential to use a plant-based transient expression system to produce affordable diagnostic reagent, especially for developing countries. This is the first study that expressed PCV-2 VLPs using a pCBP-2 expression vector and used PCV-2 VLPs as a coating reagent in the development of a lateral flow test as a proof of concept.

ABREVIATIONS

APE	acute pulmonary edema
BCIP	5-bromo-4-chloro-3-indoxyl-phosphate
BSA	bovine serum albumin
BSL	biosafety level
CP	capsid protein
ELISA	enzyme-linked immunosorbent assay
ER	endoplasmic reticulum
FDA	food and drug administration
GAG	glycosaminoglycans
GCD	glucocerebrosidase
IEC	ion exchange chromatography
IFA	indirect fluorescent antibody
IHC	immunohistochemistry
IIFA	indirect immunofluorescence assays
IPM	immune peroxidase monolayer
IPTG	isopropyl β-D-thiogalactopyranoside
LB	Luria Bertani
LPH	leader peptide (derived from murine heavy chain of mAb24)
LSD	lysosomal storage disorder
MES	morpholineethanesulforic acid
NBT	nitroblue tetrazolium
NGC	non-gas chromatography
NK	natural killer
NLS	nuclear localization signal
OD	optical density
ORF	open reading frame
PBS	phosphate buffer saline
PCR	polymerase chain reaction
PCV	*Porcine circovirus*

PCVAD	porcine circovirus associated diseases
PDNS	porcine dermatitis and nephropathy syndrome
PMWS	postweaning multisystemic wasting syndrome
PRDC	porcine respiratory disease complex
PRRSV	porcine reproductive and respiratory syndrome virus
PTGS	post-transcriptional gene silencing
PVX	potato x virus
RCR	rolling-circle replication
RFLP	restriction fragment length polymorphism
RNA	ribonucleic acid
SAB	sample application buffer
TBSV	tomato bushy stunt virus
TEM	transmission electron microscopy
TMV	tobacco mosaic virus
TSWV	tomato spotted wilt virus
VLP	virus-like particle

Table of content

1 Chapter 1: Literature review

1.1 Background

Porcine circovirus (PCV) is one of the smallest DNA viruses that infect mammals and is a global threat to swine (Kennedy *et al.*, 2000, Bolin *et al.*, 2001). There are currently four different categories of PCV in swine populations. In 1974, PCV type 1 (PCV-1) was discovered, however it has not been associated with any known animal disease although it is widespread in swine (Allan *et al.*, 1995). Since then, PCV-2 was identified retrospectively in swine herds in northern Germany from 1997 (Jacobsen *et al.*, 2009, Bolin *et al.*, 2001, Zhai *et al.*, 2014b) and in South Africa, the virus was first identified in June 2001 at a large, well-managed commercial breeding facility in Gauteng Province (Drew *et al.*, 2004). Furthermore, in 2015 PCV-3 was identified as a new subtype of PCV on a farm in North Carolina, United States of America (USA) (Palinski *et al.*, 2017a). Interestingly, in 2016 the same strain of PCV was discovered in Guangxi, China (Wen *et al.*, 2018). Recently, a novel PCV strain was discovered within the swine population of Hunan Province in China and it was referred to as PCV-4 (Zhang *et al.*, 2020a).

In Germany, PCV was initially discovered in a pig kidney cell line (PK-15) as a picornavirus-like contaminant with no cytopathic effect. It was first thought that PCV has a ribonucleic acid (RNA) genome (Tischer *et al.*, 1974). However, it was later discovered that PCV is a single stranded deoxyribonucleic acid (ssDNA) virus. Experiments revealed that PCV isolated from the PK-15 cells was PCV-1 and that it did not cause any sickness in pigs (Tischer *et al.*, 1982). Subsequently in 1991, an emergence of PCV-2 occurred in Saskatchewan, Canada, from infected pigs which had symptoms of weight loss, jaundice, discomfort in breathing and microscopic lesions in lymphoid tissues. Furthermore, PCV was also discovered on nearly all continents around the world (Allan *et al.*, 1998, Harding, 1998). The non-pathogenic strain of PCV was designated PCV-1 and the pathogenic was termed PCV-2 (Allan *et al.*, 1999b).

From 1961 to 1984, the total number of global incidences of PCV-2 was minimal compared to the number of incidences that occurred between the period of 1985 to

1998 (Jacobsen *et al.*, 2009). So far the epidemiological data shows that PCV-2 has possibly been in existence for over five decades in the swine population worldwide (Jacobsen *et al.*, 2009, Rose *et al.*, 2012, Afolabi *et al.*, 2017b).

PCV-2 is regarded as one of the major threatening pathogens affecting all swine producing countries, causing severe economic losses to the pig industry. Wild boars can also be affected by this virus. However, they rarely show clinical symptoms, although PCV-2 serological prevalence is as high as in domestic swine (Beach and Meng, 2012). In the early 1990s, PCV-2 was first discovered to be the causative agent associated with porcine circovirus associated diseases (PCVAD) (Chae, 2005). PCV-2 associated diseases were primarily seen in samples archived in 1985 (Jacobsen *et al.*, 2009). In recent years, PCV-2 has received much attention due to its negative impact on the profitability of pork production (Chen *et al.*, 2018). This literature will review PCV-2 as the major causative agent of PCVAD, the vaccines that are used to reduce PCV-2 infections, diagnosis of these diseases and challenges associated with these.

1.2 Classification

PCV-2 belongs to the genus *Circovirus*, within the family *Circoviridae*. Phylogenetic analysis of PCV-2 viruses from both symptomatic and asymptomatic infected pigs around the world, has shown that there are five major genotypes. These are grouped by their capsid protein coding sequence: PCV-2a, PCV-2b, PCV-2c, PCV-2d and PCV-2e (Meehan *et al.*, 1998, Olvera *et al.*, 2007). However, a recent study conducted in China identified new viral sequences that cluster differently from the existing sequences and classified these as genotype PCV-2f and PCV-2g (Figure 1.1) (Franzo and Segales, 2018). These genotypes have a nucleotide sequence identity of more than 94%, with 90-100% amino acid sequence identity (Melanie *et al.*, 2019, Meehan *et al.*, 1998).

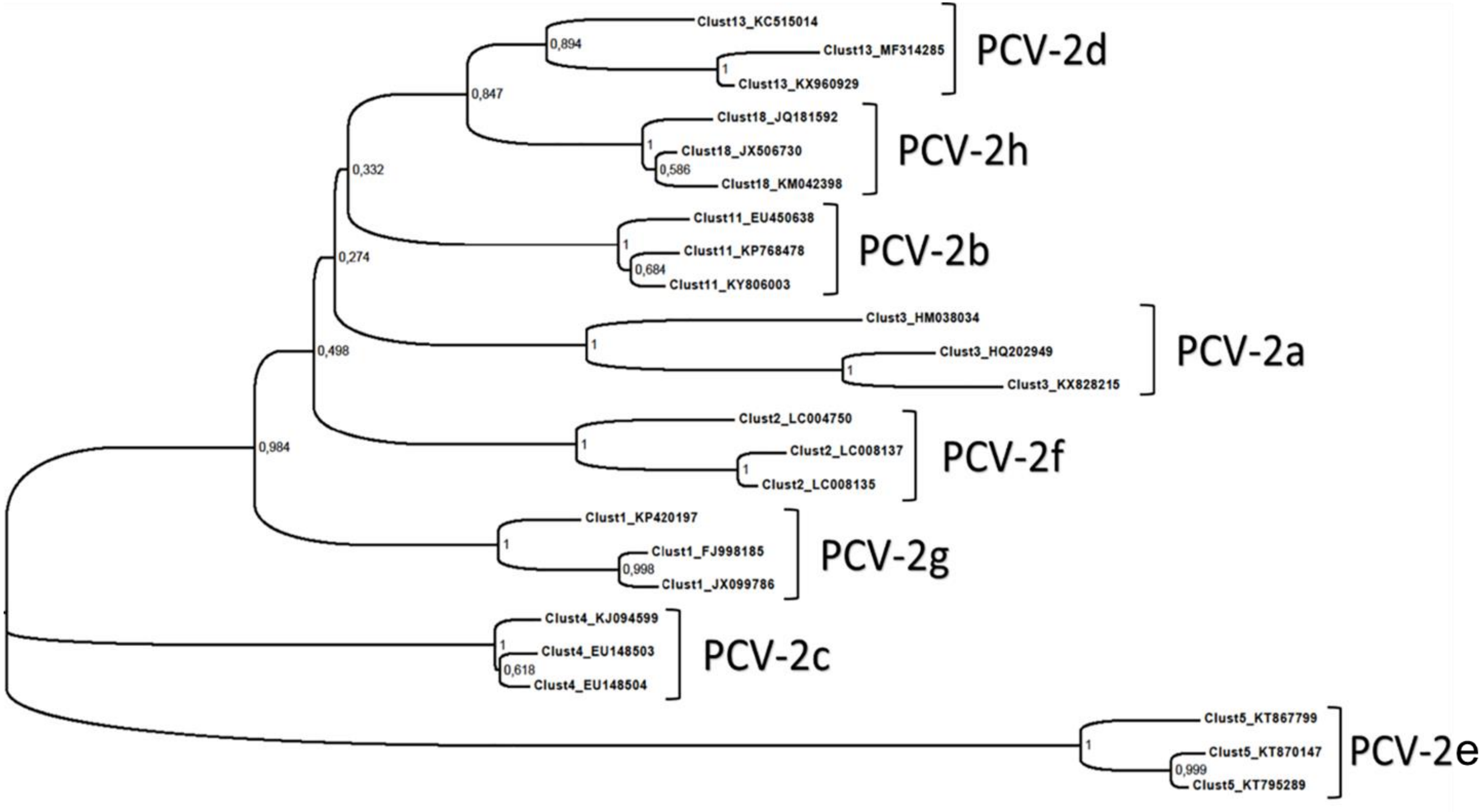

Figure 1.1 Phylogenetic tree of PCV-2 genotypes. Tree obtained with permission from Franzo and Segales (2018).

From 1996 to the early 2000's PCV-2a was the predominant genotype in global swine herds. Since then, this has changed due to a genotype shift, with the emergence of PCV-2b from Europe and North America which has been shown to be the most widely spread PCV pathogen worldwide (Figure 1.2), with an observed increase in associated disease outbreaks. A third genotype, PCV-2c, was reported in the 1980's from Denmark (Dupont *et al.*, 2008). PCV-2d first appeared in China, then a second genotype shift (from PCV-2b to PCV-2d) occurred in 1999 in which PCV-2d became the main PCV-2 pathogen. This is suggested to have been driven by the worldwide use of PCV-2 vaccines (Mo *et al.*, 2019, Beach and Meng, 2012, Franzo and Segalés, 2018, Dupont *et al.*, 2008). According to Xiao *et al.* (2015). The PCV-2d genotype now consists of PCV-2 strains previously classified as PCV-2b subtype 1C and those classified as mutant PCV-2b (mPCV-2b), arising from PCVAD clinically manifested pigs in suspected vaccine failure (Guo *et al.*, 2012, Opriessnig *et al.*, 2013). The third genotype, PCV-2c has not been of serious economic importance since it was only initially found in Danish archived samples from healthy herds and then in wild pig samples in Brazil (Dupont *et al.*, 2008).

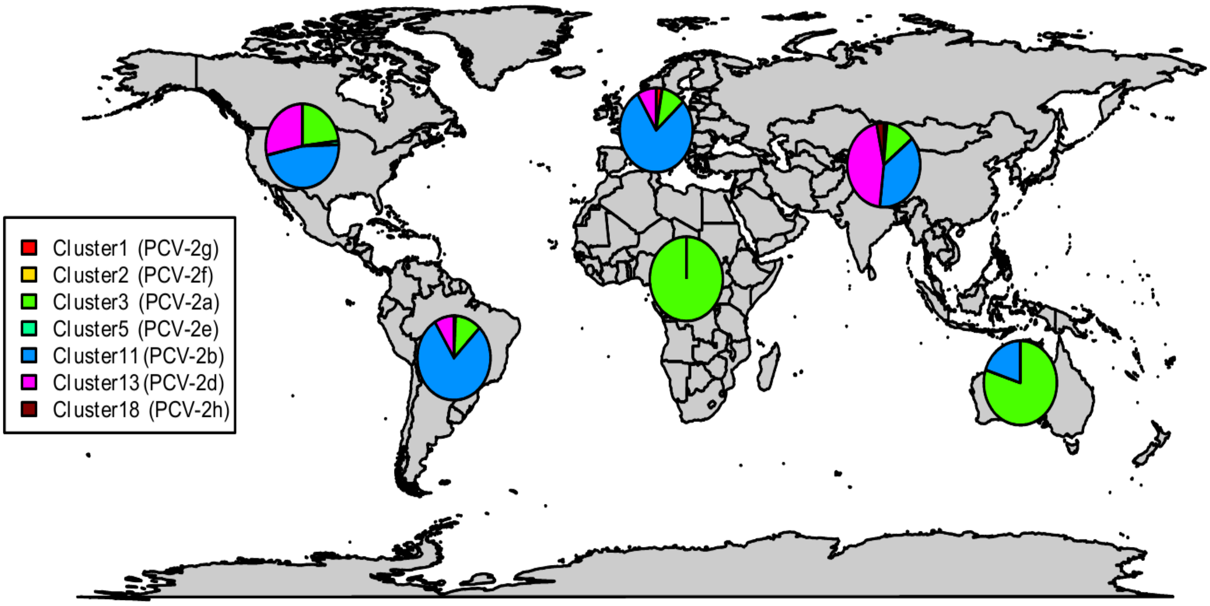

Figure 1.2 Geographic distribution of main PCV-2 groups. The PCV-2 cluster distribution was summarized using pie-charts that are specific to continents whose slide size is relative to the cluster occurrence (color-coded) (Franzo and Segalés, 2018).

It has been shown that PCV-2d shows virulence similar to that of PCV-2a and PCV-2b when inoculated into susceptible pigs. The clinical significance of PCV-2c, PCV-2e and PCV-2f are not known. New genotypes are likely to appear in the future since PCV-2 is a single stranded DNA virus with a high nucleotide substitution rate (comparable to those of RNA viruses) and there is high potential for genome mutations (Franzo and Segalés, 2018).

1.3 PCV genome

PCV has a circular, ssDNA genome of approximately 1.8 kb in size. The virion is non-enveloped with a diameter of 12 to 23 nm (Rodriguez-Cariñg and Segales, 2009, Fauquet *et al.*, 2005, Todd, 2005, Mankertz *et al.*, 2000). PCV is the smallest known animal DNA virus with a highly conserved genome in terms of the amino acid sequence. However, for a typical ssDNA virus, the rate of nucleotide substitution in the viral genome per site and year is considered to be the highest of its kind (Xiao *et al.*, 2015).

The ssDNA genome of PCV-2 encodes four major open reading flames (ORFs, Figure 1.3) (Mankertz *et al.*, 2000, Meehan *et al.*, 1998), oriented in opposite directions (Chen *et al.*, 2018, Nawagitgul *et al.*, 2000). ORF1 encodes two DNA replication-associated proteins (Rep and Rep') whereby Rep is very conserved, whereas Rep’ is a truncated form and a result of alternative splicing of a C-terminal of ORF1 (Chen *et al.*, 2018, Mankertz *et al.*, 2004).ORF2 encodes the capsid protein (CP), a structural protein of PCV-2 associated with its pathogenicity (Hu *et al.*, 2016, Nawagitgul *et al.*, 2000). In addition, ORF2 has been shown to be a good phylogenetic and epidemiological marker for PCV-2 since it gene sequences reconstruct the same phylogenetic tree when compared to using the whole PCV-2 genome (Grau-Roma *et al.*, 2008). This gene is transcribed from the complementary strand in the replicative form of the virus to produce a 233 amino acid CP that is approximately 27kDa (Karuppannan and Opriessnig, 2017a). PCV-2 CP is capable of self-assembly into virus-like particles (VLPs) that are similar to the icosahedral morphology of the native PCV-2 virions when recombinantly expressed (Yin *et al.*, 2010).

ORF3 is located within ORF1 and is not crucial in viral replication but is involved in inducing cell apoptosis/pro-apoptosis (Ren *et al.*, 2016). This is essential in the development of viral pathogenesis (Júnior *et al.*, 2012). ORF4 has been identified and is embedded within ORF3 and oriented in the same direction. Similarly to ORF3, ORF4 is not crucial in virus replication (Lv *et al.*, 2014, He *et al.*, 2013). It encodes a protein of approximately 60 amino acids with anti-apoptotic function and plays a major role in limiting ORF3 transcription thus inhibiting virus-induced apoptosis (Klaumann *et al.*, 2018, Gao *et al.*, 2014). The genome of PCV-2 has a stem loop structure at the origin of replication (ori) that is well maintained between two small intergenic regions (IR), this structure also exists in diverse ssDNA viral families that infect eukaryotes such as *Nanoviridae* and *geminiviruses* (Karuppannan and Opriessnig, 2017a). The replication associated proteins recognizes distinctive structures of stem loop in the genome of the virus and, in conjunction with the machinery of host cells that is likely to have been involved in previous DNA repair synthesis resulting in double stranded DNAs (dsDNA) form of the genome. After nicking of the DNA strand, the Rep binds to the new 5 ends covalently and initiates rolling circle replication (Finsterbusch and Mankertz, 2009).

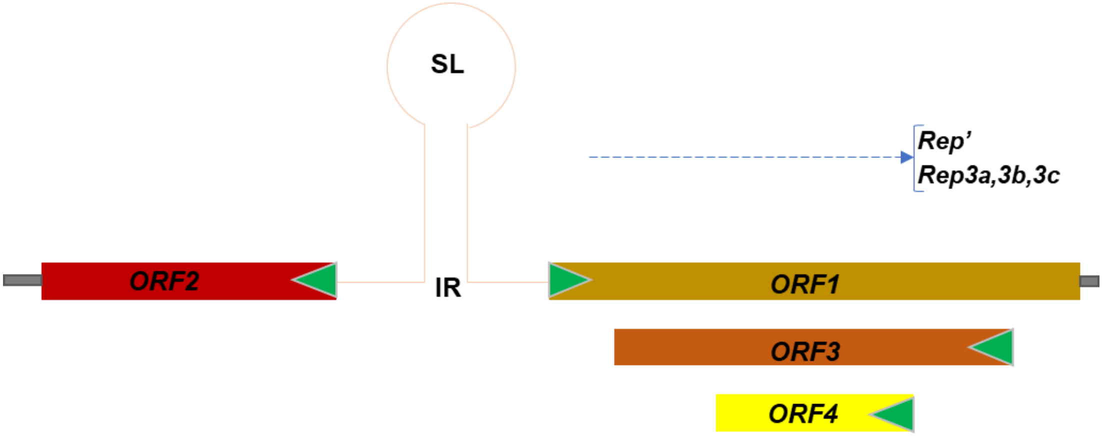

Figure 1.3 Genomic representation of PCV-2. Four ORFs are shown, with the stem loop (SL) structure located in the IR between ORF1 and ORF2. The Rep is translated from the full-length ORF1, whereas the Rep′, Rep3a, b & c are produced via alternative splicing of the Rep transcript as shown by dotted lines. Image adapted from Lv *et al.* (2014).

1.4 Structure

According to Khayat *et al.* (2011), the crystal structure of the *in vitro* assembled PCV-2 VLPs shows that these consist of 60 copies of PCV-2 CP with icosahedral symmetry and several exposed loops on the viral surface. These serve as immunodominant epitopes that trigger neutralising antibodies (Khayat *et al.*, 2011, Liu *et al.*, 2016). The crystal structure of the N-terminally truncated PCV-2 CP has a resolution of 2.3 Å, whereas the *in vitro* assembled full-length PCV-2 VLP has a 9.6 Å resolution.

A comparison of the PCV-2 capsid crystal structure and cryo-EM images of the PCV-2 capsid shows that the Cap Nuclear Localization Signal (NLS) is located at the 5-fold icosahedral axis (Figure 1.4) (Khayat *et al.*, 2011, Mo *et al.*, 2019). The NLS consist of positively charged arginine (R) residues (Figure 1.4C). The arginine-rich residues which are next to the NLS-A reach onto the adjacent capsid protein and then interact with its NLS-B fragment to stabilize VLP formation (Figure 1.4 C-D). In addition, the rate and or stability of VLP formation is greatly determined by the amino acid type and charge. A polyarginine peptide is generally recognized as a cell penetrating peptide (CPP), which can disrupt cell membranes and carry foreign proteins and chemicals (and even beads) into cells (van den Berg and Dowdy, 2011)

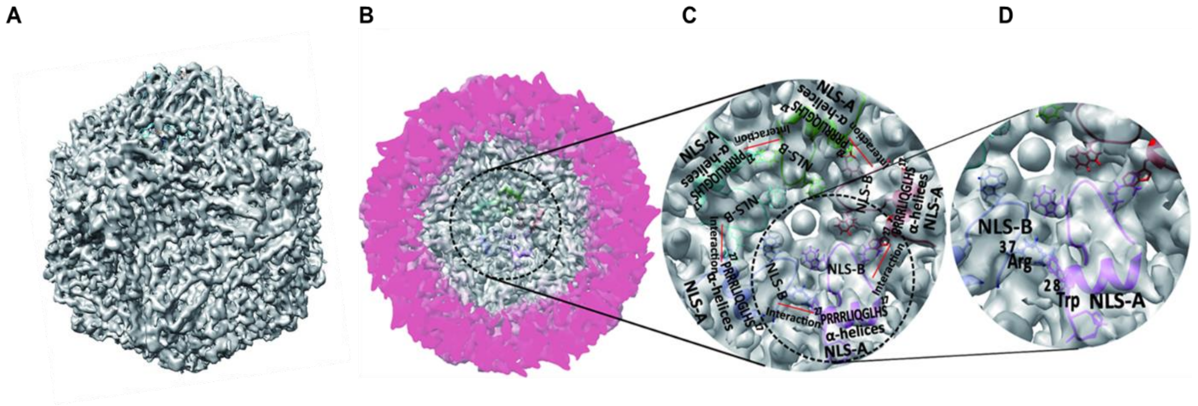

Figure 1.4 Cryo-EM of full-length PCV-2 VLP structure **A:** A 3D reassembled cryo-EM form of PCV-2 VLP showing a typical T=1 icosahedral particle fold. **B:** Internal structural feature of the NLS fragment with one-half of the density map was removed. **C:** Density map of NLS region. The density maps are shown for NLS-A, NLS-B, α-helices etc. **D:** The interaction of cation-π between 37Arg and 28Trp residues. Image obtained with permission from Mo *et al.* (2019).

1.5 PCV-2 and its associated diseases

1.5.1 Postweaning multisystemic wasting syndrome and PCVAD

PCV-2 causes postweaning multisystemic wasting syndrome (PMWS) and is strongly associated with other diseases in pigs, such as porcine dermatitis and nephropathy syndrome (PDNS) , porcine respiratory disease complex (PRDC), acute pulmonary edema (APE), proliferative and necrotizing pneumonia, myocarditis in stillborn piglets and occasionally failure in reproduction (Allan *et al.*, 1999a, Bolin *et al.*, 2001, Harding and Clark, 1997, Bogdan *et al.*, 2001). PMWS has become established in many countries worldwide as a major disease in pigs (Krakowka *et al.*, 2000).

According to Young *et al.* (2011) & Segalés *et al.* (2005), diseases linked to PCV-2 are collectively named porcine circovirus diseases (PCVD) or PCVAD in North America. It was clear that almost every pig that has the virus, became infected sometime during its growing period. Although pigs were infected with PCV-2, some of them had no clinical manifestation of PCVAD.

1.5.2 PCV-2: First occurrence in South Africa pig herds

In 2001, a PCV-2 outbreak was recorded in the Gauteng province of South Africa (Drew *et al.*, 2004). Here, 1-2-month-old pigs clinically presented PDNS. These symptoms were immediately followed by PMWS clinical signs and five months later, morbidity increased to 30-40% while the mortality rate was below 10% (Drew *et al.*, 2004). Another study in South Africa by Afolabi *et al.* (2017a), reported that swine herds of the Eastern Cape District were observed to have typical clinical symptoms of PMWS (Figure 1.5). PCV-2 was also detected and characterized in other Sub-Saharan African countries such as Uganda as indicated below.

Figure 1.5: Wasting appearance of a pig with severe respiratory difficulty within a herd of the same age at a farm in Lukhanji Local Municipality, Chris-Hani District, Eastern Cape, South Africa (Afolabi *et al.*, 2017b).

1.5.3 PCV-2 among Ugandan domestic swine

A study conducted by Jonsson (2013) in Uganda, focused on assessing PCV-2 in domestic pigs. Here, sampling and analysis of 91 pigs around Murchison Falls national park was performed. Approximately 77% of the sampled pigs tested positive for PCV-2 and were associated with PMWS. This is in agreement with the results obtained by Ojok *et al.* (2013). The sampling size was small to achieve a more reliable conclusion, therefore, Jonsson (2013) recommended that more studies need to be carried out in order to obtain reliable results .

1.6 Aetiology

1.6.1 The host and virus replication

Segales and Domingo (2002) documented that, swine are the natural host for PCV-2. The interaction between PCV-2 and its host (domestic and wild pigs) is a complex process that normally begins with the attachment of the virus to the target cells and organs by binding to specific receptors known as glycosaminoglycans (GAG) which are present on the surface of the cell as shown in figure 1.6.

The ssDNA genome enters the host cell by the help of a polyarginine peptide which is recognized as a cell penetrating peptide. It is transported to the nucleus and converted into dsDNA by the host enzymes. Protein synthesis begins when the cap and rep mRNAs are transcribed and then imported to the cytoplasm. Rolling-circle replication (RCR) is initiated when rep/rep' binds to the dsDNA, and introduces a nick, which serves as a primer and elongation of the nick leads to replication (Figure 1.6). Replication appears to be a slow process that occurs in several types of cells, mainly endothelial, epithelial cells and macrophages. (Nauwynck *et al.*, 2012, Finsterbusch and Mankertz, 2009).

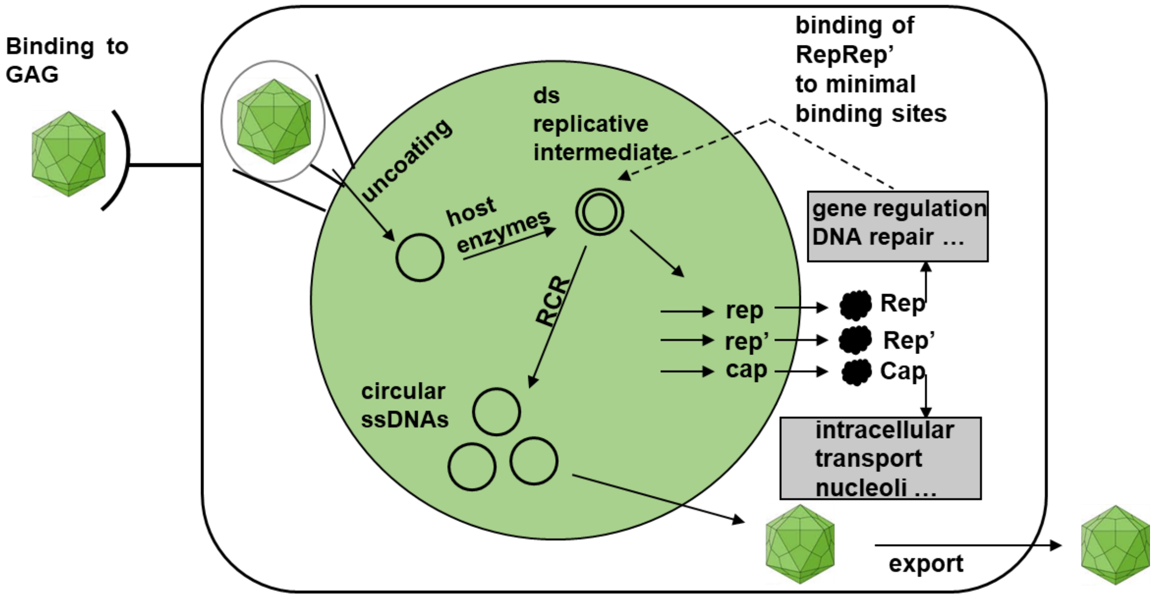

Figure 1.6 The life cycle of PCV-2. Image adapted from Finsterbusch and Mankertz (2009).

PCV-2 infection leads to host immunosuppression. Hematological examinations show a decline in the production of CD4 T lymphocytes, natural killer cells (NK cells), dendritic cells and B cells. The lymphoid depletion results from viral replication in the lymph tissues or from virus induced cellular apoptosis. The extent of lymphoid depletion has a direct correlation with the amount of PCV-2 antigen present in tissues (Júnior *et al.*, 2012).

1.6.2 Transmission and associated clinical manifestation

Generally, virus transmission occurs through vertical and horizontal transmission. In horizontal transmission, viruses are spread between individuals of the same generation whereas vertical transmission happens between mother and their offspring. PCV-2 can be transmitted to pigs from other pigs, rodents, humans, animals, pen environments and insects (Figure 1.7) (Blunt *et al.*, 2011, Yang *et al.*, 2012, Zhai *et al.*, 2014a, Verreault *et al.*, 2010, Alarcon *et al.*, 2011, Lőrincz *et al.*, 2010, Chiou *et al.*, 2010, Dupont *et al.*, 2008).

During systemic infections of PCV-2, virus can be shed in oral and nasal secretions, faecal, milk, urine in naturally and experimentally infected pigs (Patterson *et al.*, 2011a) (Patterson *et al.*, 2011b). The duration of the virus in swine naturally infected with PCV-2 at or before the age of 13 days has been shown to be at least 209 days after farrowing (Patterson *et al.*, 2011a), or 69 days after experimental PCV-2 infection (Patterson *et al.*, 2011b).

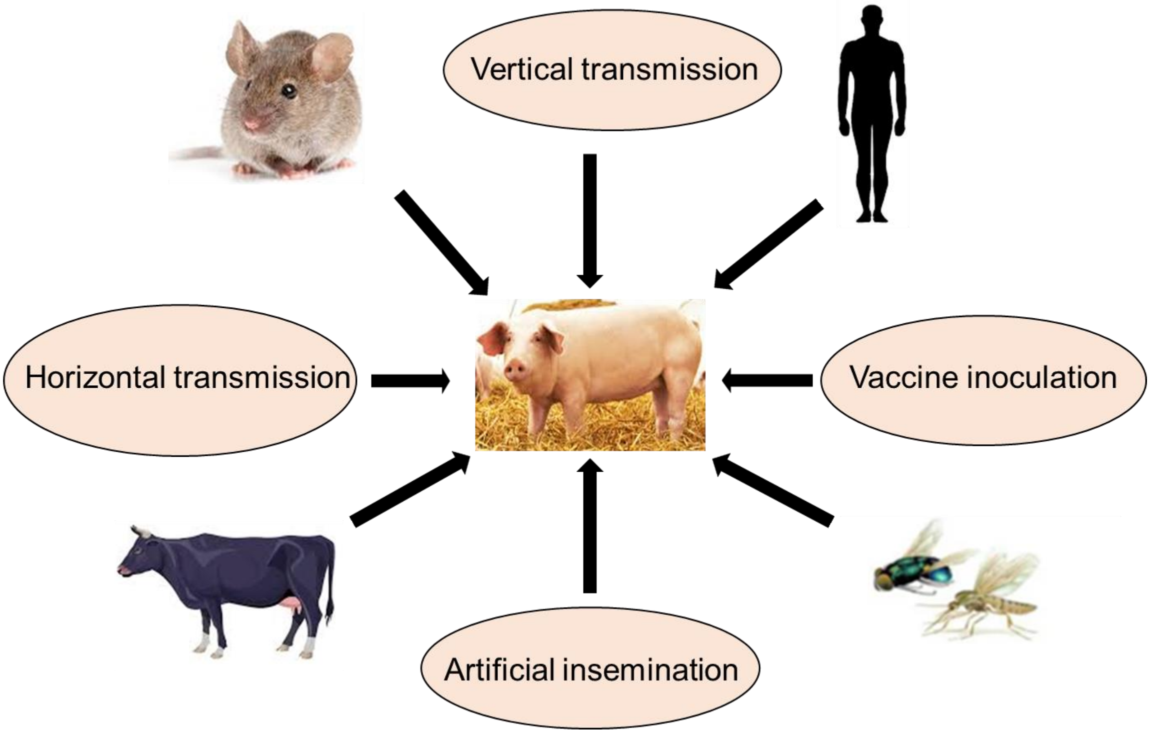

Figure 1.7 Possible sources of PCV infection and cross-species spread in pigs. Image adapted from Zhai *et al.* (2014a).

Shedding of the virus in the semen of adult boars is a concern for breeding herds. Experimentally infected boars were shown to shed PCV-2 for at least 90 days post infection (Madson *et al.*, 2008). Madson *et al.* (2009a) further reported that insemination of naïve sows with semen containing large amount of infectious PCV-2 can lead to failure in reproduction. The transmission of PCV-2 by means of insemination is dose-dependent, as semen containing lower levels of PVC-2 failed to infect sows (Madson *et al.*, 2009b).

PCV-2 coinfection with porcine reproductive and respiratory syndrome virus (PRRSV), which is another swine pathogen, results in increased duration and amount of PCV-2 shedding, which contribute to a higher environmental viral load (Sinha *et al.*, 2010). Airborne spread among farms in areas of high-density swine production is a potential concern for biosecurity. In production facilities, high levels of PCV-2 DNA (up to 107 genome copies / m^3 of air) were detected in dust particles (Verreault *et al.*, 2010).

Vertical transmission both in the field and experimentally were confirmed in individual sows (Johnson *et al.*, 2002, Ladekjaer-Mikkelsen *et al.*, 2001, O'Connor *et al.*, 2001). Additionally, this mode of PCV-2 transmission was suggested by Bogdan *et al.* (2001) as the virus was detected in neonatal piglets. This mode of transmission may not only be related to reproductive failure but also to the development of multisystemic diseases later in the life of swine (Bogdan *et al.*, 2001). According to Harding and Clark (1997), PMWS most commonly affects pigs of 2-3 weeks postweaning or at about 5-6 weeks of age. PCV-2 viral particles are stable and persists in the environment of infected herds, making virus eradication very hard (Júnior *et al.*, 2012).

PMWS have been found to be due to dual infections with PCV-2 and other virulent pathogens, such as swine influenza virus, PRRSV, *Porcine parvovirus*, *Streptococcus suis*, *Mycoplasma hyopneumoniae* to mention a few. Such co-infections may confuse and complicate the clinical representation of the disease. The manifestation of the clinical signs and lesions associated with PMWS occur in a mild form in piglets infected with PCV-2 (Júnior *et al.*, 2012).

1.7 Diagnosis of PCV-2

Since the disease caused by PCV-2 is a complicated disease with multiple clinical signs, precise diagnosis of PCV-2 infections is of paramount importance for implementing effective containment strategy on affected herds (Segalés *et al.*, 2005). Clinical PCVAD are observed with three well established criteria: (1) observation of at least one clinical manifestation of the disease such as weight loss, wasting, dyspnea, enlargement of inguinal lymph nodes, jaundice, increased mortality or respiratory signs; (2) presence of PCV-2-associated hallmark microscopic lesions in lymphoid tissue in the case of a dead animal; (3) detection of PCV-2 antigen or nucleic acids at sites of lymphoid lesions using immunohistochemistry (IHC) or *in situ* hybridization (Sorden, 2000). Analysis of histological segments for the distribution and quantity of PCV-2 by immunohistochemistry and *in situ* hybridization in affected tissues is regarded as the gold standard for PCVAD diagnosis (Opriessnig *et al.*, 2007).

Reproductive diseases among pigs infected by PCV-2 is diagnosed with the following criteria: (1) late-term abortions and stillborn, sometimes with severe foetal heart hypertrophy; (2) the development of cardiac lesions marked by severe fibrosis and/or necrotizing myocarditis; (3) high levels of PCV-2 found in myocardial lesions and other foetal tissues (West *et al.*, 1999).

1.7.1 Detection of PCV-2 antibodies by enzyme immune-linked immunosorbent assay (ELISA) and indirect fluorescent antibody (IFA)

ELISA in general is a sensitive technique which allows the detection and measurement of serum antibodies. Many commercially available ELISA kits are utilized in diagnostic laboratories to detect PCV-2 antigens and PCV-2 specific antibodies. There are two types of ELISAs for detecting PCV-2 antibodies: indirect ELISAs and competitive ELISAs. Briefly, indirect ELISA involves a two-binding process of primary antibody and secondary antibody. The antigen is bound to the micro-well plates, incubated with the primary antibody, washed, and then incubated with the secondary antibody prior to detecting by elicit of a fluorescence signal (Deng *et al.*, 2018). The competitive ELISA involves competitive binding process which is performed by the sample antigen (original antigen) and the add-in antigen. In short, the sample antigen is incubated with the primary antibody. The addition of the antigen-antibody complexes to the wells pre-coated with the same antigen then follows. Here, competition takes place since only less antibody will be able to bind to the antigen. The unbound antibody is washed off and the secondary specific antibody is added and then detection takes place. Weaker signal is observed when the concentration of sample antigen is high (Kong *et al.*, 2017). Immune peroxidase monolayer (IPM) and indirect immunofluorescence assays

(IIFA) were commonly used before these kits were developed to detect PCV-2 specific antibodies and infectious PCV-2.

The IPM is performed by labelling the anti-species secondary antibody with peroxidase. The brown staining by a substrate is then observed using a light microscope (Zhang *et al.*, 2016, Han *et al.*, 2017). For the indirect immunofluorescence assay, the antibody is detected in body fluids by labelling the specific antibodies with a compound that enable them to glow with a green colour when observed under ultraviolet light microscopically (Meroni *et al.*, 2019). These assays were however, time-consuming and require highly experienced technicians (Opriessnig *et al.*, 2007, Blanchard *et al.*, 2003b). Most commercially available PCV-2 ELISAs are coated with an inactivated PCV-2 antigen, therefore making ELISA kits unaffordable for use by most pig farmers of developing countries especially.

The IFA assay is an independent and sensitive assay which uses recombinant PCV-2 CP for the recognition of PCV-2 specific antibodies in sera as described by Racine *et al.* (2004). IFA requires the earlier infection of porcine cells with live PCV-2 virus, a process which is difficult because the replication cycle is slow (Ouardani *et al.*, 1999). Briefly, the sample is combined with the antigen at the acetone-fixed infected cells present on a slide. A secondary indicator fluorescein-labelled antibody is then added and the slide is read using a fluorescent microscope, followed by the grading of the intensity of the signal fluorescence (Racine *et al.*, 2004, Messenger and Rupprecht, 2015).

1.7.2 Neutralization assays and Micro-Bead Array (MBA)-based technology

Neutralization assays are useful for detection of PCV-2-specific antibodies. However, it is time-consuming, needs fluorescent labelled antibodies or immunoperoxidase staining to verify the absence or presence of the antigen and requires a tissue culture laboratory to be able to carry out this specific assay (Nawagitgul *et al.*, 2002, Pogranichnyyp *et al.*, 2000).

Other platforms for PCV diagnosis include the microbead-based assay, for example the Luminex® multiplex assay, a serological assay that is used to detect PCV-2 specific antibodies. The assay uses flow cytometry whereby colour-coded microbeads have different spectral addresses that enables laser-mediated detection. This diagnostic involves coupling of beads to antigens or antibodies for precise detection of antibodies or antigens diagnostic (Lin et al, 2011; Nolan & Mandy, 2001), a process that is both time consuming and expensive.

1.7.3 Polymerase Chain Reaction (PCR)

Conventional PCR assays accompanied by restriction fragment length polymorphism (RFLP) are useful for routine and quick diagnosis. Variations in RFLP models resulted in the discovery of PCV-2 as a pathogen and that of PCV-2b as an emerging genotype (Nayar *et al.*, 1997, Carman *et al.*, 2006).

Quantitative PCR (qPCR) assays that assess the number of copies of the viral genome as a measure of the viral load in body fluids and tissue samples have replaced the conventional PCR assay. qPCR is useful for detecting etiology during laboratory disease investigation, particularly in cases of reproductive failure where the viral load in the foetus is a very useful indicator. Another variation of this method is based on fluorescent probe-based PCRs, such as Taqman probes, which enable the detection of multiple PCV-2 genotypes and other pathogens in a single reaction. Diagnostic capacity and information availability of investigating clinical cases of PCV-2 have been revolutionized by fluorescence probe-based PCR assays and automated sample processing (Kekarainen *et al.*, 2014). PCR is a sensitive method; however, it is highly laboratory laborious compared to other serological tests. In addition, this method confirms the presence of the virus but does not confirm the presence of the disease.

Even though early detection and diagnosis of PCV-2 is a key step in the goal of elimination or reduction in the number of PCV-2 cases in developing countries, the majority of available diagnostic methods are expensive and time consuming. Therefore, there is a need for inexpensive yet effective diagnostic assays.

1.8 Prevention of PCV-2

PCV-2 can be prevented by effective control of PCVAD. Prevention of PCVAD can also be achieved by avoiding prompting factors through enhancing swine management, coinfection control and altering pig genetic background by careful breeding selection of boars. It is also advisable to separate unhealthy herds which show clinical manifestation of PCVAD from healthy herds as soon as possible.

Traditionally, vaccination is considered the most effective approach to manage viral diseases, however the duration of protection of the vaccine against the disease is limited (Feng *et al.*, 2014). Even though vaccinated animals may still be infected with the virus, they normally have reduced viral loads compared to non-vaccinated animals. Therefore, at present, vaccines administered as a single-dose do not grant swine herds sterilizing immunity and can potentially cause evolution of the virus (Segalés *et al.*, 2013, Kekarainen *et al.*, 2010). The potential of vaccines in preventing multifactorial diseases such as PCVAD has prompted the intense research into and the production of safer vaccines as alternatives to eradicating or regulating PCV-2 (Sun *et al.*, 2016).

1.8.1 PCV-2 vaccines

Generally, a vaccine is a pharmaceutical composition that is safe to administer to an animal and can induce protective immunity against a pathogenic micro-organism. Since the emergence of PMWS and confirmation of the PCV-2 as its causative agent, researchers have been developing ways to control the virus through the development of vaccines. Vaccines against PCV-2 have been commercially available since 2004, and have led to a decrease in morbidity and improved swine production efficiency (Grgacic and Anderson, 2006).

The main commercial vaccines available to date for decreasing the burden of the disease are derived from the PCV-2a coat protein (Opriessnig *et al.*, 2007). These vaccines are highly efficient and successful in inducing humoral and cell mediated immunity (Fort *et al.*, 2012, Fort *et al.*, 2009, Kekarainen *et al.*, 2010). Among them are the inactivated virus vaccines grown in different cell cultures, DNA vaccines and subunit vaccines containing the viral capsid proteins produced in modified insect cells (Karuppannan and Opriessnig, 2017a).

The introduction of PCV-2 commercial vaccines begun in 2004. Their availability has led to a reduction in the disease. These vaccines are currently the best-selling prophylactic agent in swine farming practices (Karuppannan and Opriessnig, 2017b, Alarcon *et al.*, 2013). Circovac® (Merial, France), an inactivated oil-adjuvanted virus vaccine was the first to enter the market. There are three subunit vaccines that are based on the PCV-2 CP-encoding ORF2, expressed using the system of recombinant baculovirus cell expression. These vaccines are Circumvent® (Merck, USA); Ingelvac CircoFlex® (Boehringer, Ingelheim USA) and Porcilis® PCV (Merck, Germany). In addition to these vaccines, there is Fostera® PCV (Pfizer, USA) which is an inactivated chimaeric PCV-1/2 that has a genomic backbone of a non-pathogenic PCV-1 and a CP of PCV-2 that is genetically engineered (Chae, 2012). These vaccines are produced based on genotype PCV-2a which shows cross-reactivity against the prevalent genotypes PCV-2b and PCV-2d (Karuppannan and Opriessnig, 2017b, Xiao *et al.*, 2016, Carman *et al.*, 2006).

Although vaccinated pigs can still become infected with PCV-2, they are expected to have lower viral loads compared to non-vaccinated pigs hence current vaccines applied as single-dose protocol do not provide sterilizing immunity (Kekarainen *et al.*, 2010).

1.8.1.1 Inactivated virus vaccines

Generally, inactivated vaccines can be composed of either whole viruses or bacteria, or fractions of either while live attenuated vaccines are produced by modifying a disease-producing (“wild”) virus or bacterium in a laboratory. Conventional vaccines meant to prophylactically protect pigs against PCV-2 infection may be based on whole inactivated PCV-2 virus as a non-replicating immunogen (antigen) (Melanie *et al.*, 2019). Circovac® and Fostera™ PCV are examples of inactivated virus vaccines and they are for piglets that are 3 weeks and older. Drawbacks associated with inactivated vaccines are improper deactivation which may lead to reversal of replication and harmfulness. It is therefore important ensure that these viruses are effectively deactivated while sustaining immunogenicity, a process which can be expensive (Liu *et al.*, 2016).

1.8.1.2 Live-attenuated vaccines

Suvaxyn® vaccine from Zoeitis, Netherlands (Melanie et al., 2019) is a live-attenuated vaccine. Normally, these vaccines are produced by propagation of the virus in a tissue or cell line. The collection of the virus then follows, and its replication ability is either disabled physically or chemically but the antigen displaying the CP is intact. Live attenuated vaccines consist of a less virulent virus that can undergo partial replication without producing a complete disease, this can typically be achieved by altering an amino acid sequence of the virus. A study conducted by Fenaux *et al.* (2004b) has demonstrated the ability to produce an attenuated PCV-2 candidate vaccine in porcine kidney cells. In other studies by Hemann *et al.* (2014) and Beach *et al.* (2010), a chimaeric PCV-1/2b attenuated virus showed protection against PCV-2a and PCV-2b. The main draw-back with live-attenuated vaccines is the ability of their viral antigen to reverse to a complete virulence form.

1.8.1.3 Vectored vaccines

Viral vector vaccines are viruses that lack replication and are non-pathogenic. These viruses have been altered to express antigens derived from pathogenic viruses. One of the common approaches for viral vector vaccine production is the use of replication defective adenovirus. Wang *et al.* (2007), vaccinated pigs with a recombinant human adenovirus expressing the CP of PCV-2, this resulted in a specific immune response. In another study by Liu *et al.* (2013), an immune response was elicited in mice that were vaccinated intranasally with PCV-2 CP expressed by a non-replicating adenovirus. Since PCV-2 is mostly spread via nasal and oral route, these strategies of vaccine administration are needed. However, there is a need for further improvement to decrease the regularity of immunisation that is necessary.

1.8.1.4 DNA vaccines

DNA vaccines are made up of protein-encoding DNA which is administered to elicit cellular and humoral immunity. The plasmids normally have enhancers or promoters to increase the expression of the gene in the recipient of the vaccine. These vaccines are easier to store and transport in comparison to conventional vaccines (Krishnan, 2000). Chimaeric PCV-1/2 DNA is among some of the initial DNA candidate vaccines. Its development required a non-pathogenic PCV-1 backbone in which the pathogenic PCV-2 CP was inserted. Pigs which were injected intramuscularly with the DNA to produced PCV-2 CP specific antibodies and achieve defensive immunity (Fenaux *et* *al.*, 2004a, Beach *et al.*, 2010). Another study utilised combination of DNA from the three major ORFs as potential candidates vaccine in mice. In this study, only constructs consisting of ORF2 resulted in PCV-2 specific antibody responses, emphasizing the antigenic importance of the ORF2 encoded CP (Aravindaram *et al.*, 2009). Although DNA-based vaccines often have less immune potency compared to conventional vaccines, more research by Guo *et al.* (2015) and Li *et al.* (2015) has focused on either co-expressing porcine interleukin-6 or actually adding CpG motifs to the CP coding DNA constructs to attain an improved cellular and humoral immunity.

1.8.1.5 Subunit and virus like particles vaccines

The baculovirus-insect cell expression system has been a powerful tool in the development of subunit vaccines. PCV-2 CP expressed in this system have been shown to have immunogenic and protective properties (Blanchard *et al.*, 2003a).These vaccines do not cause a disease and are not associated with side effects because they do not contain a live virus (Chae, 2012). Subunit vaccines has been shown to successfully protect pigs against PCV-2 and they are registered as a single dose to pigs that are about two weeks old. These vaccines have demonstrated superior prophylactic efficacy compared to traditional PCV-2 vaccines made from inactivated PCV-2 viruses (Balka et al., 2016, Weibel et al., 2012). As mentioned earlier, there are currently three subunit PCV-2 vaccines produced in insect cell culture expression systems that are commercially available. These vaccines are effective; however they do not produce sterilizing immunity and the virus continues to replicate and spread to a lesser degree (Song *et al.*, 2007).

It has been shown that CP recombinantly expressed using the baculovirus expression system self-assembles into virus like particles (VLPs), which when used to vaccinate swine produced immunogenic responses (Melanie *et al.*, 2019, Fan *et al.*, 2007). VLPs are nearly identical in terms of morphology to the original virions and present an array of epitopes mimicking the structure of the pathogen but lack the viral genome. VLPs are more immunogenic than soluble CP preparations, as a result of their size and structure with repetitive display of immunogenic epitopes. Vaccination with VLPs against PCV-2 has been applied to control disease outbreaks in swine herds (Polayes and Hughes Jr, 1994).

Apart from the baculovirus expression system, other expression systems such as *Escherichia coli* (*E. coli*) cells, yeast and plants have drawn the attention of researchers in order to produce PCV-2 VLP-based vaccine candidates with improved efficacy and safety (Yin *et al.*, 2010, Gunter *et al.*, 2019). Studies have shown the successful production of PCV-2 VLPs in *E.coli* cells that can be used as diagnostic agents as well as vaccine candidates (Wu *et al.*, 2012, Zhang *et al.*, 2014). High quantities of PCV-2 CP have also been expressed in *Pichia pastoris* and *Saccharomyces cerevisiae* yeast cells (Zhang *et al.*, 2014, Bucarey *et al.*, 2009). Vaccines produced using these expression systems are expensive due to their complexity requirement of bioreactors and technically skilled operator.

Over the years, plants have gained traction as a cost-effective system to conventionally used expression systems. Our group was the first to successfully produce immunogenic PCV-2 VLPs in plants. This was the first report describing the expression and purification of PCV-2 CP in plants and confirmation of its assembly into VLPs. The VLPs have further been demonstrated to be highly immunogenic in mice. The yields of purified PCV-2 VLPs were approximately 2 mg/kg of fresh plant material (Gunter *et al.*, 2019). This was a proof of concept study showing that plants can be used to make affordable and immunogenic vaccines.

1.9 The role of plants in the development of biopharmaceuticals

Recombinant proteins can be produced in various expression systems including yeast, bacteria, mammalian cells and plants. Plants have recently become a reliable system for manufacturing recombinant proteins which are useful in disease prevention, treatment, or diagnosis.

Plants have been occupying a vital position in biopharmacy and promised rapid developments in the field of plant-derived biopharmaceutical agents since 1986 (Fahad *et al.*, 2015, Rybicki, 2014). The production of human growth hormone in sunflower and tobacco tissues was the first evidence of the use of plant expression systems (Barta *et al.*, 1986). In addition, Hiatt *et al.* (1989) successfully demonstrated the use of plant-based expression for production of a monoclonal antibody. Since then, a vaccine antigen of *Streptococcus mutants* was produced in plants (Curtis and Cardineau, 1990). One of the most important innovations in plant expression and vaccine production is the development of an influenza vaccine consisting of quadrivalent VLPs by Medicago Inc. in phase II human trials, this vaccine showed efficacy and safety in humans (Pillet *et al.*, 2019). Phase III results of this vaccine are expected to come out in 2020 with promising data. With the recent outbreak of Coronavirus (SARS-CoV-2), British American Tobacco is developing a potential vaccine produced in tobacco plants. Meanwhile Medicago Inc is pursuing a similar effort to combat Covid-19 which has now reached a global pandemic level. This is showing the relevance and strength of using plant-transient expression system in vaccine development. In addition, it only takes approximately 2 months to express a vaccine transiently in tobacco which makes it good to use especially in pandemic situations.

Interestingly, the authorization of a first plant-based enzyme substitution therapy for commercial use in human by the food and drug administration (FDA) was done in May 2012 (Fox, 2012). Gaucher's disease is caused by a deficiency of glucocerebrosidase (GCD) enzyme known as Elelyso ™ which leads to the development of a lysosomal storage disorder (LSD). This enzyme can be produced transgenicaly in carrot cells by Pfizer and Protalix Biotherapeutics (Carmiel, Israel) (Shaaltiel *et al.*, 2007).

In 2014 during the West Africa Ebola epidemic, treatment with a triple cocktail consisting of antibodies (4G7, 2G4 and 13C6) produced in *Nicotiana benthamiana* (*N. benthamiana*) was permitted for use to control the outbreak (Qiu *et al.*, 2014). In addition, there are several plant made vaccines, antibodies, therapeutic proteins and diagnostic reagents that are in clinical progression such as the Norwak virus CP and intrinsic factor for vitamin B among others (Yusibov *et al.*, 2011). All these studies provide evidence that plant-based expression systems have the ability to produce affordable biopharmaceuticals for use, particularly in developing countries.

With the high incidence of emerging viral diseases in the world, particularly developing countries, there is a need to focus on plant-based expression systems for the rapid development of vaccines. Plant-based expression systems have lower upfront investment costs compared to other expression systems such as insect cell and mammalian cell expression systems, making them suitable for deployment in developing countries where infrastructure cost presents an entry barrier for research, development and manufacturing. The use of antibiotics in livestock production has led to an emergence of antibiotic-resistant pathogens. These variables have motivated the creation of cost-effective, scalable veterinary pharmaceutical manufacturing and distribution platforms. Production systems based on plants are suitable to meet these requirements (Sack *et al.*, 2015, Gómez *et al.*, 2009, Chen and Davis, 2016). It offers to produce the recombinant proteins in low cost biomass at large scale with yields up to 5 mg per kg of fresh leaves which can be subjected to processing to obtain pure antigens for making vaccines (Marillonnet *et al.*, 2005). In accordance with Chen and Davis (2016), the majority of commercially available vaccines are produced in mammalian and other cell cultures. Biopharmaceuticals produced in these systems however require capital intensive facilities fermenters, expensive downstream processing, cold storage and transportation, and sterile delivery methods. The development of alternative manufacturing technologies is encouraged by these constraints.

There are two methods for the expression of recombinant proteins in plants, namely transgenic or transient (Scotti and Rybicki, 2013). Traditionally, plant expression methods depended largely on plants that are stably transformed whereby a transgene is incorporated into the plant's nucleus or plastid (Schillberg *et al.*, 2005). Transgenic plants are attained via gene delivery into dicots by *Agrobacterium tumefaciens* or monocots using biolistic method (Mason *et al.*, 1992). The system of generating transgenic plants is however time consuming.

Recently, transient expression systems outperformed transgenic expression systems since it has a brief manufacturing time that yields high quantities of protein (Rybicki, 2010, Schillberg *et al.*, 2005). Transient expression systems have the ability to deliver target protein manufacturing in less than two months, including the time needed to synthesize and optimize target gene expression in plants (Musiychuk et al, 2007). Interestingly, it only took Medicago Inc 20 days to produce SARS-CoV-2 VLPs in *N. benthamiana*. This method involves the expression of a foreign DNA that cannot be inherited but is transcribed and translated within a host cell. There are two main methods that are regularly used to accomplish a heterologous protein's transient expression in crops: via viral vectors derived from Potato X virus (PVX), or tobacco mosaic virus (TMV) (Sala *et al.*, 2003, Curtis and Cardineau, 1990). When using viral vectors, the gene of interest is cloned into the plant virus genome, with a subgenomic promoter. Plants are then infected with a recombinant virus construct that carries the transgene to the plant cell to produce the anticipated protein without transforming the plant stably (Porta and Lomonossoff, 2002). Although immunogenic proteins were produced with this method, the levels of protein expression were low compared to that of the transgenic expression system (Turpen *et al.*, 1995, Mason *et al.*, 1992).

These low yields have led to the development of deconstructed plant virus vectors and agroinfiltration to deliver the gene of interest into plants (Marillonnet *et al.*, 2005). The gene remains as an episome and it does not become a portion of the plant genome hence it is not passed on to the following generation. Modified plant viruses such as tobamoviruses, bean yellow dwarf virus, mastrevirus, geminiviruses and bromoviruses are regularly used. This method utilizes the viral replicative machinery to make non-infectious vectors that can generate expression and translation of the gene of interest in plants (Lomonossoff and D’Aoust, 2016, Gleba *et al.*, 2005). Another method which utilizes a highly translational efficiently is the non-replicating expression system which aims to produce high yields of recombinant protein (Peyret and Lomonossoff, 2013, Hefferon, 2014). These features have enabled a scalable, flexible system to escalate the speed and yields of biopharmaceutical production, with time and cost reduction (Pogue and Holzberg, 2012, Tiwari *et al.*, 2009).

A variety of plant hosts such as *Arabidopsis thaliana, Nicotiana tabacum* and *Lactuca sativa* have been used to produce biopharmaceuticals, but tobacco plants and more specifically, *N. benthamiana* has become the preferred experimental plant species for the expression of recombinant proteins at industrial and laboratory scale. *N. benthamiana* is the most exceptional host, mainly due to the large number of various plant viruses that can infect it successfully (Goodin *et al.*, 2008, Tremblay *et al.*, 2010), furthermore they produce substantial leaf biomass and have a high soluble protein content (Tremblay *et al.*, 2010).

1.10 Objectives and rationale of the study

PCV-2 is known as an emerging swine pathogen of great economic importance, causing significant losses in the piggery industry. Even though pig production is relatively small in South Africa compared to other countries around the world, it is one of Africa’s highest pork producers. The country currently has a pig population of more than 1.5 million produced commercially by more than 400 farmers. The Western Cape province contributes about 11% to the country's swine population commercially (Figure 1.8) (DAFF, 2018).

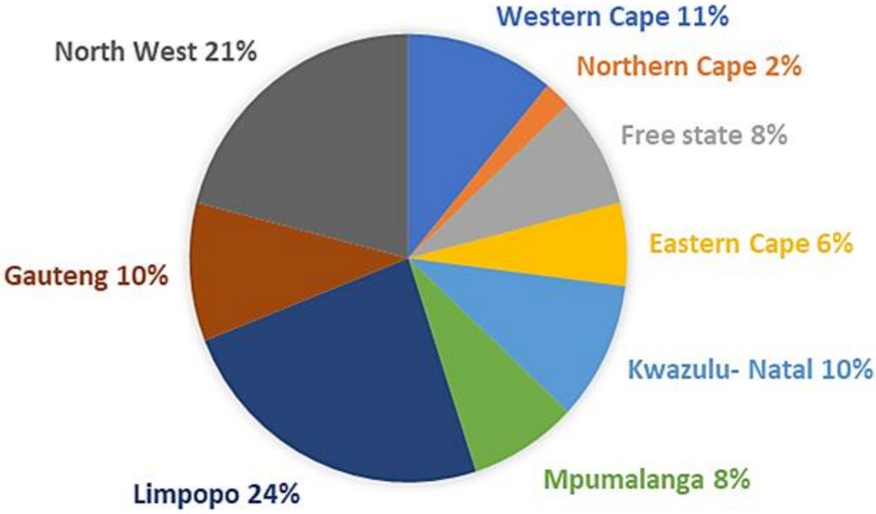

Figure 1.8 The distribution of pig per province in 2017. Source: (DAFF, 2018).

PCV-2 has attracted the attention of researchers since the early 1990s due to the economic fallout it has caused in many pig-producing countries of the world. As discussed previously, PCV-2 subunit vaccines are produced using baculoviral-based expression systems. Additionally, these vaccines rely on expensive growth media and sterile bioreactors for production prior to protein extraction. Since such proteins are in demand, it provides an opportunity for complementary production platforms to be explored. Moreover, plant-based transient expression systems can be promptly implemented and scaled up. Plants also negate contamination with animal pathogens, a concerning drawback with conventional eukaryotic expression systems.

Firstly, only PCV1 and PCV2 (PCV2a, PCV2b, PCV2c, PCV2d, PCV2e, and PCV2f) were known, but a recently diagnosed distant porcine circovirus (PCV3) was publish ed (Phan *et al.*, 2016b, Chen *et al.*, 2017, Wang *et al.*, 2020). The recent discovery and characterization of PCV-3 stresses the importance of continued research and development of vaccines and diagnostics for PCV (Klaumann *et al.* (2018). This strain of PCV, with a genome of about 2000 bp, has been found circulating in Asia and North America in cases of reproductive failure, PDNS (Fan *et al.*, 2017).

Since PMWS still presents a threat to emerging and backyard farmers, early detection of PCV-2 is of great importance. This attracted researchers' interest to continue searching for affordable, reliable and fast diagnostics against PCV-2. Gunter *et al.* (2019) showed that PCV-2 VLPs can be successfully produced in plants, these findings have unlocked the opportunity to develop affordable plant-made serological assays to detect PCV-2. Particularly because the ELISAs that are commercially available are expensive (approximately R18 000 per kit for 100 reactions) and must be imported.

Therefore, the aim of the study is to develop a plant-made diagnostic immunoassay for the detection of PCV-2 antibodies in South African swine herds. The main objectives for this study are as follows:

1. To clone the PCV-2 CP gene into the pCBP-2 proprietary plant expression vector and compare expression levels and VLP formation to that obtained when using the pEAQ-*HT* plant expression vector, which has previously been used to produce VLPs (Gunter *et al.*, 2019).
2. Development of a lateral flow device immunoassay for adaptation to a diagnostic laboratory and field setting.

2 Chapter 2: Transient expression optimisation of PCV-2 capsid protein (CP) in *Nicotiana benthamiana*

2.1 Introduction

PCV-2 has been infecting swine for many years and the leading cause of PCVAD (Wei *et al.*, 2020, Chae, 2004). Over the years various expression systems has been used to express recombinant PCV-2 CP to manage the disease. These include insect cells, yeast, bacteria, plant-based and mammalian expression systems (Fan *et al.*, 2007, Fan *et al.*, 2008, Marcekova *et al.*, 2009, Nawagitgul *et al.*, 2002, Tu *et al.*, 2013, Wang *et al.*, 2008, Lai and Chen, 2012, Chen, 2008). In these studies, the expression of PCV-2 CP was achieved by optimizing the codon composition, truncating the gene to remove the arginine-rich N terminal, or by adding various tags that are useful for purification. These approaches were successful in producing full-length or truncated PCV-2 CP. This capsid protein is the only structural protein and the major antigenic determining factor of this virus. The CP has a great potential to be used as both a vaccine candidate and or in diagnostic assays. The PCV-2 CP has antigenic peptides that maximizes its capacity to be used as a diagnostic reagent and vaccine (Santos *et al.*, 2018). In addition, the CP has unique patterns on its surface that possibly helps with the pathogenesis, virus function and cell entry (Wang *et al.*, 2016).

Insect cells, yeast, bacteria, mammalian cells expression methods depend on the use of sterile bioreactors and expensive growth media which makes them costly and complex. Consequently, vaccine and diagnostic reagents produced using these production systems may be unaffordable and therefore do not serve their purposes in resource-poor countries. The increase in demand for industrially and biomedically useful proteins, demands highly scalable, robust, cost-effective, easy-to-use, more secure, and sustainable production systems. Transient plant expression systems can fulfil these criteria from laboratory expression level to the industrial manufacturing of bioactive compounds. Plant cells carry insignificant risk of cross-contamination with animal pathogens and are able to carry out the necessary post-translation modifications and assembly of recombinant proteins (Fahad *et al.*, 2015, Rybicki, 2009, Diamos *et al.*, 2016). Moreover, the prerequisites for transient expression of proteins in plants are a greenhouse for plant cultivation and a biosafety level-1 (BSL-1) laboratory, making this innovative system accessible for exploration to a bigger research community. Although plant expression can be either transient or transgenic, lately, transient expression systems have gained attention over transgenic expression (Rybicki, 2010). The transient expression is a contained system in itself that can be used to produce large quantities of proteins rapidly, thus saving time (Figure 2.1) (Marsian and Lomonossoff, 2016, Lico *et al.*, 2008).

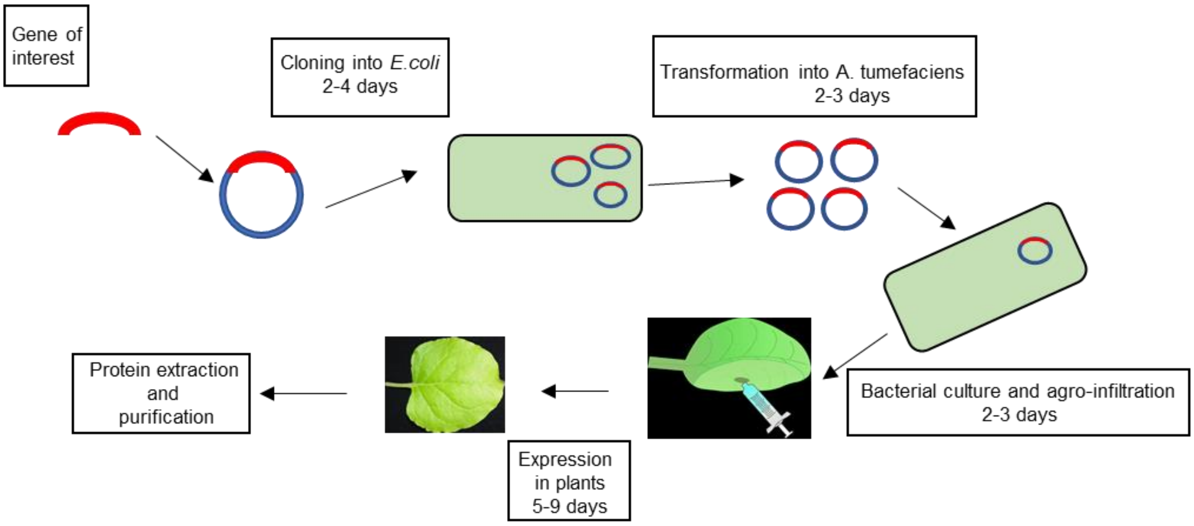

Figure 2.1 Schematic representation of transient expression. Cloning and expression of the protein of interest may occur within 2-3 weeks. The image was adapted from Peyret and Lomonossoff (2013).

A. tumefaciens is a plant and soil pathogen and is known as rhizobium radiobacter. This bacterium can transmit genetic information by transferring transfer DNA (T-DNA) into the plant nucleus carried on a plasmid that induces tumours (Ti plasmid). It integrates into the genome of the host causing the alteration of cells and develop into tumours. The proliferating tissue gives the bacterium unusual amino acids specific to the bacteria called opines, which are an important source of nitrogen and carbon (Zupan *et al.*, 2000, Depicker *et al.*, 1982).

Only some of the T-DNA is incorporated into the genome, numerous copies remain in the nucleus as episomes whose mRNAs are translated and subsequently transiently expressed. A suitable expression vector is required to achieve transient expression of proteins in plants. The *A. tumefaciens* strain and expression vector used plays a vital role in the plant expression speed and yield of recombinantly expressed protein. Generally transient recombinant expression via agroinfiltration of plant leaves is faster, easier, and results in higher yields of protein in comparison to transgenic plants (Krenek *et al.*, 2015, Hefferon, 2014).

The main challenges encountered with plant-produced biopharmaceuticals has been the low accumulation levels of some recombinant proteins within the plant cell and the subsequent purification thereof (Martínez *et al.*, 2010, Islam *et al.*, 2019, Marques *et al.*, 2019). In an effort to optimise the expression of proteins in plants, it has been shown that targeting heterologous proteins to a suitable intracellular compartment leads to higher levels of protein accumulation (Ahmad *et al.*, 2010). The process of folding, assembly, post-translational modifications as well as prevention of immediate degradation and intervention of the protein sequences with cell metabolism can be directly influenced by the type of cell organelle in which the protein is found (Leite *et al.*, 2019, Ahmad *et al.*, 2010). This is because each organelle has a distinct physical size, protease component and biochemical environment which impact the levels of protein production (Streatfield, 2007, Pillay *et al.*, 2014). Normally, recombinant proteins are targeted to the major compartments which includes the vacuole, the cytosol, the apoplast, the chloroplast and the endoplasmic reticulum (ER) using transit and signal peptides (Pereira *et al.*, 2014, Miletic *et al.*, 2016, Conley *et al.*, 2009b).

Notably, RNA silencing can also affect protein yield in plants. RNA silencing is known as a post-transcriptional gene silencing (PTGS) system which acts as a defence against viral infection (Waterhouse *et al.*, 2001b, Kant and Dasgupta, 2019, Takeda *et al.*, 2002). The mechanism for RNA silencing recognizes 'abnormal' RNAs, derived from certain double-stranded RNAs (dsRNAs), transgenes and intermediate replicants of viral RNAs, and breaks down homologous RNA in the cytoplasm. RNA silencing begins when 21-25 nucleotide small interfering RNAs (siRNAs) which corresponds to the target RNA are produced. Once the PTGS induction has begun at one location, the systemic silencing stimuli spread and eventually triggers PTGS in the rest of the tissues. (Waterhouse *et al.*, 2001a). The silencing suppressor is considered to interfere with dsRNA-generating steps and thus inhibit silencing. Silencing suppressors are encoded by various plant viruses such as Tomato spotted wilt virus (TSWV) and Tomato bushy stunt virus (TBSV). The NSs and P19 proteins of TSWV and TBSV respectively were shown to suppress transgenic PTGS. Interestingly, the

P19 protein has shown up to 50 times greater expression for various proteins (Takeda *et al.*, 2002, Voinnet *et al.*, 2003, Margaria *et al.*, 2015). In this study, the NSs protein was used. This silencing suppressor has been used widely and shown to improve protein expression since it increases viral siRNAs (Hedil *et al.*, 2015, Huddy *et al.*, 2018).Our group was the first to transiently express PCV-2 CP in tobacco plants (Gunter *et al.*, 2019). The authors used a plant-codon optimised gene, targeted to the cytoplasm which showed promising results.

The knowledge of the genetic components responsible for the replication and expression of plant viruses has led to the creation of plant-based viral vector systems. One of those vectors is the newly synthesized non-replicating pCBP-2 plant expression vector which targets protein expression to the ER. This vector is designed based on the pTRAc vector (Maclean *et al.*, 2007). The pTRAc vector uses the chalcone synthase 5' UTR which is believed to increase the translation rate, which in turns improves expression yield (Gallie *et al.*, 1995). Interestingly, the 5' UTR widely used and has demonstrated higher protein expression levels (Gallie, 2001, Shopan *et al.*, 2020, Hinnebusch *et al.*, 2016, Peyret *et al.*, 2019).

As mentioned earlier, the PCV-2 CP is not only a structural protein of the virus, but it is of immunogenic importance. It has potential to be utilised as a vaccine and a diagnostic reagent. The increasing outbreak of PMWS, especially in developing countries, motivates the use of CP for vaccine development and as a diagnostic reagent to improve management capabilities such as disease surveillance of PCV-2. The aim of this study was to investigate if the new plant expression vector, pCBP-2, resulted in higher PCV-2 CP expression levels compared to the pEAQ-HT vector which was previously shown by Gunter *et al.* (2019) to be the best for CP expression.

2.2 Materials and Methods

2.2.1 Expression vectors

Two expression vectors were used in this study; pCBP-2, a new non-replicating expression vector that targets expression of proteins to the ER. The codon-optimised PCV-2 *cp* gene (GenBank accession number KJ128269) was synthesized by Genscript Inc (USA) and maintained in the pUC57 vector (Figure 2.2). PCV-2 *cp* was previously cloned into pEAQ-*HT* by (Gunter *et al.*, 2019) (Figure 2.3 B). This vector targets protein expression to the cytoplasm (Sainsbury *et al.*, 2009).

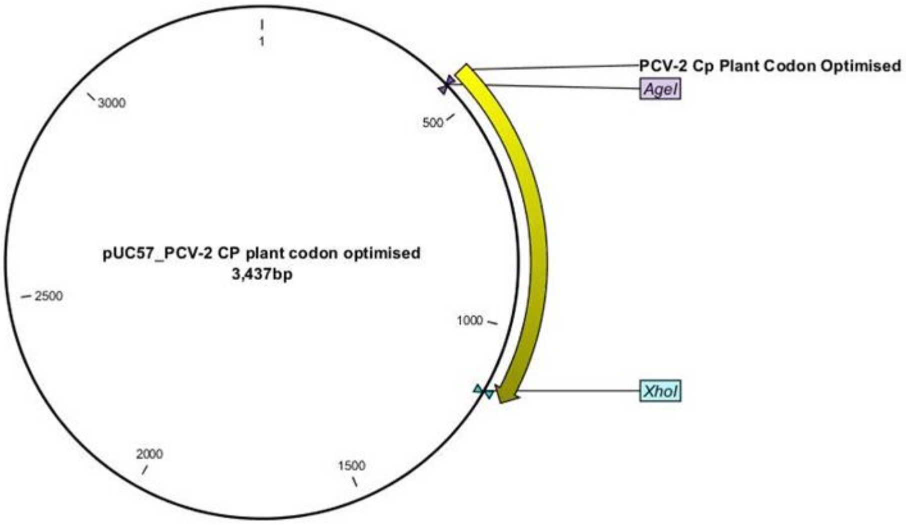

Figure 2.2: A- The pUC-57 cloning vector harbouring the PCV-2 ORF2 gene. The PCV-2 gene is shown in the pUC57 plasmid as indicated in figure A, together with *Age*I and *Xho*I restriction sites used to subclone the gene.

2.2.2 Strains of bacteria and antibiotics used

For *E. coli* transformation, chemically competent *E. coli* DH5α cells (E. cloni®, Lucigen) were used while for *A. tumefaciens* transformation the GV3101:pMP90RK and LBA4404 strains were utilized in this study. Recombinant *E. coli* and *A. tumefaciens* were cultured in the presence of specific antibiotics (Table 2.1) to sustain selective pressure. All liquid cultures of *E.coli* were grown with agitation at 37°C overnight in Luria Bertani medium (LB; 0.5% yeast extract, 1% sodium chloride [NaCl] and 1% tryptone) as described by Sambrook *et al.* (1989). *Agrobacterium* cells were grown 3 days on solid media plates after which they were screened for positive transformants. LBB (LB media with additional yeast extract (12.5 g/L) and 10 mM morpholineethanesulforic acid (MES)) was used for *A. tumefaciens* liquid culture growth with agitation at 27 °C. Single colonies were inoculated into 10 ml LBB for liquid cultures, supplemented with specific antibiotics and grown overnight. The 10 ml culture was used as inoculum to initiate a 50 ml culture, which in turn was used for inoculating 500 ml LBB for large-scale infiltrations. The LBA4404 500 ml cultures were supplemented with 1M $MgSO_4$ to prevent clumping of the cells. Glycerol stocks (2 ml) to preserve cultures were prepared by mixing the cultures with 50% glycerol in a 1:1 ratio. These were stored at -80 °C for later use.

Table 2.1: Plant expression vectors and their antibiotic working concentrations in *E. coli* and *A. tumefaciens* cultures

Vectors	Strains	Antibiotic	Concentration
pEAQ- *HT*	*E. coli* DH5α cells	Kanamycin	50 µg/mL
	LBA4404	Kanamycin	30 µg/ml
		Rifampicin	50 µg/ml
pCBP-2	*E. coli* DH5α cells	Ampicillin	100 µg/mL
	GV3101::pMP90RK	Carbenicillin	50 µg/ml
		Kanamycin	30 µg/ml
		Rifampicin	50 µg/ml

2.2.3 Subcloning into the pCBP plant expression vector

Single colonies of *E. coli* DH5α transformed with pUC57-PCV-2-CP, pCBP-2 empty vector and pEAQ-PCV-2-CP were inoculated into 10 mL LB media supplemented with their respective antibiotics as indicated in Table 2.1. Plasmid DNA was extracted using the QIAprep® Spin DNA Miniprep Kit (Qiagen) as per manufacturer's guidelines. All

DNA quantification were performed using a NanoDrop™ 2000C spectrophotometer (Thermo Fischer Scientific, USA).

The PCV-2 *cp* gene was excised from pUC57 using the *Age*I and *Xho*I restriction enzyme sites and subcloned into the pCBP-2 vector linearized with *Bsa*I and *Xho*I to yield the pCBP-PCV-2-CP-SP construct (Figure 2.3 A). Briefly, after digesting pUC57-PCV-2-CP and pCBP-2 with the relevant restriction enzymes (according to the manufacturer's (NEB) instructions), the digested DNA was resolved on 1% agarose gels. The expected bands for *cp* and the linearized vector were excised from the gel and purified with the QIAquick® Gel Extraction Kit (Qiagen, USA) as instructed by the manufacturer.

The pCBP-2 backbone and PCV-2 *cp* DNA fragment were ligated in 1:3 vector to insert ratio overnight at 4 °C using T4 ligase (Roche, Basel, Switzerland) as described by the manufacturer. The ligation mixture was transformed into chemically competent *E. coli* DH5α cells (E. cloni ®, Lucigen). Briefly, 5 µl of ligated plasmid was mixed with 15 µl of competent cells before incubating the mixture on ice for 30 minutes. After that the mixture was heat shocked for 45 seconds at 42 °C then placed back on ice. Five hundred microlitres LB was added to the tube prior to incubation at 37 °C with agitation for an hour after which cells were plated onto LB agar media supplemented with 100 µg/mL ampicillin. Single colonies were screened with vector specific primers as described in Table 2.2 using colony PCR.

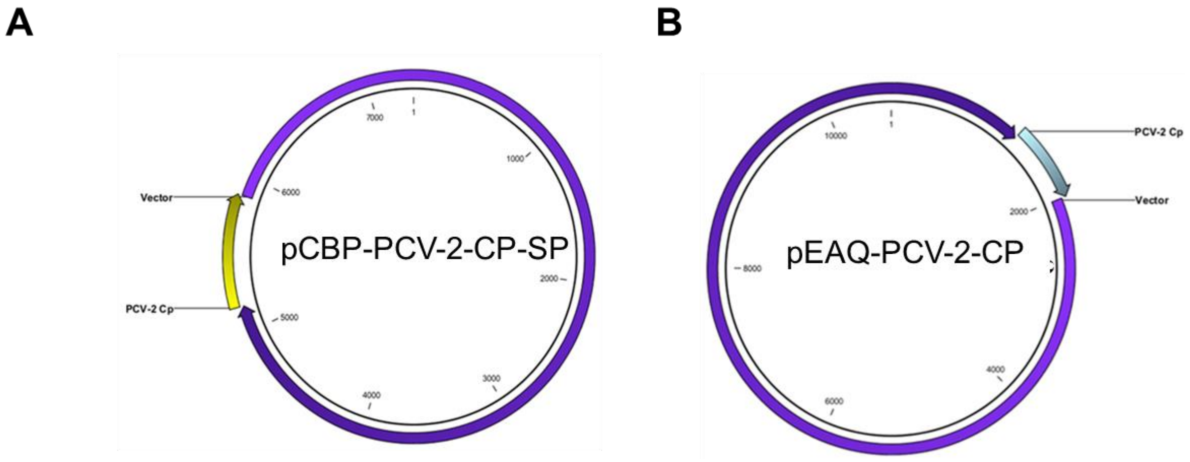

Figure 2.3: The pCBP-2 and pEAQ-*HT* plant expression vectors harbouring the PCV-2 *cp* gene. A- The PCV-2 *cp* gene was sub-cloned into the pCBP2 vector and

resulted in the final recombinant pCBP-PCV-2-CP-SP plasmid. B- The pEAQ-*HT* vector harbouring the PCV-2 gene (Gunter *et al.*, 2019).

A BioRad Biocycler was used to perform all PCRs. All colony PCR reactions were performed with Taq DNA polymerase 2x Master Mix Red ampliqon (Thermo Fisher Scientific), together with 0.2 µM of each primer and 2 mM $MgCl_2$ as instructed by the manufacturer. The reactions were performed using the following cycling conditions: an initial denaturing step for 5 minutes at 95 °C, followed by 30 cycles of denaturation at 95 °C for 30 seconds, annealing based on the temperature given in Table 2.2 for 30 seconds, and extension for 30 seconds at 72 °C. A final elongation step followed at 72 °C for 5 minutes. For every PCR experiment, a negative control that did not contain DNA template was used. The separation of all PCR products was carried out on 1% agarose gels stained with ethidium bromide. O'GeneRuler™ 1kb DNA ladder from Thermo Fisher Scientific was used as molecular size marker.

Table 2.2: Primers used in this study

Primer name	**5'-3' primer sequence**	**Length (bp)**	**Tm (°C)**
FW CBP	TTT CAT TTG GAG AGG ACC AG	20	51
RV CBP	GCG AAA CCC TAT AAG AAC C	19	51
pEAQ-HTf	TTC TTC TTC TTG CTG ATT GG	20	56
pEAQ-HTr	CAC AGA AAA CCG CTC ACC	18	56

2.2.4 Transformation of *A. tumefaciens*

The pCBP-2 vector, pCBP-PCV-2-CP-SP and pEAQ-PCV-2-CP were electroporated into their respective *Agrobacterium* strains as indicated in Table 2.1 based on the method described by Shen and Forde (1989). Briefly, in a 0.1 cm electroporation cuvette (Bio-Rad), 300ng of each recombinant plasmid was mixed with 100µl of competent *Agrobacterium* cells and chilled on ice for 5 minutes. Electroporation was carried out using a Gene Pulser Xcell™ (Bio Rad) at 200Ω, 25µF and 1.8kV. Nine hundred microlitres LB medium was added to the cuvettes and mixed with the cells.

The cell suspension was subsequently incubated at 27 °C for 2 hours with agitation before plating onto LB agar plates supplemented with the relevant antibiotics (Table 2.1) and grown for 3 days. Colony PCR with relevant specific primers was performed as described in section 1.2.3 to confirm positive *Agrobacterium* clones. DNA isolated from positive *Agrobacterium* clones were back-transformed into *E. coli* DH5α cells to further verify the recombinant plasmids. Plasmid DNA from recombinant *E. coli* was digested with *PstI* and *XhoI* restriction enzymes for further confirmation. The restrict digests were set up according to Thermo Fisher Scientific DoubleDigest calculator and was incubated for 2 hours at 37 °C before resolving on a 1% agarose gel.

2.2.5 Transient expression of PCV-2 CP in *N. benthamiana*

2.2.5.1 Preparation of *N. benthamiana* plants

All plants used in this study were grown in a plant growth room with a 16 hour light and 8 hour dark photoperiod and a temperature range of 18 °C (night time low) to 25 °C (day time high), with 50-60% humidity. *N. benthamiana* were grown from seeds that were planted in trays filled with soil that was supplemented with Margaret Roberts supercharger fertilizer and Gaucho (0.05 g/L). Seedlings of about 2-3 weeks old were transplanted into individual soil-filled pots supplemented with Multi Booster fertilizer and Gaucho. Plants were fertilized once every week and watered every 2-3 days. Four to six weeks old plants were used for agroinfiltration.

2.2.5.2 Small scale expression optimization

A preceding study in the BRU conducted by Gunter *et al.* (2019) focused on optimizing PCV-2 CP expression with the pEAQ-*HT* vector in *N. benthamiana.* In the present study expression of PCV-2 CP with the pCBP-2 vector was optimized to determine cell concentration [Optical density (OD_{600})] and day post infiltration (dpi) at which the highest levels of CP protein was expressed. The pCPB-2-CP construct was also co-infiltrated with the pBIN-NSs (LBANSs) silencing suppressor construct to determine if CP yields could be improved.

In short, 2 ml of the frozen glycerol stocks consisting of the recombinant *Agrobacterium* constructs were revived in 10 ml LBB medium consisting of specific antibiotics and grown with agitation overnight at 27 °C. The next day, the 50 ml LBB medium was inoculated with the 10 ml pre-inoculums and incubated overnight in the presence of appropriate antibiotic (excluding rifampicin) and 200 mM acetosyringone to induce the expression of the virulent genes. Cultures were prepared for syringe infiltration by diluting the 50 ml overnight cultures to OD_{600} of 0.25 and 0.5 in resuspension buffer (10 mM $MgCl_2.6H_2O$, 5 mM MES, pH 5.6). *N. benthamiana* leaves of 4-6 old weeks were syringe-infiltrated with the diluted cultures. Similar infiltration parameters were tested for the empty vector negative control, pCBP-2.

Three leaf discs per construct were harvested at 3, 5 and 7 dpi by using the lid of a 1.5 ml microcentrifuge tube. A volume of 200 µl DB_{150} extraction buffer (1 mM $CaCl_2$, 150 mM NaCl, 10% glycerol (v/v), 0.001% Triton X-100, 1 M Tris, 250 mM L-Arginine, pH6.5) supplemented with cOmplete™ Protease Inhibitor (EDTA-free) was added to the leaf discs and these were subsequently homogenised with a micropestle. The extracts were clarified at 11 142.9 × *g* for 5 minutes using a benchtop microcentrifuge. The supernatant was recovered and denatured at 95 °C in the presence of sample application buffer (SAB, 0.5 M EDTA, 25% (v/v 0,001% (w/v) bromothymol blue, 5% (w/v) SDS, glycerol) for 10 minutes and stored at -20 °C.

2.2.6 Protein purification using density gradient ultracentrifugation

Expression was scaled up in order to produce enough biomass for purification. Vacuum infiltration for medium scale expression optimization was carried out as described earlier in section 1.2.5.1 except that the 50 ml overnight culture was further scaled up by to 500 ml supplemented with the relevant antibiotics (except rifampicin) and acetosyringone and incubated at 27°C overnight. *N. benthamiana* plants were vacuum infiltrated at -90 kPa by submerging the plants into the bacterial suspension and quickly releasing the vacuum. The leaves were harvested collectively at 3 and 5 dpi and weighed. Fresh biomass was homogenised in 2 x volumes of DB_{150} buffer and protease inhibitor using a T25 digital ULTRA-TURRAX® homogenizer (Sigma-Aldrich®). The homogenate was incubated for 60 minutes at 4 °C before clarification with centrifugation for 20 minutes at 8000 × *g*.

The clarified crude extract comprising of the PCV-2 CP was filtered through four layers of 22-24 µm Miracloth® (Millipore Sigma) prior to loading onto sucrose gradients. Sucrose solutions were prepared in DB_{150} buffer. The gradients consisted of two steps: 6 ml 45% sucrose (w/v) overlayed onto 2 ml 65% sucrose (w/v) in 38 ml Ultra-Clear™ ultracentrifuge tubes (Figure 2.4). Samples were centrifuged for 4 hours at 120 000 × *g*, 4 °C using a SW32Ti rotor (Beckman). The resulting pellet was resuspended in 1 ml of 1× phosphate buffered saline (PBS, pH 7.4) and subsequently analysed (Gunter *et al.*, 2019).

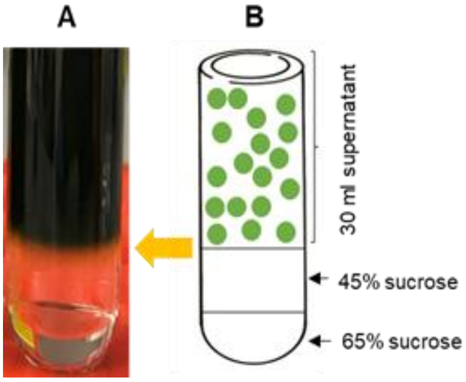

Figure 2.4: Set up of sucrose gradient purification of plant produced PCV-2 CP protein. Photo and schematic representation (A and B respectively) of a discontinuous sucrose gradient (45% w/v and 65% w/v) on which the plant homogenate is loaded prior ultracentrifugation.

2.2.7 SDS-Page and western blot analysis

SAB was added to the PCV-2 CP at a final concentration of 1×, before denaturation at 95 °C for 10 minutes. Denatured PCV-2 CP was resolved at 120V on 12.5% SDS-PAGE gels and either stained at room temperature overnight in Coomasie blue stain (48% v/v methanol, 0.1% (w/v) brilliant blue G-250, 15% v/v glacial acetic acid) and destained (10% v/v glacial acetic acid, 30% v/v methanol) at room temperature overnight; or protein expression was analysed on western blots. For western blot analysis, proteins were transferred onto nitrocellulose membranes pre-soaked in transfer buffer (2.93 g glycine, 5.82 g Tris base, 200 mL methanol in 1000 mL water, pH 9.2) with a semi-dry TransBlot® system, (Bio-Rad) at 15V for 90 minutes. After transfer, membranes were washed in blocking buffer (5% long life fat-free milk, 1x PBS, 1% Tween-20) with agitation for 30 minutes at room temperature. PCV-2 CP rabbit antisera diluted in blocking buffer (1:1000) was used to probe the membranes by incubating overnight with agitation at 4 °C. Blots were washed 4× 15 minutes in blocking buffer after which they were incubated in 1: 5000 dilution of the secondary antibody (alkaline phosphatase conjugated anti-rabbit, Sigma-Aldrich®) in blocking buffer at 37 °C for 60 minutes with shaking. Following incubation in the presence of the secondary antibody, the blots were washed 4x 15 minutes with blocking buffer without milk. Finally, 5-bromo-4-chloro-3-indoxyl-phosphate (BCIP) and nitroblue tetrazolium (NBT) phosphatase substrate (BCIP/NBT 1-component) was added to the blots for 30 minutes for detection of the PCV-2 CP.

2.2.8 Protein quantification

In order to quantify PCV-2 CP, gel densitometry was utilised with Bovine serum albumin (BSA, (Sigma-Aldrich®)) as reference protein standard. BSA with a starting concentration of 1 mg/mL was diluted (2- fold) in 1x PBS (pH 7.4) to create a standard curve. SAB was added to 25 µl of the PCV-2 CP samples and BSA standards to a final concentration of 1x. Samples were denatured for 10 minutes at 95°C and resolved on 12.5% SDS-PAGE gels. The gels were Coomassie-stained and protein quantification was performed using StudioTM Lite version 5.2 software (LI-COR®).

2.3 Results

2.3.1 Confirmation of recombinant *E. coli* and *Agrobacterium* clones

Restriction enzyme digest was successfully performed to linearize the pCBP-2 vector with *Bsa*I & *Xho*I and yielded a 6610 bp fragment as shown by the blue arrow in figure 2.5 A. Similarly, the PCV-2 *cp* was excised from the pUC57 vector using *Age*I & *Xho*I restriction enzyme digests as evidenced by the presence a 712 bp fragment constituting *cp* on an agarose gel (yellow arrow, Figure 2.5 A), this band was purified from the agarose gel for ligation into the linearized pCBP-2 vector to yield the pCBP-PCV-2-CP-CP-SP construct.

Colony PCR with vector-specific primers were carried out on *E. coli* colonies transformed with pCBP-PCV-2-CP-SP, a total number of 21 colonies were screened of which 4 of the colonies harboured the gene of interest, as evidenced by the detection of an expected band at 1071 bp for colonies 1,3 17 and 18 (purple arrow). Colony PCR of an *E. coli* colony transformed with the empty vector resulted in amplification of a band of approximately 423 bp (orange arrow) (Figure 2.5 B), which was expected since it did not contain the gene of interest. The pEAQ-PCV-2-CP construct was also screened along with pCBP-PCV-2-CP-SP whereby vector specific primers were utilized, 1 colony was screened and showed to be positive as shown by the purple allow in figure 2.5 B which shows the presence of the gene of interest. The amplified product was slightly smaller, which was expected, since the constructs were in different vectors and amplified with vector-specific primers and the size of the fragment amplified is dependent on where the primers bind in the vector backbone. A no DNA template PCR negative control was also carried out and as expected no bands were observed.

Before transformation into *A. tumefaciens*, RE digests with *Xho*I and *Pst*I were carried out for confirmation of the selected positive clone. Here, two bands of size 6596 bp (red arrow) and 726 bp (green arrow) were observed as expected as seen in figure 2.6 C. Single digests of the plasmid using individual enzymes were done to assess the functionality of the enzymes along with an undigested plasmid which served as a control (Figure 2.5 C).

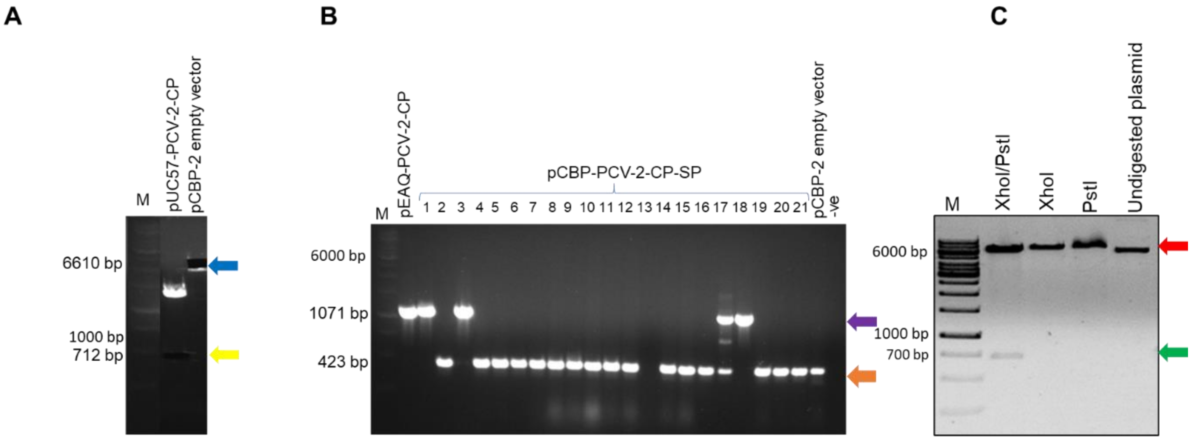

Figure 2.5: Cloning of PCV-2 *cp* into the pCBP-2 vector, colony PCR screening of recombinant *E. coli* transformants and RE digest confirmation. A) Gel after the excision of the expected 712 bp PCV-2 *cp* digested with *Age*I and *Xho*I (yellow arrow) from the backbone of the pUC-57 vector not excised (visible band). The pCPB-2 vector was linearized with *Bsa*I and *Xho*I giving rise to a 6610 bp as indicated with the blue arrow. B) Colony PCR confirmation of successful *E. coli* transformants. Positive clones harbouring the gene of interest is indicated by the purple arrow at approximately 1071 bp. The orange arrow at approximately 423 bp indicates the empty vector and for the PCR negative control, no DNA fragments were amplified. C) Double digest (*Pst*I and *Xho*I) of the pCBP-PCV-2-CP-SP plasmid yielding two bands; 6596 bp (red arrow) and 726 bp (green arrow) which were expected. Single digests with each enzyme gave rise of the expected band size along with the undigested plasmid, respectively. M – molecular weight marker shows fragment sizes in nucleotide base pairs (O'GeneRuler 1kb ladder).

Following confirmation of positive pCBP-PCV-2-CP-SP clones in *E. coli*, plasmid DNA was extracted and used to transform *A. tumefaciens* GV3101::pMP90RK. Colony PCR with vector specific primers was carried out as described for the *E. coli* clones above and all the *A. tumefaciens* colonies screened were shown to contain the gene of interest as indicated by amplification of a band of approximately 1071 (Figure 2.6, black arrow). An *A. tumefaciens* colony transformed with the empty pCBP-2 vector yielded a band of approximately 423 bp (grey arrow) after colony PCR as expected (Figure 2.6). Just like for *E. coli* screening, colony PCR of pEAQ-PCV-2 CP transformants were also carried out for confirmation of the *A. tumefaciens* clones.

Here, the amplified product appeared to be was slightly smaller as expected. A no DNA template PCR negative control was carried out and as expected no bands were observed after amplification (Figure 2.6).

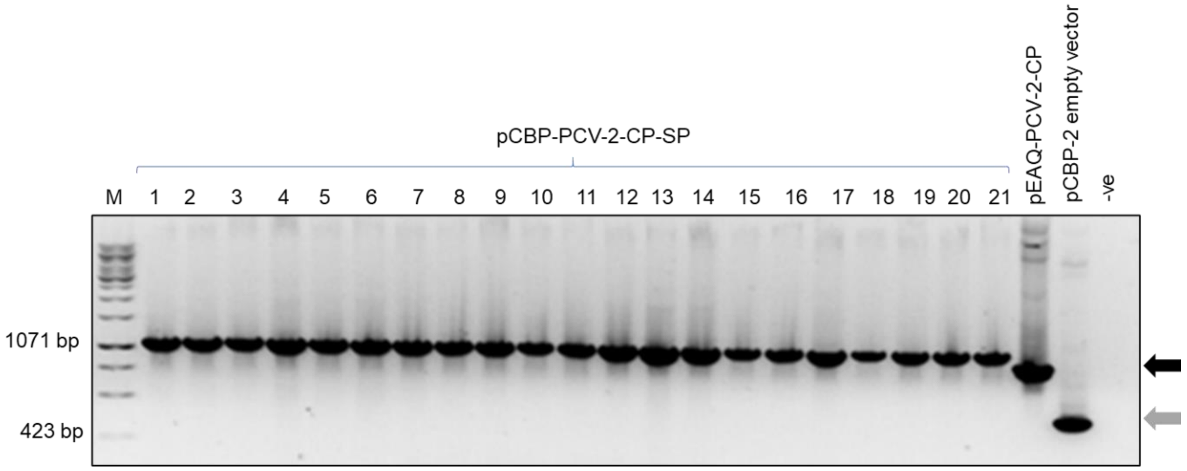

Figure 2.6 *A. tumefaciens* colony PCR confirmation. Positive clones harbouring the gene of interest is indicated by the black arrow at approximately 1071 bp. The grey arrow at approximately 423 bp indicates the empty vector and for the PCR negative control no DNA fragments were amplified. M – molecular weight marker shows fragment sizes in nucleotide base pairs (O'GeneRuler 1kb ladder).

2.3.2 Optimization of protein expression in *N. benthamiana*

To assess plant-based transient expression as a tool for producing PCV-2 CP that is suitable for making an affordable PCV-2 diagnostic reagent, which will be especially useful in developing countries, optimization was performed to determine the day post infiltration and cell density at which the best protein expression was achieved.

Small-scale expression studies of PCV-2 CP was first conducted where plants were syringe-infiltrated at different cell densities with the recombinant *Agrobacterium* constructs and biomass was harvested for analysis at 3, 5 and 7 dpi.

Figure 2.7 shows images of the phenotype of plant leaves expressing PCV-2 CP when infiltrated at a cell density of OD_{600}=0.5 and 0.25 as observed at 3, 5 and 7 dpi respectively (Figure 2.7 A-C) and empty vector (Figure 2.7 D). Plants infiltrated with the recombinant pCBP-2-PCV-2-CP-SP construct developed necrosis from 5 dpi onwards with browning and drying out of the leaves, the negative control empty vector plant was still healthy at 7 dpi. No difference in phenotype was observed between the two cell densities tested.

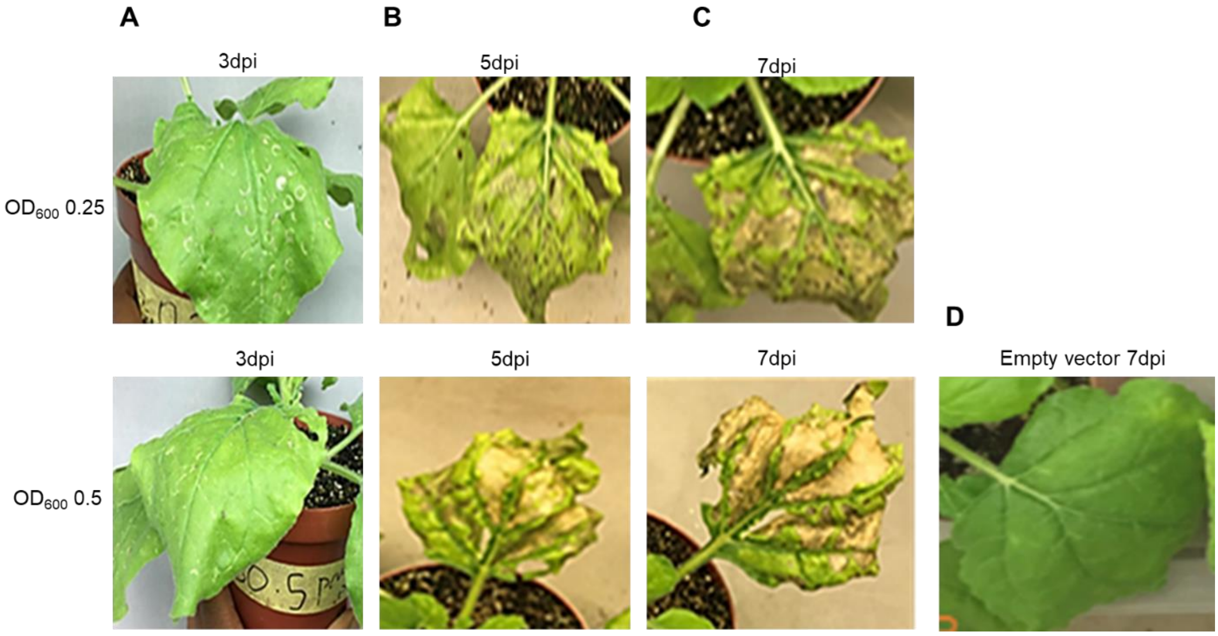

Figure 2.7 Phenotype of plant leaves infiltrated with pCPB-PCV-2-CP-SP. A-C) leaves of PCV-2 infiltrated at OD_{600} 0.25 and 0.5 examined at 3, 5 and 7 dpi respectively. D) empty vector representative.

Since the plants were severely necrotic from 5 dpi onward, which resulted in a loss of biomass and potentially reduced protein expression and resulted in protein degradation, co-infiltration with the pBIN-NSs silencing suppressor was carried out to determine if it would improve both phenotype and protein accumulation levels. The usage of viral gene-silencing suppressors may enhance the transient expression of heterologous proteins (Burgyán, 2008, Takeda *et al.*, 2002). RNA silencing functions as an antiviral defensive strategy in plants. Co-expression with the NSS silencing suppressor showed significant improvement of the symptoms previously observed (Figure 2.7), and biomass appeared to be relatively healthy, with the development of chlorosis at 7 dpi (Figure 2.8). No significant difference in phenotype was observed between the two cell densities for pCBP-PCV-2-CP-SP tested.

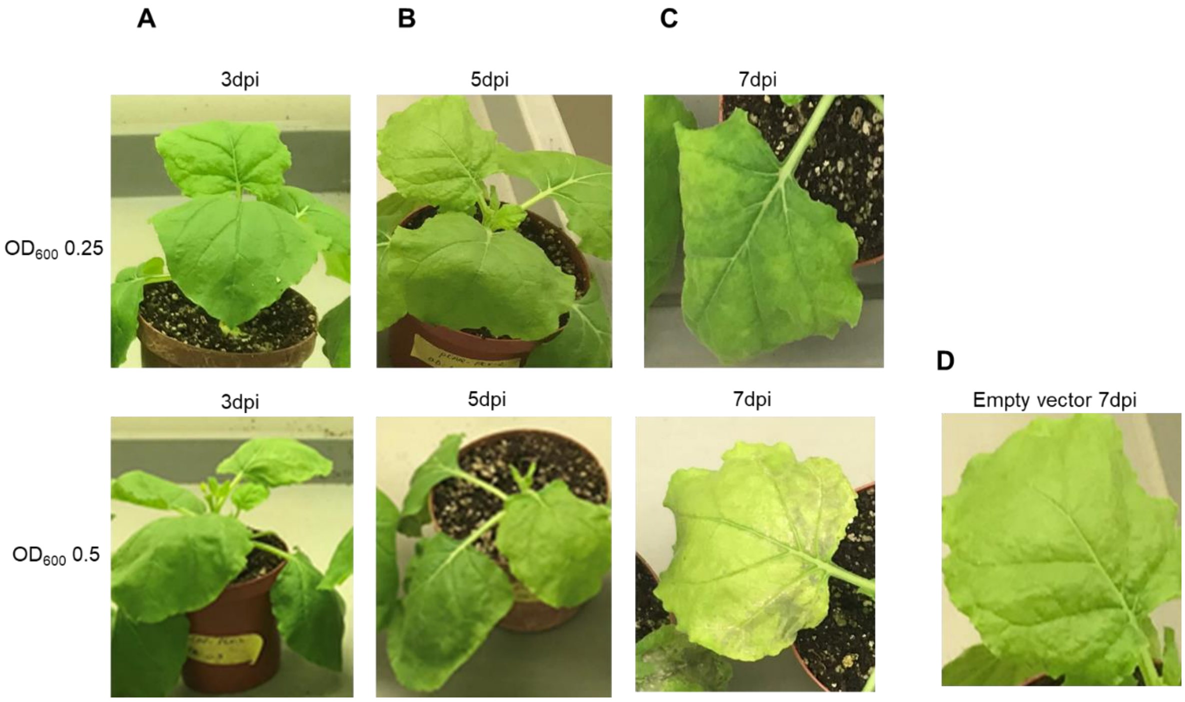

Figure 2.8 Phenotype of plant leaves co-infiltrated with a silencing suppressor. A-C) leaves of pCBP-PCV-2-CP-SP co-infiltrated with a silencing suppressor at OD_{600} of 0.25 and 0.5 examined at 3, 5 and 7 dpi, respectively. D) empty vector representative.

Biomass was collected for analysis at 3 and 5 dpi of plants infiltrated at both OD 0.25 and 0.5, with or without the presence of the NSs silencing suppressor. CP expression was analysed on western blots probed with either rabbit-raised PCV-2 antisera or mouse PCV-2 antisera. Non-specific binding of the antibodies to host cell proteins in the crude extracts were observed on the western blots, which made it difficult to reliably detect the expressed CP protein in crude extract obtained from leaf discs. Pre-absorption of the rabbit PCV-2 antisera with crude plant extract was also carried out prior to detection of CP on western blots, however no significant difference was observed (results not shown).

Therefore, medium scale expression was carried out where more plants were vacuum infiltrated, and protein was purified to remove contaminating plant proteins. Plants were infiltrated with at ODs of 0.25 and 0.5 in the presence or absence of the NSs silencing suppressor and harvested at 3 and 5 dpi. PCV-2 CP was extracted in DB_{150}

buffer and purified on discontinuous sucrose gradients, the protein was concentrated in the pellet and resuspended in 1× PBS (pH 7.4) and subsequently analysed on Coomassie-stained gels (Figure 2.9 A) and western blots (Figure 2.9 B). The empty vector negative control was purified and analysed using the same methods. On both the Coomassie-stained gels and western blots probed with rabbit-raised PCV-2 antisera successful expression of the CP was confirmed with the detection of a band at approximately 27 kDa (blue arrow). Based on the intensity of the bands detected, the highest overall protein expression was observed at 3 dpi at both cell densities tested. Infiltration at a cell density of 0.5 in the presence of the silencing suppressor resulted in higher CP accumulation at 3 and 5 dpi, compared to infiltration at an OD of 0.25 as evidenced on the Coomassie-stained gel (Figure 2.9 A). The absence of the silencing suppressor negatively impacted both the health of the biomass (Figure 2.7) as well as protein expression levels (Figure 2.9). No bands were observed in the negative control (empty vector). The experiment was repeated two times to validate the results obtained.

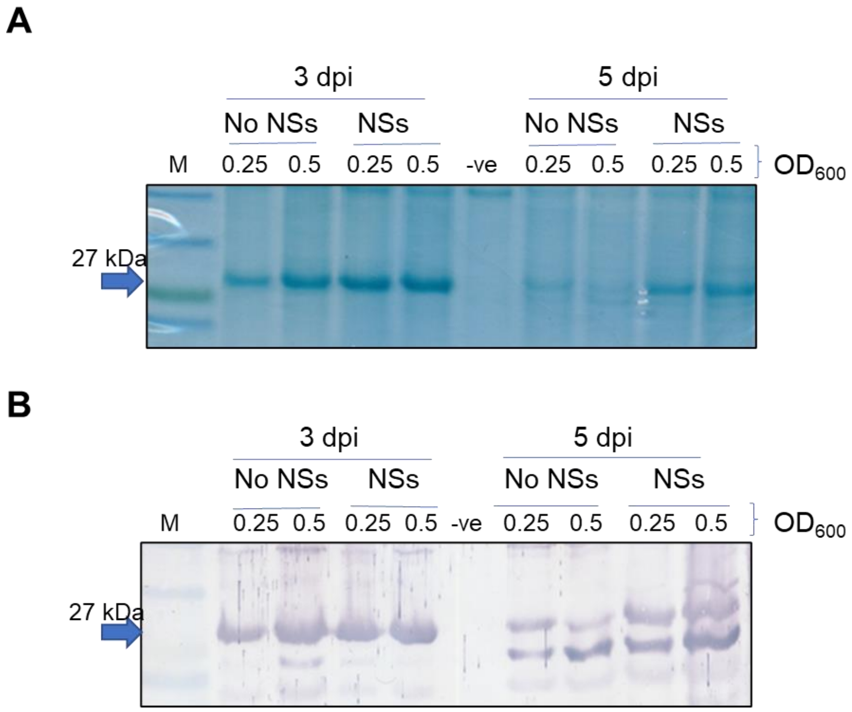

Figure 2.9 Optimization of plant-produced PCV-2 CP. A) Coomasie-stained SDS-PAGE gel of PCV-2 CP; B) Western blot analysis of PCV-2 CP probed with rabbit PCV-2 antisera (1:1000 dilution) and anti-rabbit IgG alkaline phosphatase-conjugated secondary antibody (1:5000 dilution). Samples were analysed at OD_{600} 0.25 and 0.5,

with or without a silencing suppressor (NSs or No NSs), biomass was harvested at 3 and 5 dpi. Labels: M: PageRuler ^{TM} pre-stained protein standard in kilodaltons (kDa), Blue arrow: PCV-2 CP (~27 kDa), -ve: Negative control (pCBP-2 empty vector).

2.3.3 Large scale purification of pEAQ-*HT* and pCBP-2 – produced PCV-2 CP

PCV-2 CP was previously successfully expressed by Gunter *et al.* (2019) with the pEAQ-*HT* plant expression vector and a reasonable amount of recombinant protein was obtained. The aim of the present study was to determine if expression levels could be further improved upon by using the new plant expression vector, pCBP-2.

Based on the results obtained from the medium-scale expression studies, large scale expression and purification of PCV-2 CP was carried out by infiltrating plants with pCBP-PCV-2-CP-SP at an OD_{600} 0.5 with the silencing suppressor as described in section 1.3.2. Biomass was harvested at 3 dpi. At the same time, plants were also infiltrated with pEAQ-PCV-2 CP at an OD_{600} of 1.0 and harvested at 4 dpi as per previous optimization by Gunter *et al.* (2019). Biomass infiltrated with pCBP-2-PCV-2-CP-SP and pEAQ-PCV-2 CP was purified using the same method to ultimately compare which vector resulted in the highest expression levels of PCV-2 CP. Figure 2.10 shows a Coomassie-stained gel and a western blot probed with rabbit-raised PCV-2 antisera. Based on the detection of bands at approximately 27 kDa (blue arrow), the pCBP-PCV-2-CP-SP construct that targets protein expression to the ER yielded the best expression levels compared to pEAQ-PCV-2-CP based on the band intensity observed. The band size of pCBP-PCV-2-CP-SP appears to be slightly higher which is possibly due to the presence of a signal peptide on the pCBP-2 vector which might have added extra amino acids to the N-terminal of the PCV-2 CP. As expected, no bands were observed in the empty vector negative control.

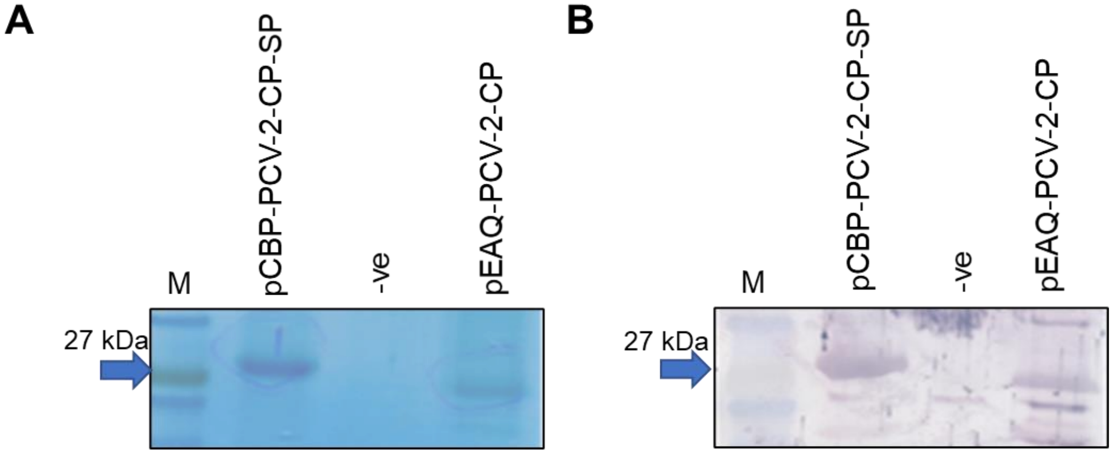

Figure 2.10 Comparison of pCBP-2 and pEAQ-HT expression of plant-produced PCV-2 CP. A- Coomasie Blue stained SDS-PAGE gel of PCV-2 CP, B- Western blot analysis of PCV-2 CP probed using rabbit PCV-2 antisera (1:1000 dilution) and anti-rabbit IgG alkaline phosphatase-conjugated secondary antibody (1:5000 dilution), M: pre-stained protein standard (kDa), -ve: Negative control (pCBP-2 empty vector).

2.3.4 Quantification of PCV-2 CP

The yields of the expressed PCV-2 CP produced in plants with the two different plant expression vectors were quantified using gel densitometry. BSA standard curves were generated from which the unknown protein concentrations were calculated (Figure 2.11). Resuspended pellets from the sucrose gradients were analysed on a Coomasie-stained gel together with the 58 kDa BSA reference protein prepared at a two-fold dilution. For both pCBP-2 and pEAQ-expressed PCV-2 CP bands were detected at the expected size of approximately 27 kDa (Figure 2.11 A and D). A total CP yield (per kg fresh weight [FW]) at least 18.15 mg/kg FW and 8.39 mg/kg FW were obtained for pCBP-PCV-2-CP-SP and pEAQ-PCV-2 CP, respectively.

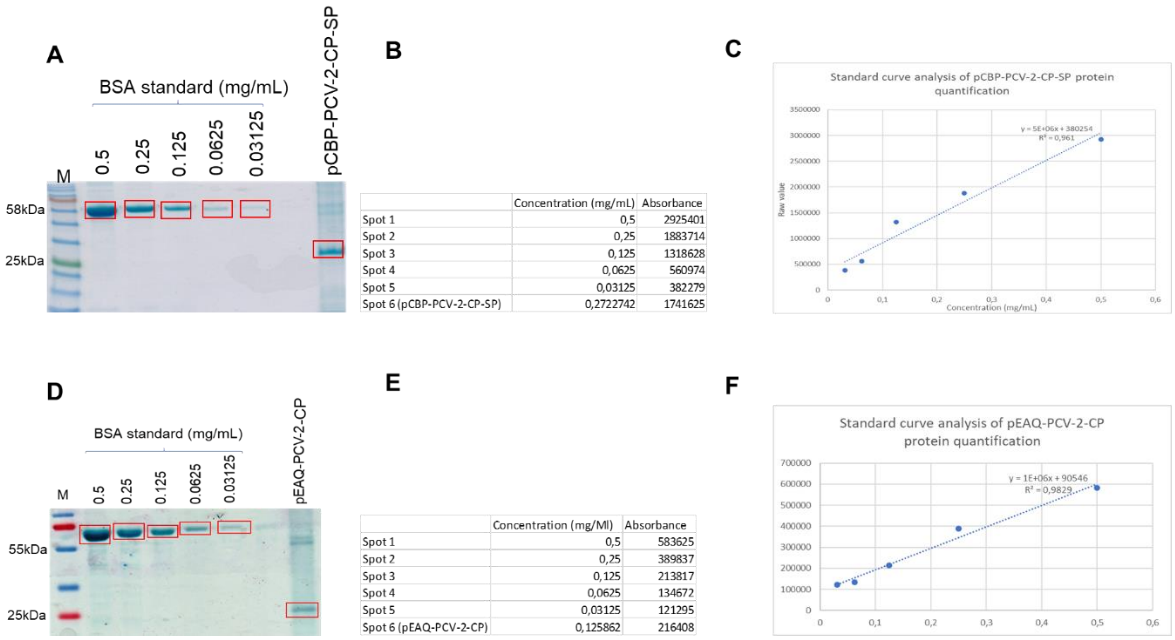

	Concentration (mg/mL)	Absorbance
Spot 1	0,5	2925401
Spot 2	0,25	1883714
Spot 3	0,125	1318628
Spot 4	0,0625	560974
Spot 5	0,03125	382279
Spot 6 (pCBP-PCV-2-CP-SP)	0,2722742	1741625

	Concentration (mg/Ml)	Absorbance
Spot 1	0,5	583625
Spot 2	0,25	389837
Spot 3	0,125	213817
Spot 4	0,0625	134672
Spot 5	0,03125	121295
Spot 6 (pEAQ-PCV-2-CP)	0,125862	216408

Figure 2.11 Analysis of acrylamide gel stained with Coomassie Brilliant Blue by densitometry. The quantification of plant expressed pCBP-PCV-2-CP-SP and pEAQ-PCV-2-CP (A and D, respectively) assessed through densitometry evaluation of the appropriate band. The marker used for A is the Colour Prestained Protein Standard Ladder while for B is the PageRuler^{TM} Plus Prestained Protein Ladder. Each BSA standard concentration is indicated above the lane (A & D). The determined absorbance (signal) is shown in the table for each standard and sample (B & E). C and F shows standard curves of BSA protein concentration. The equations were used for quantification of recombinant plant produced pCBP-PCV-2-CP-SP and pEAQ-PCV-2 CP respectively.

2.4 Discussion

The objective of this study was to assess plant-based transient expression as a tool for producing PCV-2 CP that is suitable for making an affordable PCV-2 diagnostic reagent, especially useful in developing countries. Thus far, only one study has focused on the development of PCV-2 VLPs in plants using pEAQ-*HT* as a plant expression vector (Gunter *et al.*, 2019). This has led to the rise of this study, which explored the expression of PCV-2 CP using the pCBP-2 plant expression vector.

The PCV-2 viral CP has been shown to be the most important part of the PCV-2 genome because of its immunogenic properties and capabilities to serve as a reagent in diagnostics. Recombinant protein production systems such as yeast, bacterial cells and insect cells have demonstrated promise for the development of PCV-2 CP capable for use as a vaccine or in diagnostics (Xi *et al.*, 2016, Wu *et al.*, 2012, Nainys *et al.*, 2014, Zhang *et al.*, 2020b). In recent years plants have been utilised to produce a wide range of important proteins used to manage diseases such as influenza, cervical cancer, rabies, Ebola, HIV, African horse sickness, African swine fever etc. (Tsekoa *et al.*, 2020). PCV-2 CP has previously been successfully expressed in *N. benthamiana* with promising results, this was the initial step towards the aim of producing a cheaper PCV-2 vaccine (Gunter *et al.*, 2019).

In the current study, expression of recombinant PCV-2 CP in *N. benthamiana* was optimized by testing the new pCBP-2 plant expression vector. To this end we evaluated the optimal *Agrobacterium* cell concentration for infiltration, the ideal day of leaf harvesting as well as the effect of co-expression with or without the NSs silencing suppressor on CP expression levels. The pCBP-2-expressed protein was partially purified to enable detection on Coomasie-stained gels and Western blots (Figure 2.9).

In previous studies it has been shown that the cell density used for infiltration can influence protein expression levels (Wroblewski *et al.*, 2005), therefore in this study, plants were infiltrated with the recombinant constructs at an OD_{600} of 0.25 and 0.5 to determine at which cell density the highest protein expression occurred. Protein analysis at OD_{600} of 0.5 had a better yield compared to OD_{600} of 0.25 at 3 dpi while at 5 dpi OD_{600} of 0.25 had a better yield (Figure 2.9). These results were inconclusive since severe necrosis was observed across the two ODs (Figure 2.7) which has potentially affected the expression. For this reason, the PCV-2 CP was co-expressed with a silencing suppressor to potentially improve the expression.

RNA silencing is known in plants as a post-transcriptional gene silencing (PTGS) system which acts as a defence against viral infection (Waterhouse *et al.*, 2001b, Kant and Dasgupta, 2019, Takeda *et al.*, 2002). The mechanism for RNA silencing recognizes 'abnormal' RNAs, derived from certain double-stranded RNAs (dsRNAs), transgenes and intermediate replicants of viral RNAs, and breaks down homologous RNA in the cytoplasm. RNA silencing begins when 21-25 nucleotide small interfering RNAs (siRNAs) which corresponds to the target RNA are produced. Once the PTGS induction has begun at one location, the systemic silencing stimuli spread and eventually triggers PTGS in the rest of the tissues. (Waterhouse *et al.*, 2001a). The silencing suppressor is considered to interfere with dsRNA-generating steps and thus inhibit silencing. The silencing suppressor used in this study was NSs which is derived from TSWV (Margaria *et al.*, 2015, Takeda *et al.*, 2002). This silencing suppressor has been used widely and shown to improve protein expression since it increases viral siRNAs (Hedil *et al.*, 2015, Huddy *et al.*, 2018).

CP was successfully expressed with the pCBP-2 vector, with the highest protein accumulation levels obtained when plants were co-infiltrated with the pBIN-NSs silencing suppressor construct at an OD_{600} of 0.5 and harvested at 3 dpi. Co-expression with the silencing suppressor protein resulted in significantly increased accumulation of PCV-2 CP (Figure 2.9), with a significant improvement of the health of the plant (Figure 2.8). Protein expression levels observed after co-expression with NSs, resembled findings shown by Gunter *et al.* (2019) in which plants infiltrated with the pEAQ-*HT* vector, which contains the P19 silencing suppressor on the same T-DNA as the gene of interest (Sainsbury *et al.*, 2009), resulted in very little development of chlorosis and necrosis (Gunter, 2017).

As the overall aim of this study was to produce a plant-made diagnostic reagent for PCV-2 based on the CP, we had to determine which plant expression vector would give the highest yields of PCV-2 CP. In order to achieve this, large scale expression studies were carried out with the recombinant pCBP-2 and pEAQ-*HT* constructs. Biomass was partially purified on discontinuous sucrose gradients and overall protein yield was determined with gel densitometry (Figure 2.11). A 2-fold higher yield of CP was obtained with the pCBP vector (~18 mg/kg) compared to yields obtained from pEAQ-*HT* (~8 mg/kg). The difference in protein levels achieved by the two vectors could be attributed to localisation within the plant cell compartment. The increase in recombinant protein yield is highly improved by targeting proteins to specific cellular compartments for isolation and post-translational modifications (Maclean *et al.*, 2007). The pCBP-2 vector directs protein to the ER while the pEAQ-*HT* vector targets protein expression in the cytoplasm (Sainsbury *et al.*, 2009). Based on the results obtained in this study, the amount of protein expressed using the pCBP-2 vector is ~two-fold higher than when expressed with the pEAQ-*HT* vector and it might be because in the cytoplasm the protein is more exposed to proteases which can degrade the protein, whereas in the ER the protein is protected by membranes (Schwarz and Blower, 2016). The presence of the signal peptide on pCBP-2 may result in continuous interaction with ER chaperones to promote proper protein folding (Benchabane *et al.*, 2008), a low level of proteolytic activity (Vitale and Pedrazzini, 2005) or a stabilizing effect of glycosylation in the ER compartment (Floss *et al.*, 2009). Similar results have been described earlier for other recombinant proteins expressed in *N. benthamiana*. Miletic *et al.* (2016) obtained low levels of the tailspike protein Gp9 accumulation when targeted to other compartments compared to the ER. Another study has demonstrated higher subcellular accumulation of polygalacturonase when targeted to the ER in comparison to other compartments (Pereira *et al.*, 2014). Notably, since the ER is the most suitable organelle for post-translational modifications, ER targeting has usually been associated with increased yields of recombinant proteins in plants (Tschofen *et al.*, 2016, Conley *et al.*, 2009a).

It has also been observed (Figure 2.10) that the size of the ER-targeted PCV-2 CP is slightly higher than the cytoplasm-targeted PCV-2 CP which is likely due to the additional sequence of the leader peptide derived from the murine heavy chain of mAb24 (LPH signal peptide) which is present in the pCBP-2 expression vector. The signal peptide may add extra amino acids sequences to the N-terminal of the PCV-2 CP hence an increase in the size may occur. Similar results were obtained in a study by Pêra *et al.* (2015) where the VP6 protein of Rotavirus was targeted to various compartments such as the cytoplasm, chloroplast, ER and apoplast and a higher molecular weight band was observed for VP6 protein targeted to the ER.

Even though the CP yield obtained using the pEAQ-*HT* vector in this study was lower than that of the pCBP-2 vector, we showed improved protein yields compared to a previous study by (Gunter *et al.*, 2019) which utilized the same vector where only ~2 mg/kg FW CP was produced (Gunter *et al.*, 2019). Although the infiltration conditions and the purification conditions were exactly the same as that of the previous study, this variation could be attributed to factors such as plant handling during infiltration, time of harvest and purification, storage of the protein as well as the growth conditions of plants (Fahad *et al.*, 2015).

In conclusion, the CP encoded by ORF2 of the PCV-2 genome was successfully expressed in *N. benthamiana* using the novel pCBP-2 plant expression vector. Here we found that the pCBP-2 vector can be utilized to achieve high yields of PCV-2 CP compared to the previously used pEAQ-*HT* vector. The study serves as a major initial step towards the aim of transiently producing the PCV-2 CP in *N. benthamiana* with improved yield, which may potentially be useful as an immunogenic protein of biomedical and industrial importance. To the best of our knowledge this is the first study to report on the expression of PCV-2 CP with the pCBP-2 plant expression.

3 Chapter 3: Optimization of PCV-2 VLPs production and the use of VLPs in diagnostic assays

3.1 Introduction

The ability to predict, monitor, and manage the spread of porcine circoviruses is not only vitally important for veterinary observations but also plays a significant role in the surveillance of human diseases resultant of zoonotic viruses.

Since clinical and epidemiological data is usually limited during the emergence of diseases caused by viruses, it is extremely important to be able to track the spread of the culpable virus and to record the manifestation and clinical symptoms associated with that specific disease. Early diagnosis of the pathogen responsible for the disease is the most important step in managing diseases of any sort as this allows proper implementation of appropriate preventative measures in unaffected animals, and limitation of further spreading thereof. In addition, proper diagnostic procedures of viral diseases are essential to monitor disease progression. In general, diagnosis of viral diseases are hindered by the lack of reagents for identifying the viral antigen in suspected cases for use serology-based studies (Boivin *et al.*, 2016, Burbelo *et al.*, 2019). This is the same with PCV-2, which is one of the major burdens within the pig industry, especially in developing countries. The lack of diagnostic assays can be resolved by developing quick yet effective diagnostic techniques that do not necessitate specialized expertise, equipment, and facilities in comparison with assays that require viral culture, that is still a pillar of viral diagnosis.

The CP of PCV-2 has been demonstrated to be highly immunogenic in infected hosts which makes it an effective vaccine candidate. Globally, strict PCV-2 vaccination procedures have led to effective control of both the virus and its related diseases in swine (Afghah *et al.*, 2017, Chae, 2016, Wozniak *et al.*, 2019). The PCV-2 CP elicits specific antibody responses in swine, therefore making it an ideal target for PCV-2 serology-based diagnosis (Nawagitgul *et al.*, 2000). The choice of utilising the ORF2 CP and not the ORF1 protein (Rep protein) is based on certain factors such as the ability of the CP to attach itself to host receptor and activation of an immune response (Nawagitgul *et al.*, 2002, Saporiti *et al.*, 2020b, Melanie *et al.*, 2019, Kim *et al.*, 2018).

In the course of PCV-2 infection, antibodies are made against the three proteins (Rep, ORF3 and CP) , but mostly to the abundant CP (Juhan *et al.*, 2010, Peng *et al.*, 2016). The potential to detect antibodies elicited against the CP in the infected host's serum makes it possible to diagnose present or previous infection as well as viral exposure.

Recombinantly expressed CP has the ability to self-assemble into structures referred to as VLPs which are immunogenically and structurally identical to native virions (Bucarey *et al.*, 2009, Fan *et al.*, 2005, Duan *et al.*, 2019, Liu *et al.*, 2012, Gunter *et al.*, 2019, Liu *et al.*, 2020, Chae, 2012). The potential to produce VLP-based vaccines in yeast, insect and bacterial cell-based systems that have the ability to elicit cell mediated and humoral immunity in animals has provided a platform to utilise the same foundation for the development of a highly specific diagnostic tool (Xi *et al.*, 2016, Nainys *et al.*, 2014, Chae, 2012).

There are different methods to diagnose PCV-2 infections in swine herds, these include qPCR, indirect fluorescent antibody tests (IFATs) and ELISAs. Currently there are two commercially available kits used to diagnose and manage PCV-2. The PCV-2 antigen test kit (qPCR) enables the detection and quantification of PCV-2 DNA which provides information about the viral load of the virus depending on the presence/absence of the virus (https://www.biochekbulletin.com/wp-content/uploads/2015/06/MZ-16390-BIOCHEK-Folder-PCV2_V1.0_web.pdf). On the other hand, the PCV-2 antibody test kit (ELISA) detects IgG antibodies in swine sera elicited by all strains of PCV-2. In this ELISA, the plates are coated with inactivated virus which can be bound by antibodies present in sera, the results of the test are quantitative. Furthermore, the test provides important information such as antibody titres after vaccination or infection with field virus, the uniformity of immunity and the optimal vaccination time. Additionally, the test can detect antibodies as soon as 14 days post vaccination/infection (https://www.biochek.com/swine-elisa/porcine-circovirus-type-2-antibody-test-kit/). Although diagnosis based on clinical symptoms manifested is widely used, performing PCV tests among the swine population is an important aspect in diagnosis since asymptomatic infection in swine is widespread (Patterson *et al.*, 2011c). Additionally, proper preventative measures can then be put in place based on the results obtained from testing.

With an increase in viral diseases across the globe, the use of lateral flow devices in diagnostics has been explored over the years since it is a rapid testing method which allows faster decision making. The use of such devices enables early stage diagnosis, observation, and treatment of diseases. In addition, these tests can be used with little training and requires less time to perform (Koczula and Gallotta, 2016, Sigmund *et al.*, 2018, Soh *et al.*, 2020).

To obtain recombinant proteins that is of industrial and biopharmaceutical importance, the purification method that allows efficient processing is of paramount importance. Several methods for the purification of PCV-2 VLPs have been studied to ensure that the protein is efficiently separated from other cellular material in the extract and that VLPs are free of contaminants. Fully assembled PCV-2 VLPs of high purity were obtained when using ion-exchange chromatography (Xi *et al.*, 2016, Masuda *et al.*, 2018, Zaveckas *et al.*, 2015, Lin *et al.*, 2019), or affinity tag columns accompanied by size-exclusion chromatography (Wu *et al.*, 2016, Trundova and Celer, 2007, Yang *et al.*, 2019) for purification. Although these methods are effective for purifying the protein of interest, they require the addition of affinity tags to the protein and chromatography columns which adds additional costs for overall protein production and purification. Moreover, production becomes more complex since the affinity tags have to be removed after protein purification since its presence might present a disadvantage for the use of the protein, especially in clinical application (Arnau *et al.*, 2006, Mahmoodi *et al.*, 2019). PCV-2 VLPs produced in different expression systems have been purified successfully over the years using a simple separation technique known as density gradient ultracentrifugation. This method is a preparative technique that is not scalable for commercial production (Khayat *et al.*, 2019, Nainys *et al.*, 2014, De Almeida *et al.*, 2017, Wu *et al.*, 2012, Gunter *et al.*, 2019).

Several studies have investigated the potential to develop IgG PCV-2 VLP-based ELISAs to detect PCV-2 IgG specific antibodies in swine sera. However, these studies used costly expression systems such as yeast, insects and *E. coli* to produce VLPs (Blanchard *et al.*, 2003b, Nainys *et al.*, 2014, Ilha *et al.*, 2020). For this reason, there is a need to explore a cheaper and simpler expression system to produce VLPs that can potentially be used as a coating reagent in serological assays, such as ELISAs, which will in turn lower the production costs and ultimately the costs of the final testing kit. Recently, a Covid-19 diagnostic reagent was successfully expressed in plants for use in RT-PCR, indicating the relevancy of plant-based expression system (Chan *et al.*, 2020). There is also the potential to use these VLPs for the development of lateral flow devices which may help with faster diagnosis and better management of the disease. These lateral flow devices can be used in real time by farmers as it does not require expertise to read the results.

In the work described in this chapter, the production of plant-expressed PCV-2 VLPs was optimised. This involved the cloning of the PCV-2 *cp* gene into the pCBP-2 vector (Chapter 2), lacking an ER-targeting signal peptide. Methods based on density gradient centrifugation and Ion exchange chromatography (IEC) were also optimised for the purification of VLPs from plants. Purification of high yields of PCV-2 VLPs from *N. benthamiana* is a crucial first step towards producing a plant-made coating reagent for the development of an ELISA-based diagnostic assay. Furthermore, *E. coli* expressed VLPs were also produced and both the transiently expressed VLPs and *E. coli* made VLPs were used as a coating reagent in the development of a lateral flow diagnostic immunoassay, as a proof of concept.

3.2 Material and methods

3.2.1 Cloning

The purpose of this chapter was to optimize the production of PCV-2 VLPs. Several attempts were made to produce VLPs using the previous construct (pCBP-PCV-2-CP-SP) (Chapter 2), with no success. It was thought that the ER signal peptide on the pCBP-2 vector might be hindering the formation of VLPs, this led to the design and cloning of a new construct without the ER signal peptide. New forward (2019FP) and reverse (2019RP) primers were designed to add the *Bsp*HI site to the 5' end of the *cp* gene and *Xho*I to the 3' end of the gene (Table 3.1, restriction enzyme sites in bold and underlined). The pUC57-PCV-2 plasmid DNA was used as DNA template for PCR amplification of *cp*.

Table 3.1 Primers used for re-cloning

Primer name	5'-3' primer sequence	Length (bp)	Tm (°C)
2019FP	GC**T CAT GA**C CTA CCC CAG GAG GAG GT	26	64
2019RP	CG**C TCG A**GT CAG GGG TTG AGA GGT GGG T	28	67

PCR reactions were carried out as described in Chapter 2, section 2.2.3 with a few modifications. Here, Phusion® High-Fidelity DNA polymerase was used according to the manufacturers protocol. As done for all PCRs, a negative control that contained no DNA template was used. PCR products were separated on 1% agarose gels, with O'GeneRuler™ 1kb DNA ladder (Thermo Fisher Scientific) as size marker.

After adding the restriction enzyme sites using PCR, the PCV-2 *cp* PCR fragment was gel purified using the QIAquick® Gel Extraction Kit (Qiagen, USA) as instructed by the manufacturer before digesting it using *Bsp*HI and *Xho*I restriction enzymes. The pCBP-2 vector was linearized using *Nco*I and *Xho*I. The restriction sites: *Bsp*HI and *Nco*I have compatible cohesive ends which can be ligated; however, the restriction sites are both destroyed after ligation. The digested *cp* PCR fragment and pCBP backbone was excised from the gels and purified using the above-mentioned gel purification kit. This was followed by overnight ligation, as described in Chapter 2, Section 2.2.4.

After ligation, the ligation mix was transformed into *E. coli* competent cells as described in Chapter 2 (Section 2.2.4). Transformants were screened by PCR using vector specific primers (Chapter 2, Section 2.2.3, Table 2.2) and confirmed using restriction enzyme digestion. The recombinant plasmid was subsequently transformed into GV3101::pMP90RK *A. tumefaciens* electrocompetent cells and positive clones were confirmed as described above.

3.2.2 Infiltration of *N. benthamiana*

N. benthamiana plants were infiltrated with the recombinant pCBP-PCV-2-CP, pEAQ-PCV-2-CP, and the pCBP-2 empty vector constructs. The pCBP-PCV-2-CP and pCBP-2 empty vector were co-infiltrated with pBIN-NSs at an OD_{600} of 0.5 each. Time-trials were carried out where biomass was harvested at 4, 5 and 6 dpi and analysed for VLP formation. The pEAQ-PCV-2-CP construct was infiltrated at an OD_{600} of 1.0 and biomass was harvested at 4 dpi as described by Gunter *et al.* (2019).

3.2.3 Purification of VLPs by ultracentrifugation

VLPs were extracted and purified as described in Chapter 2. Briefly, after the plant extract was clarified with slow speed centrifugation of 8000 ×g, the supernatant was loaded onto discontinuous 65% and 45% sucrose gradients which were subjected to ultracentrifugation for 4 hours at 120 000 × *g* at 4 °C. Putative VLPs were concentrated in the pellets which were resuspended in 1× PBS (pH 7.4) for further analysis.

The resuspended pellets obtained after sucrose density gradient centrifugation were further purified on caesium chloride (CsCl) gradients. To this end 4.5, 5, 5.5 and 10 g of CsCl were dissolved in 10 ml DB_{150} buffer lacking arginine (Nainys *et al.*, 2014). Five hundred microlitres of each of the 4 CsCl dilutions were under layered in Thinwall Ultra-Clear™ ultracentrifuge tubes (Beckman) to prepare the step gradients. Resuspended pellets were layered onto the CsCl gradients and gradients were centrifuged at 4 °C for 16 hours at 180 000 × *g* using a Beckman SW55Ti rotor. Five hundred microlitre fractions were collected from the bottom of the tubes after ultracentrifugation. CsCl was removed from the samples by dialysing the samples at 4 °C overnight in 1× PBS (pH 7.4) with stirring.

3.2.4 Transmission electron microscopy (TEM) analysis

Transmission electron microscopy (TEM) analysis was carried out to assess if the expressed CP had assembled into VLPs. Sucrose purified pellets of the construct with the signal peptide (pCBP-PCV-2-CP-SP) as described in Chapter 2 were also assessed for VLP formation. Briefly, carbon-coated copper grids of a 200-mesh size were glow discharged for 30 seconds at 25 mA using a Model 900 SmartSet Cold Stage controller (Electron Microscopy Sciences). The carbon side of the grids were floated on the samples for 4 minutes to trap samples onto the grids. Grids were washed 4 x with deionized water and negatively stained with 2% w/v uranyl acetate for 30 seconds. Grids were viewed using a FEI Tecnai 20 transmission electron microscope. After the construct with the signal peptide showed no VLP formation, the signal peptide was removed and the new construct (pCBP-PCV-2-CP) lacking the signal peptide was assessed for VLP formation as per the procedure above.

3.2.5 Purification optimisation

To produce VLPs for use in diagnostic assays we set out to optimise the VLP purification method to obtain fully assembled VLPs of high purity that were free of bacterial contamination.

3.2.5.1 Density gradient purification

To improve on the purity and sterility of VLPs, two methods of density gradient ultracentrifugation purification were explored. For the first method, VLPs were extracted in 1× PBS (pH 7.4) and the homogenate incubated at 4 °C for 1 hour. The crude extract was clarified at 8000 × *g* for 20 minutes at 4 °C and the resulting supernatant filtered through 4 layers Miracloth. The clarified crude extract was loaded onto discontinuous sucrose gradients consisting of 20%, 30%, 40% and 50% sucrose steps of 3 ml each. Gradients were centrifuged for 18 hours at 20 000 × *g*, 4 °C using a SW32Ti rotor. After ultracentrifugation, 1 ml fractions were collected from the bottom of the tubes. Fractions were analysed on Coomasie blue-stained gels, western blots, and with TEM. Additionally, 100 µl of each sample was plated out on LB agar media plates without antibiotics to observe any viable microbial growth.

The second density gradient purification method involved extraction of the VLPs in DB_{150} buffer. Briefly, 15 g of fresh biomass was homogenised in 20 ml of DB_{150} buffer and incubated at 4 °C for 1 hour. The crude extract was clarified as described above and loaded onto gradients consisting of 20%, 30%, 40%, 50%, 60% and 68% sucrose steps of 3 ml each in DB_{150} buffer. Ultracentrifugation was performed at 100 000 × *g* for 15 hours at 4 °C using a SW32Ti rotor. Fractions of 1 ml were collected from the bottom of the tubes and analysed on dot blots and plated out on LB agar to screen for contamination.

The fractions confirmed to contain PCV-2 CP with no bacterial contamination were subjected to a further purification step. Here, the PCV-2 CP fractions were pooled and loaded onto 20-50% Optiprep^{TM} (Sigma Aldrich) gradients consisting of 1.5 ml steps each. Optiprep^{TM} is a sterile gradient density medium that is endotoxin free and is normally used to purify and isolate macromolecules. This medium is obtained as a 60% iodixanol stock solution. A 50% Optiprep^{TM} stock solution was prepared by diluting the Optiprep^{TM} in 6x PBS (pH 7.4), this ensures that the final buffer concentration in all the Optiprep™ steps are 1x. Optiprep^{TM} steps of 40%, 30% and 20% were prepared from the 50% stock solution diluted in 1x PBS (pH 7.4). The gradients were centrifuged at 120 000 × *g* for 2 hours using a SW32Ti rotor, 750 µl fractions were collected from the bottom of the tubes for analysis.

3.2.5.2 Ion exchange chromatography (IEC) purification

Biomass was harvested at 6 dpi, weighed, and homogenised in 3 volumes (weight: volume) 1× PBS (pH 7.4). The homogenate was filtered through 2 layers of Miracloth. After filtration, all downstream processing was carried out on ice or at 4 °C. The crude extract was split in two: for the one half the pH was adjusted to pH 4; and for the other half the pH was not adjusted and remained at pH 6.8 (this pH of the crude extract was obtained after the leaf material was homogenised in 1× PBS of pH 7.4). These extracts were centrifuged at 8000 × *g* for 20 minutes at 4 °C. After centrifugation, the supernatant was recovered, and the exact volume was measured.

The clarified extracts were subjected to ammonium sulphate $(NH_4)_2SO_4$ precipitation. The desired amount of $(NH_4)_2SO_4$ required for each percentage saturation was calculated using the online tool at http://www.encorbio.com/protocols/AM-SO4.htm. The pH 4-adjusted sample was treated with 80% $(NH_4)_2SO_4$ while the other sample whose pH was not adjusted was treated successively with 20%, 30%, 40%, 50% and 80% $(NH_4)_2SO_4$. The pH 4- adjusted sample was treated with only 80% $(NH_4)_2SO_4$ because the pH drop would facilitate the removal of most host cell proteins. After each step of adding the $(NH_4)_2SO_4$, centrifugation was carried out at 8000 × *g* for 20 minutes at 4 °C in order to recover the pellet containing precipitated proteins, the supernatant was kept for additional precipitation at a higher percentage $(NH_4)_2SO_4$. $(NH_4)_2SO_4$ was slowly added to the supernatants at 4 °C with constant stirring to avoid protein crash out. Pellets collected after centrifugation were stored at 4 °C for later evaluation. The precipitated pellets were each resuspended in 5 ml 0.05 M Tris buffer (pH 8), and the samples were subsequently dialysed overnight in 0.05 M Tris (pH 8) to remove $(NH_4)_2SO_4$.

The dialysed samples were centrifuged at 3730 × *g* for 20 minutes at 4 °C followed by filter-sterilization of the recovered supernatant through 0.22 µm syringe filters. The pH 4-adjusted sample, and the 30% $(NH_4)_2SO_4$ sample of the non-pH adjusted batch were subjected to IEC using anion exchange columns. The procedure was obtained from (Masuda *et al.*, 2018) with few modifications. Briefly, samples were diluted in 50 ml 0.05 M Tris buffer (pH 8) and the IEC column (Praesto® Jetted Q35, Purorite Life Sciences, UK) was washed with the same buffer to provide an equilibrium environment. Columns of 5 ml (5 ml = 1 column volume) were prepared and equilibrated with 10 column volumes of binding buffer (0.05M Tris, pH 8). After which the sample was loaded onto the columns. The proteins were eluted with ten steps of 5 ml each of binding buffer (0.05 M Tris, pH 8), containing 0.15 M, 0.3 M, 0.45 M, 0.6 M, 0.75 M, 0.9 M, 1.05 M, 1.2 M, 1.35 M and 1,5 M NaCl each. The column was washed with 10 column volumes of 0.1 M sodium hydroxide for cleaning before storing in 20% ethanol. The eluted fractions together with the flow through and washes were analysed on western blots, trapped on grids for EM analysis, and plated on LB plates lacking antibiotics to evaluate for bacterial contamination.

3.2.6 Production of PCV-2 VLPs in *E. coli*

While the optimization of VLP production in plants was underway, PCV-2 VLPs were made in *E. coli* and trialled for their use in lateral flow devices. *E. coli* expression is the most frequently used laboratory system for the production of recombinant proteins because of its relatively low cultivation costs, rapid growth and increased genetic characterization (Chen, 2012).

The PCV-2 *cp* was cloned into the pROEX-HTc vector, transformed into *E. coli* DH5α competent cells and VLP production was optimised by Gunter *et al.* (2019). For large scale expression and purification, 10 ml LB supplemented with 100 µg/ml ampicillin was inoculated with the pPROEX-HTc-PCV-2 construct. The same was done with the empty pROEX-HTc vector which served as a negative control. These constructs were incubated overnight with agitation at 37 °C and transferred to 50 ml LB and incubated as before. The following day, the 50 ml culture was diluted 1:100 and incubated with agitation until the OD_{600} reached 0.5-1.0 after 1 hour of incubation. The bacterial culture was induced with the non-hydrolysable lactose equivalent; isopropyl β-D-thiogalactopyranoside (IPTG) to a final concentration of 0.6 mM. After adding IPTG the culture was incubated for 1 hour before centrifugation at 10 000 × *g* for 10 minutes at 4 °C, the wet pellet was weighed and stored at -80°C until further use.

Partial purification of the PCV-2 CP was carried out according to the inclusion body cell extract preparation protocol of BugBuster™ (Merck, Germany). In short, the wet cell pellet was resuspended in the BugBuster reagent and 25 units/ml Benzonase (Sigma-Aldrich ®, Missouri, USA) was added to the mixture, followed by 20 minutes incubation at room temperature. The cell lysate was centrifuged at 16 000 × *g* for 20 minutes (4 °C) and the pellet was recovered by centrifugation. The pellet was resuspended in BugBuster™ and 200 µg/ml lysozyme (Sigma-Aldrich®) after which the mixture was incubated at room temperature for 5 minutes. Following incubation, 6× volumes of 1:10 diluted BugBuster™ was added to the suspension and vortexed before centrifuging at 16 000 × *g* for 15 minutes at 4 °C. The pellet was washed with 1:10 diluted BugBuster™ a further two times. Following the BugBuster™ washes, the pellet was washed six times with 1x PBS (pH 7.4) before resuspending the final pellet in endotoxin-free PBS (pH 7.4, Sigma Aldrich) and storing it at -20 °C. The final pellet was analysed on SDS-PAGE gels and TEM analysis was carried out.

3.2.7 Lateral flow development

After quantification of the PCV-2 protein on a SDS-PAGE gel and TEM analysis, the *E.coli* and plant-made PCV-2 VLPs were handed over to Antrum Biotech, a biotechnology company specialising in the development of diagnostic assays, for the development of a lateral flow device (Figure 3.1).

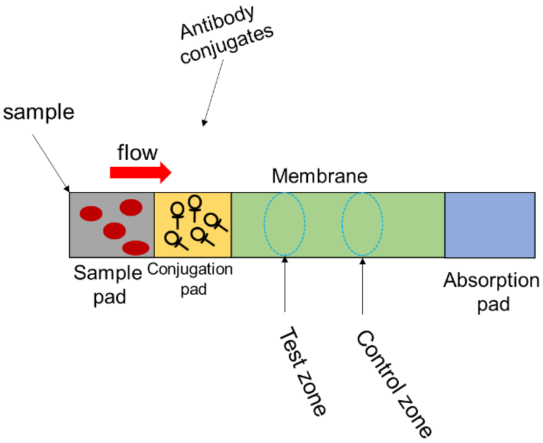

Figure 3.1 A schematic representative of a lateral flow device. Different parts of the device such as the sample pad, conjugation pad, membrane, and absorption pad are indicated. Blood sample is added to the sample pad, flows through to the conjugation pad where it binds to antibodies and migrate along the device. As the sample migrates, the binding reagents on the nitrocellulose membrane will bind to the antibody-antigen complex at the test line. If the target is present, a colour line will appear. The sample then migrates further to the absorption pad in order to absorb excess sample. The control line consists of affinity ligands which indicates if the sample flowed through. Here, a line must always show.

In addition, the company was also supplied with rabbit serum obtained from rabbits that were immunized with *E.coli*-produced PCV-2 VLPs as well as IgG precipitated from the serum with sodium acetate (Gunter, 2017). Antrum Biotech carried out and designed all the methods employed for the lateral flow device development, this included: antibody isolation, concentration, purity, and conjugation. Antibodies were isolated using two methods; Protein A was isolated from sera using the non-gas chromatography (NGC) system. $(NH_4)_2SO_4$ precipitation was done to obtain the IgG precipitated antibody. Briefly, fresh saturated $(NH_4)_2SO_4$ was prepared. One millilitre of sera sample was diluted to 10 mL with deionised water. Ten millilitres of saturated $(NH_4)_2SO_4$ was added to the diluted sera and the mixture shaken for 1 hour at room temperature. After incubation, the homogenate was centrifuged for 5 minutes at 1409 × *g* using a JA-14 rotor. The pellet obtained after centrifugation was resuspended in 1 ml of 1× PBS (pH 7.4) and then dialysed in 1× PBS (pH 7.4) before analysing the sample on 12.5% SDS-PAGE to confirm antibody concentration and purity.

In order to optimize the lateral flow assay, two alternative strategies were developed for detecting antibodies; these were: double mix and triple mix (Figure 3.2). Briefly, for the double mix strategy, the lateral flow strip was coated with *E. coli* expressed antigen and the unconjugated precipitated antibody. At the same time, the anti-rabbit secondary antibody conjugated to biotin and strep-HRP was mixed in microcentrifuge tubes for 5 minutes and the mixture was applied to the lateral flow strip for detection. On the other hand, the triple mix strategy involved coating the strip with *E. coli* expressed VLPs together with the unconjugated precipitated antibody. Separately, equal amounts of unconjugated precipitated antibody plus the anti-rabbit secondary antibody conjugated to biotin and strep-HRP was added to the microcentrifuge tube and incubated for 10 minutes. After incubation the mixture was applied to the coated lateral flow strip for detection.

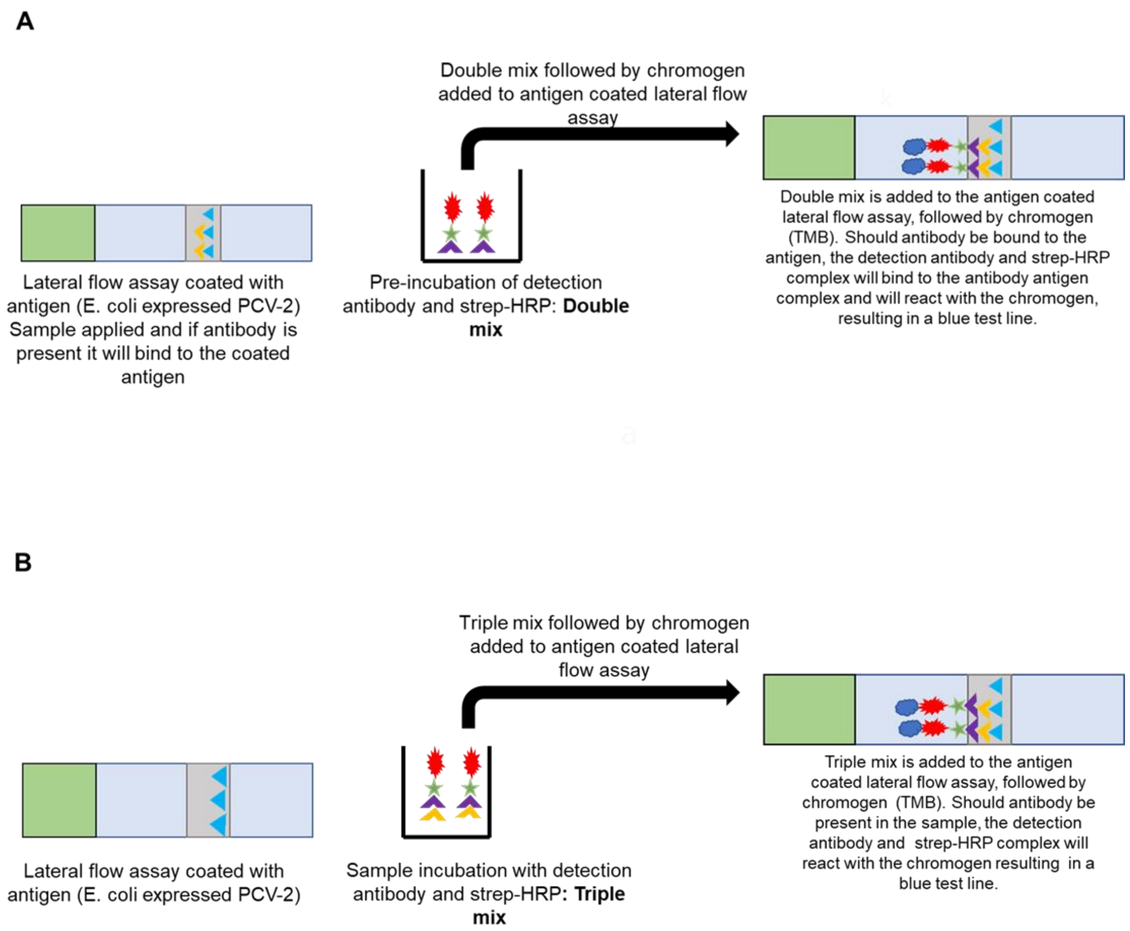

Double mix followed by chromogen added to antigen coated lateral flow assay

Lateral flow assay coated with antigen (E. coli expressed PCV-2) Sample applied and if antibody is present it will bind to the coated antigen

Pre-incubation of detection antibody and strep-HRP: **Double mix**

Double mix is added to the antigen coated lateral flow assay, followed by chromogen (TMB). Should antibody be bound to the antigen, the detection antibody and strep-HRP complex will bind to the antibody antigen complex and will react with the chromogen, resulting in a blue test line.

Triple mix followed by chromogen added to antigen coated lateral flow assay

Lateral flow assay coated with antigen (E. coli expressed PCV-2)

Sample incubation with detection antibody and strep-HRP**: Triple mix**

Triple mix is added to the antigen coated lateral flow assay, followed by chromogen (TMB). Should antibody be present in the sample, the detection antibody and strep-HRP complex will react with the chromogen resulting in a blue test line.

Figure 3.2: Mixing strategies. A) Double mix approach: Application of sample followed by pre-incubation of detection antibodies and strep-HRP. B) Triple mix approach: pre-incubation of detection antibody and strep-HRP with sample.

3.3 Results

3.3.1 Cloning

Primers were designed to add the *BspH*I restriction enzyme site to the 5’ end of PCV-2 *cp* to facilitate sub-cloning into pCBP-2 without the ER targeting signal peptide. PCR amplification yielded the expected band of approximately 714 bp. Restriction enzyme digests were carried out on PCV-2 *cp* with *BspH*I and *Xho*I and pCBP-2 with *Nco*I and *Xho*I. The PCV-2 *cp* plant codon-optimised gene was ligated into the pCBP-2 vector without a signal peptide to yield the pCBP-PCV 2 CP construct and was subsequently transformed into *E. coli*.

The PCV-2 *cp* was successfully cloned into the pCBP-2 vector as colony PCR of *E. coli* transformants showed the presence of an expected band of 1011 bp (Figure 3.3 A, green arrow) after amplification. Colony PCR of the empty vector control resulted in amplification of a fragment of approximately 423 bp (Figure 3.3 A, blue arrow), which was expected since the vector did not contain the gene of interest. Plasmid DNA was isolated from a positive *E. coli* clone and confirmed with DNA sequencing before transforming into *A. tumefaciens* GV3101::pMP90RK. A total of 20 *A. tumefaciens* colonies were screened with colony PCR, all of which were shown to contain the gene of interest (Figure 3.3 B, green arrow). As expected, a band of approximately 423 bp was observed in an empty vector negative control (Figure 3.3 B, blue arrow). For the positive control (pEAQ-PCV-2-CP) in both experiments, a band of approximately 1000 bp was observed as expected, and the no DNA template PCR negative control yielded no bands.

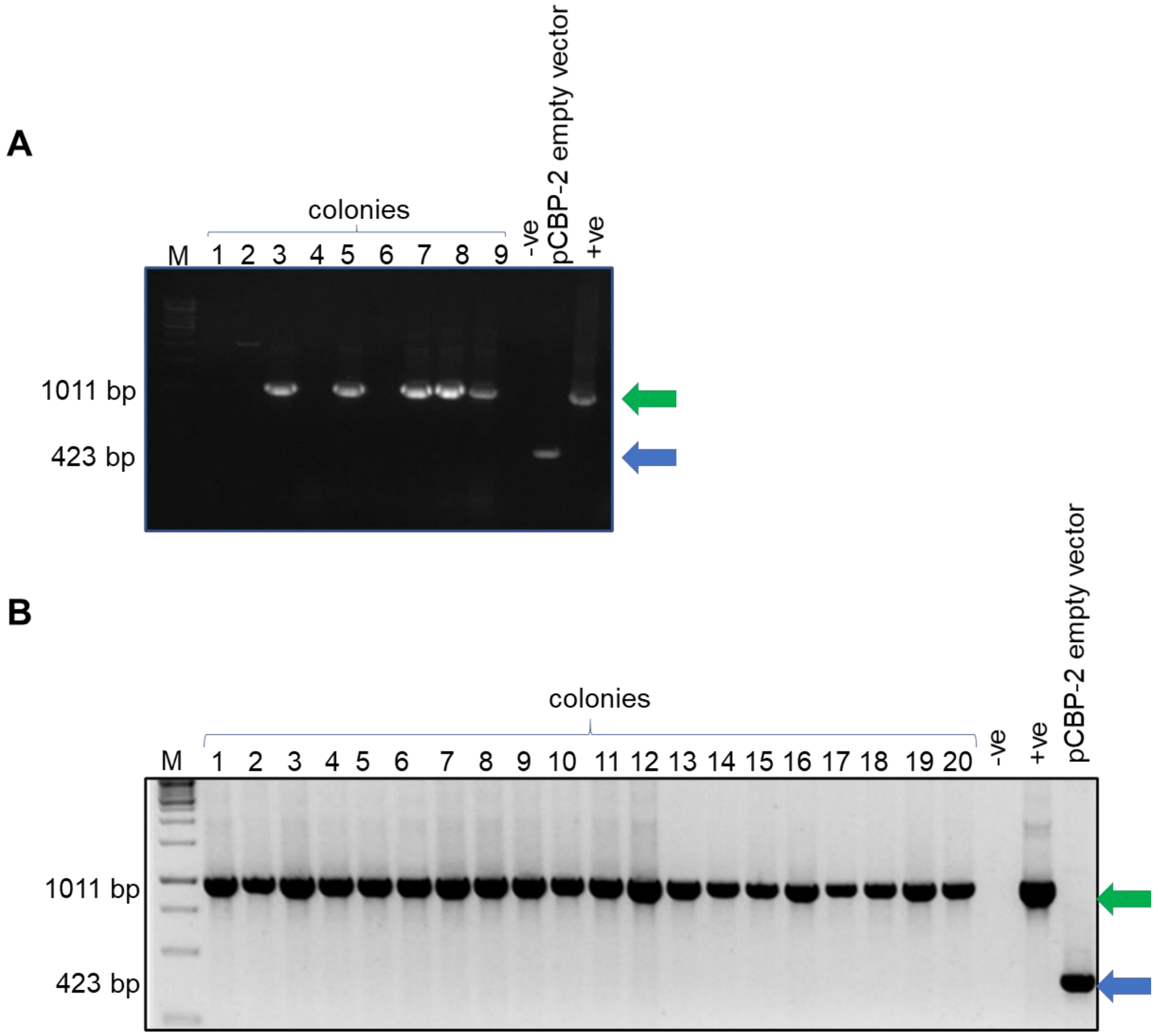

Figure 3.3 Colony PCR confirmation A) *E. coli* transformants. B) *Agrobacterium* transformants. The PCV-2 *cp* positive clones are indicated by the presence of PCR fragments of approximately 1011 bp (green arrow). The +ve control (pEAQ-PCV-2-CP) yielded a band of approximately 1000 bp (green arrow). A band of approximately 423 bp (blue arrow) was observed in the empty vector control and no bands were amplified in the no DNA template PCR negative control. M: represents the DNA molecular weight marker in base pairs.

3.3.2 Large scale purification by ultracentrifugation

Plants infiltrated with pCBP-PCV-2 CP in the presence of the pBIN-NSs silencing suppressor were harvested at 3 dpi, whereas pEAQ-PCV-2 CP-infiltrated plants were harvested at 4 dpi. Biomass was partially purified according to the method described by Gunter *et al.* (2019), Chapter 2. The pellets obtained after ultracentrifugation were resuspended in buffer and analysed on western blots and Coomassie-stained gels (Figure 3.4). From both the western blot (Figure 3.4 A) and the Coomassie-stained gel (Figure 3.4 B) it can be seen that the highest levels of PCV-2 CP (bands of approximately 27 kDa, black arrow) were obtained when expressed with pCBP-PCV-2 CP compared to pEAQ-PCV-2 CP. As expected, no bands were observed in the empty vector negative control.

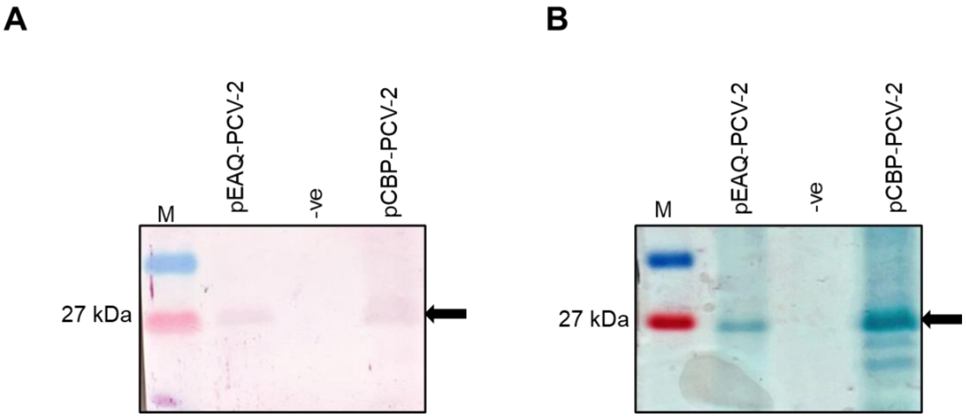

Figure 3.4 Large scale expression and purification of PCV-2 plant-produced CP. A) Western blot analysis of PCV-2 CP probed using rabbit PCV-2 antisera (1:1000 dilution) and anti-rabbit IgG alkaline phosphatase-conjugated secondary antibody (1:5000 dilution). B) Coomassie Blue stained SDS-PAGE gel of PCV-2 CP. M: Protein standard (kDa), -ve: Negative control (pCBP-2 empty vector).

3.3.3 Caesium chloride (CsCl) purification

To further purify PCV-2 VLPs, the pellet obtained after sucrose gradient centrifugation was subjected to CsCl density gradient centrifugation. Gradients were centrifuged until they reached isopycnic equilibrium. Isopycnic equilibrium is reached when the particles become concentrated in the gradient based on their densities. After centrifugation an opaque white band was observed in the CsCl gradient, indicated with a red arrow in Figure 3.5 A. The densities of the gradient fractions collected were determined using a refractometer. The refractometer analysis showed that the densities of the fractions varied from 1.658 g/cm^3 to 1.285 g/cm^3, fractions were further analysed by dot blot. Based on dot blot analysis, the PCV-2 CP was concentrated in fractions 3-5 (Figure 3.5 C), corresponding to a CsCl density of 1.564 g/cm^3-1.450 g/cm^3. No protein was detected on the dot blots of the negative control samples

(Figure 3.5. D). Protein yields were too low for detection on western blots and Coomassie-stained gels (results not shown).

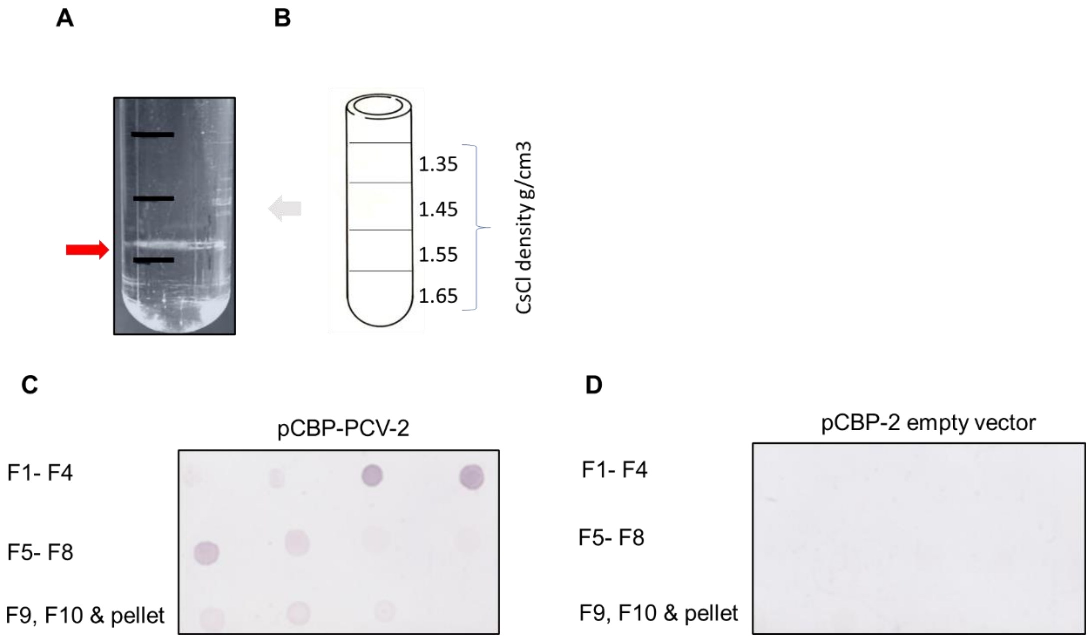

Figure 3.5 PCV-2 CP CsCl density gradient purification. A and B) Photo and schematic representation of CsCl density gradient obtained after ultracentrifugation. C) Dot blot analysis of the pCBP-PCV-2-CP without a signal peptide and (D) the pCBP-2 empty vector negative control. Dot blots were probed with rabbit PCV-2 antisera at a dilution of 1:1000, followed by probing with anti-rabbit IgG alkaline phosphatase-conjugated secondary antibody (1:5000).

3.3.4 TEM analysis of plant-made PCV-2 VLPs

At first, after successful expression and purification (sucrose ultracentrifugation and CsCl density gradient) of PCV-2 CP in *N. benthamiana* using a construct that consist a signal peptide (Chapter 2, section 2.3.3), we evaluated if the CP has successfully assembled into VLPs. However, no VLPs were observed in expression time-trials (3, 4, 6 dpi). A representative is shown (Figure 3.6 A). Our group has previously expressed VLPs using the pEAQ-*HT* vector and it was used as a positive control in the VLPs optimisation in this study. VLPs measuring between 12-20 nm were observed for the positive control at 4 dpi and were consistent with the results obtained in Gunter et al. (2019) (Figure 3.6 B, yellow arrows). As expected, no VLPs were observed in the pCBP-2 empty vector negative control (Figure 3.6 C).

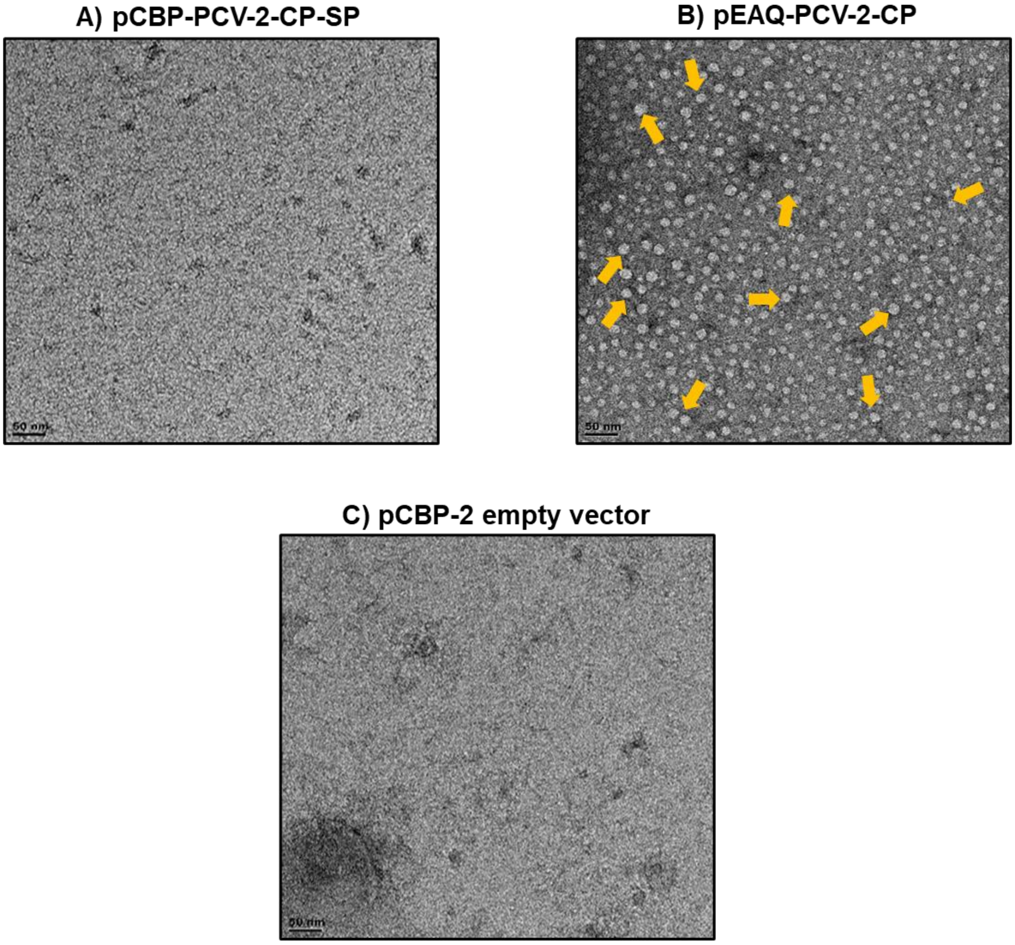

Figure 3.6 TEM analysis of purified plant-produced PCV-2 CP: A) Construct pCBP-PCV-2-CP-SP with an ER signal peptide, B) pEAQ-PCV-2-CP and C) The negative pCBP-2 empty vector. Samples were purified on sucrose discontinuous gradients and visualised at a magnification of 40 000 ×. Scale bars are 50 nm in size. Labels: yellow arrows: VLPs.

Failure of the pCBP-2-expressed CP to assemble into VLPs was potentially due to the presence of the ER targeting signal peptide present on the pCBP-2 vector. It could be that the signal peptide sequence interferes with the normal cycle of production which potentially stop VLP formation. Therefore, PCV-2 *cp* was cloned into pCBP-2 without the signal peptide.

Expression time-trials were carried out with the construct lacking the signal peptide, pCBP-2-PCV-2-CP, protein was purified on sucrose gradients at 4, 5 and 6 dpi and analysed for VLPs. Pellets were diluted 1:10, 1:20 and 1:40 in 1 x PBS, pH 7.4 and TEM analysis showed the presence of fully assembled VLPs ranging from 12-20 nm in diameter at 6 dpi (Figure 3.7 A-C, yellow arrows). Samples of the empty vector negative control were visualised at each dilution and no VLPs or similar structures were observed, a representative electron micrograph is shown in Figure 3.7 D.

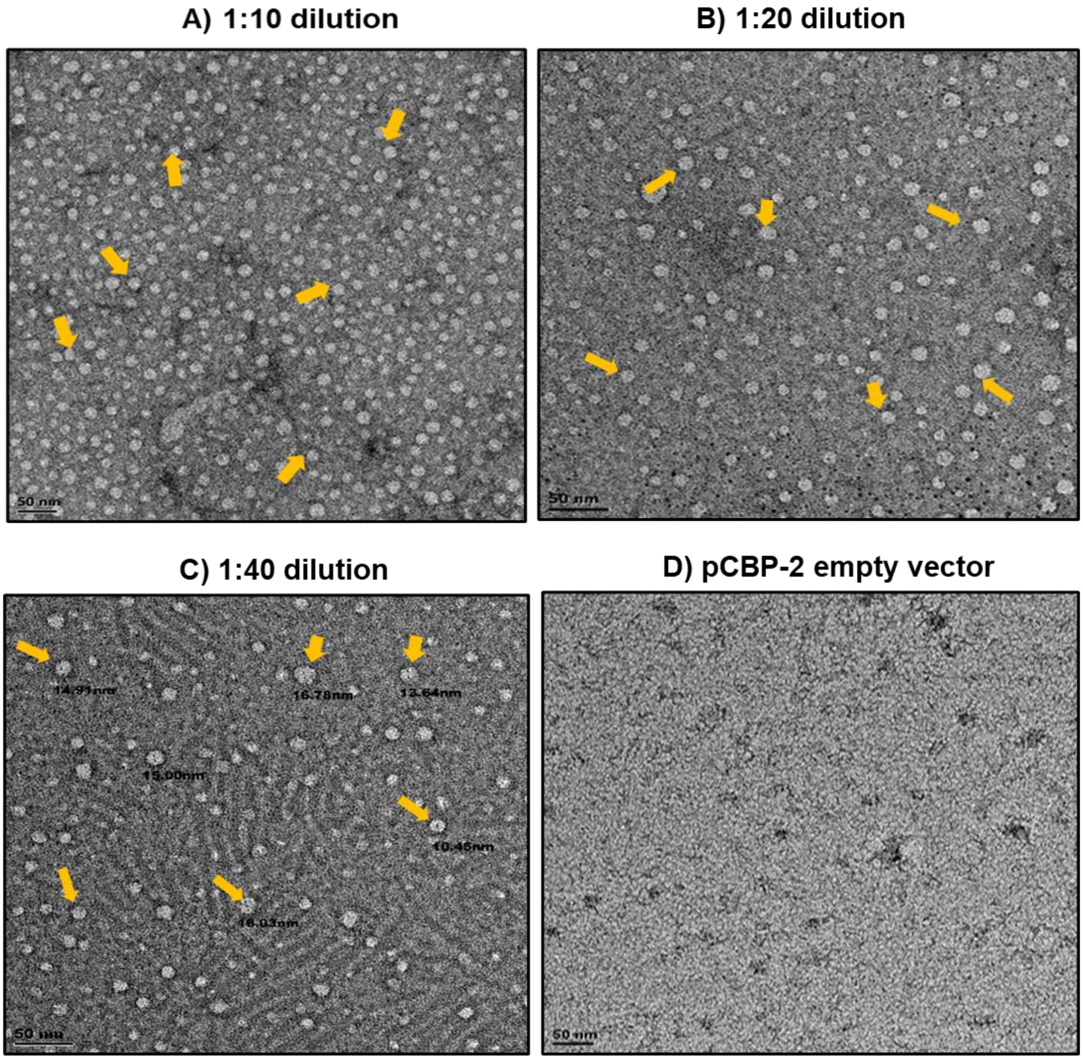
A) 1:10 dilution

B) 1:20 dilution

C) 1:40 dilution

D) pCBP-2 empty vector

Figure 3.7 Electron micrographs of plant-produced PCV-2 VLPs (pCBP-PCV-2-CP): VLPs were purified by discontinuous sucrose gradient centrifugation and resuspended in 1x PBS, pH 7.4 before TEM analysis. Grids were observed at a magnification of 40 000 ×. The negative control (D, empty pCBP-2 vector) was also analysed, and a representative electron micrograph is shown. Scale bars are 50 nm in size. Labels: yellow arrows: VLPs.

3.3.5 Optimisation of VLP purification

3.3.5.1 Density gradient purification

The recombinantly expressed PCV-2 CP was shown to successfully assemble into VLPs, however after plating the partially purified pellets on LB agar lacking antibiotics it was found that the samples were contaminated with bacteria. Therefore, purification of these VLPs was optimised in order to remove bacterial contamination, this is of the utmost importance in order to achieve accurate results in diagnostics.

In an attempt to obtain VLPs free of contamination, the resuspended pellet obtained after sucrose gradient centrifugation was filter sterilized through a 0.22 µm syringe filter. The sterile filtered protein was analysed on a western blot and Coomassie-stained SDS-PAGE gel as well as with TEM. Unfortunately, no VLPs were recovered from the filter as no band was observed on either the western blot or Coomassie-stained gel; furthermore, no VLPs were observed with TEM analysis (results not shown). Another approach was to freeze and thaw the VLPs at -20 °C for a duration of 1 hour for 5 cycles. Samples were collected after each freeze-thaw cycle and analysed. No VLPs were recovered after the 3rd freeze and thaw cycle (results not shown) and samples remained contaminated with bacteria.

Since the pelleted VLPs could not be treated to remove bacterial contaminants, we investigated optimisation of the purification method as we hypothesised that bacteria present in the crude plant extract may have been pelleted with the VLPs during ultracentrifugation. Two methods of density ultracentrifugation were explored where VLPs were not pelleted during centrifugation.

The first purification method involved extracting PCV-2 VLPs in 1x PBS, pH 7.4 and subsequent ultracentrifugation of the homogenate on discontinuous sucrose gradients for 18 hours at 20 000 × *g* at 4°C. Fractions of 1 ml were collected from the gradients and analysed on western blots (results not shown) and Coomassie-stained gels. PCV-2 CP (approximately 27 kDa) was observed across almost all the fractions with the highest concentration of CP observed in fractions 3-5 (Figure 3.8 A & B). The fractions were assessed for bacterial contamination and all fractions, except fraction 3, were free of contamination. Fractions 3–6 were analysed with TEM and showed the presence of fully assembled VLPs, an EM image of fraction 5 is shown as a representative (Figure 3.8 C, green arrows). Based on the Coomasie-stained gels, host cell proteins were co-purified together with the protein. This could explain the reason why protein aggregates were observed under EM analysis.

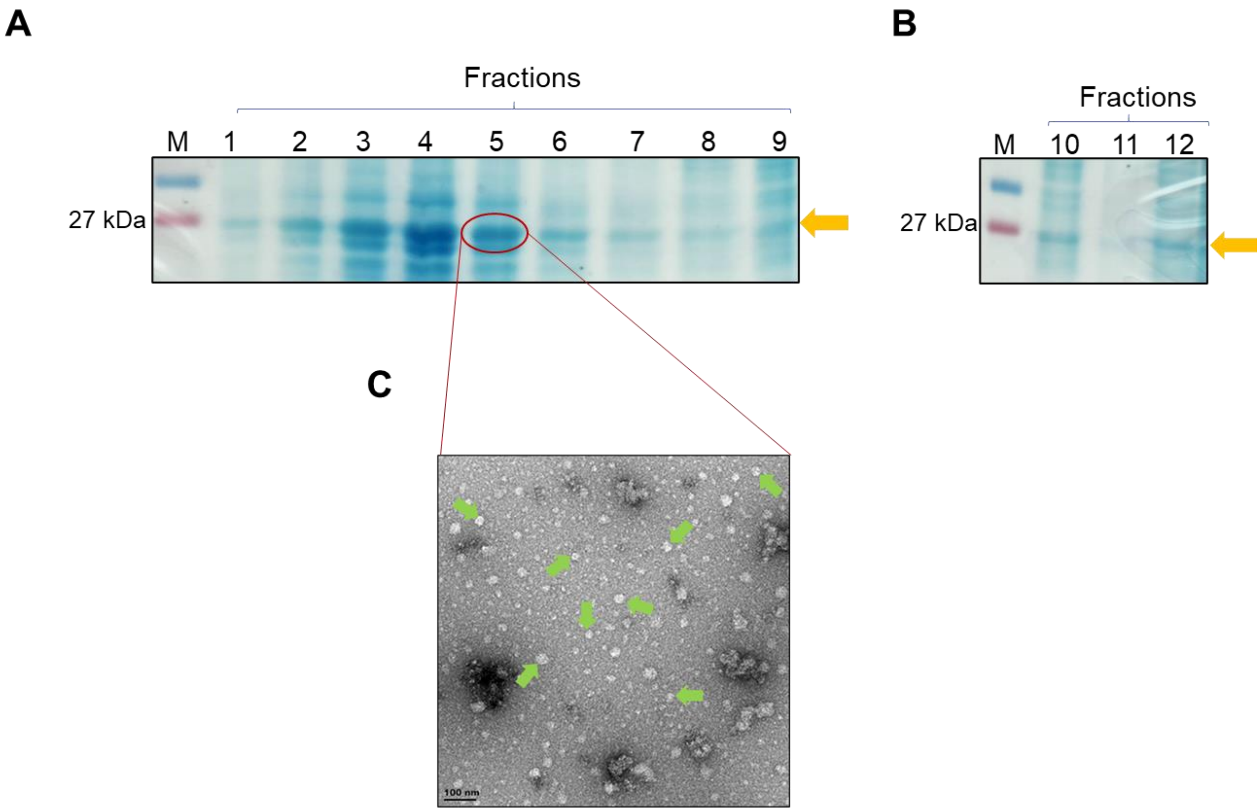

Figure 3.8 Sucrose gradient purification. A and B) Coomassie blue stained gel of the sucrose fractions. A band of 27 kDa was observed across all fractions (F1-F12). C) EM analysis of fraction 5 as a representative for fraction 3-6. VLPs ranging between 12-20 nm in size are indicated with the green arrow. Scale bars: 100 nm. M: Protein molecular ladder in kDa

The second gradient purification method involved extracting PCV-2 VLPs in DB_{150} buffer and centrifugation on discontinuous sucrose gradients (Section 2.2.5.1), followed by further purification on an Optiprep™ gradient. After sucrose gradient ultracentrifugation, the 30-50% sucrose fractions appeared brownish to green (blue arrow), with a green band observed (purple arrow) at or just above the 50% sucrose fraction (Figure 3.9 A and B).

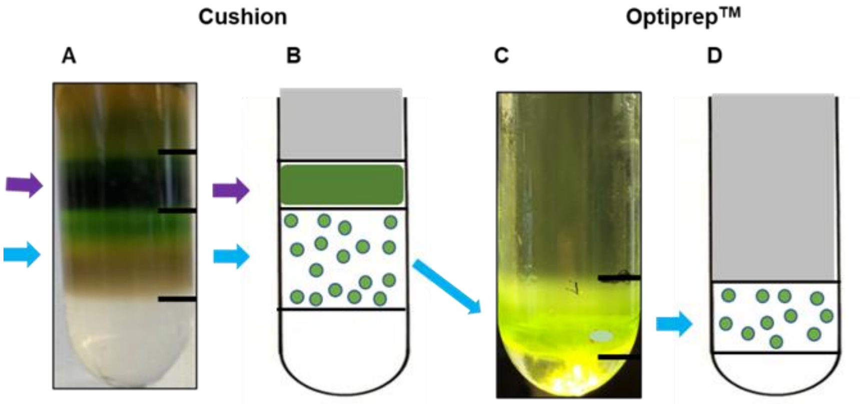

Figure 3.9 Two-step gradient centrifugation for purification of plant-produced PCV-2 VLPs. Photo and schematic representations of; A and B) discontinuous sucrose gradient (20%, 30%, 40%, 50%, 60% and 68%); C and D) discontinuous Optiprep^{TM} gradient (20%, 30%, 40% and 50%). Labels: Blue arrows - VLPs; purple arrows - native plant proteins.

No pellet was observed after ultracentrifugation. Fractions (1 ml) of 20-68% sucrose were collected by bottom puncture and analysed on dot blots. Dot blot analysis of the 18 fractions collected from the sucrose gradient showed the presence of CP in fractions 8-11 (Figure 3.10 A). No protein was detected on dot blots of the negative control empty vector (Figure 3.10 B). For contamination screening only the PCV-2 CP F1 and F4 had bacterial contamination, whereas F2, F3, F6, F9 and F16 of the negative control were shown to have contamination and was excluded from further purification.

Fractions that were free of contamination (F8, F9, F10, F11, F12, F16, F17 and F18) were pooled and diluted in 1× PBS (pH 7.4) before loading onto discontinuous Optiprep^{TM} gradients. After ultracentrifugation, a light green band was observed in the 30%-50% Optiprep^{TM} fractions (Figure 3.9 C and D, blue arrow), this is where assembled PCV-2 VLPs were expected. No pellet was observed after ultracentrifugation. A volume of 750 µl fractions were collected from the bottom of the tubes for analysis. The negative control pCBP-2 empty vector was purified using the same method.

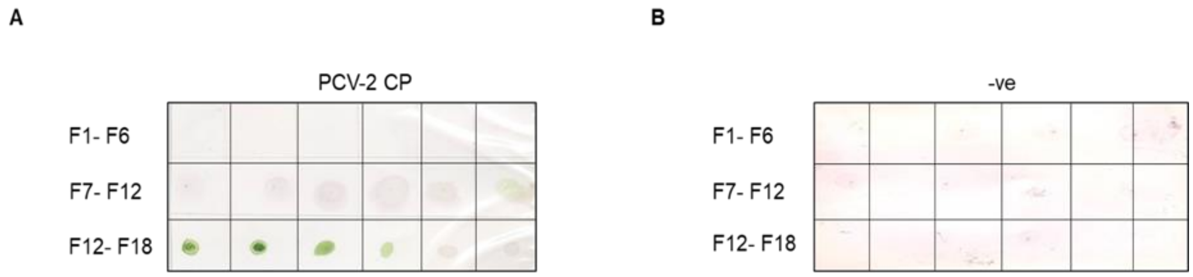

Figure 3.10 Dot blot analysis of sucrose fractions second purification attempt for plant-made PCV-2 VLPs. A: Sucrose fractions for PCV-2 CP and B: negative control pCBP-2 empty vector. The blots were probed with PCV-2 rabbit antisera (1:1000 dilution) and anti-rabbit IgG alkaline phosphatase-conjugated secondary antibody (1:5000).

After Optiprep™ purification the gradients were analysed on western blots. Western blots showed the presence of a band of approximately 27 kDa in fractions 2-6 (Figure 3.11 A, green arrow). The intense band observed just below the expected CP band in Fractions 3-5 could potentially be a cleaved product which can be explained by multiple proteases present in tobacco plants. No band was observed in the negative control empty vector samples (Figure 3.11 B). Fractions 2-5 collected from the Optiprep^{TM} gradients were analysed with TEM and showed the presence of PCV-2 CP aggregates and very few VLPs (results not shown). Fractions 2 and 4 were contaminated while the rest of the fractions were free of contamination. These purification experiments were carried out twice and some fractions were free of contamination while others had contamination, rendering the method non-reproducible. Additionally, too low yields of CP were recovered after gradient purification.

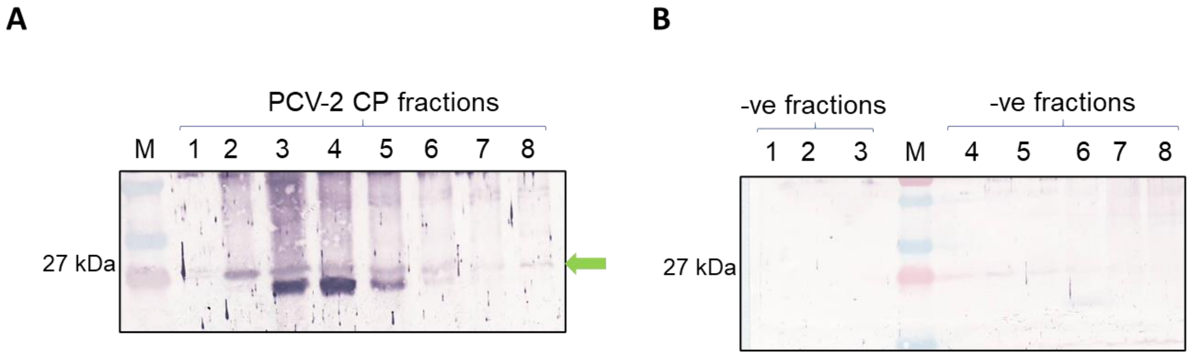

Figure 3.11 Western blot analysis of Optiprep™ fractions second purification attempt for plant-made PCV-2 VLPs. A-B) Western blot (Optiprep^{TM}) for PCV-2 CP and negative control pCBP-2 empty vector, respectively. Purified PCV-2 CP were probed with PCV-2 rabbit antisera (1:1000 dilution) and anti-rabbit IgG alkaline phosphatase-conjugated secondary antibody (1:5000). Labels: M: pre-stained protein standard (kDa); green arrow PCV-2 CP (approximately 27 kDa).

3.3.5.2 Ion exchange chromatography purification (IEC)

Since ultracentrifugation purification showed inconsistent results, purification of PCV VLPs using IEC was explored. After centrifugation and filtration, the crude extract was split in two: for one half the pH was dropped to pH 4; and for the other the pH was not adjusted and remained at pH 6.8 (which was the pH measured after extraction). After centrifugation, the supernatant was recovered, and the exact volume was measured. Both crude extracts were subjected to $(NH_4)_2SO_4$ precipitation. Following $(NH_4)_2SO_4$ precipitation and subsequent IEC purification, western blot analysis of fractions eluted from the column showed that the pH 4 samples contained PCV-2 CP (approximately 27 kDa) in the flow through and in the 1st wash. The bulk of the protein was detected in fractions 2, 3 and 4 eluted off the column (Figure 3.12 B). No bands were observed in the 30% $(NH_4)_2SO_4$ sample where the pH of the crude was not adjusted (Figure 3.12 A). All fractions that contained the CP were free of contamination.

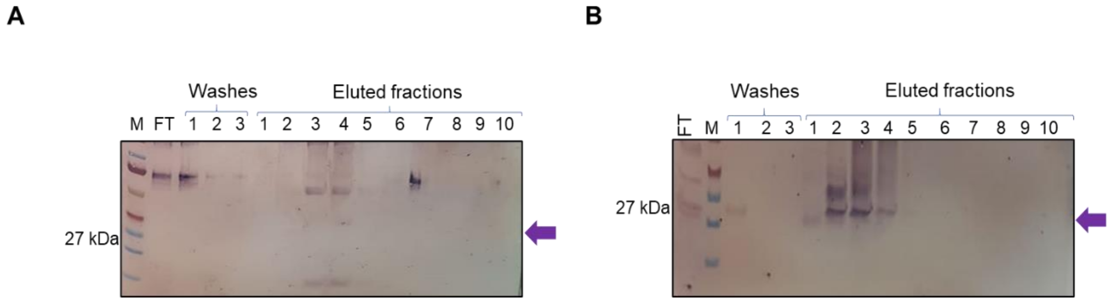

Figure 3.12 Western blot analysis of IEC purified PCV-2 VLPs. A) The 30% $(NH_4)_2SO_4$ (No pH adjustment). B) 80% $(NH_4)_2SO_4$ pH 4. Purified PCV-2 CP were probed with PCV-2 rabbit antisera (1:1000 dilution) and anti-rabbit IgG alkaline phosphatase-conjugated secondary antibody (1:5000). Labels: FT: Flow-through; M: pre-stained protein standard (kDa); purple arrow PCV-2 CP (~ 27 kDa).

Based on the western blot results, fractions 2, 3 and 4 were trapped on grids for EM analysis. PCV-2 VLPs ranging from 12-20 nm were observed in all these fractions (Figure 3.13). The highest concentration of VLPs was observed in fraction 2. Due to time constraints and COVID-19 global pandemic, I was unable to repeat this experiment or do a negative control. However, these results were promising and warrants further investigation. A summary of the purification methods is provided in Table 3.2.

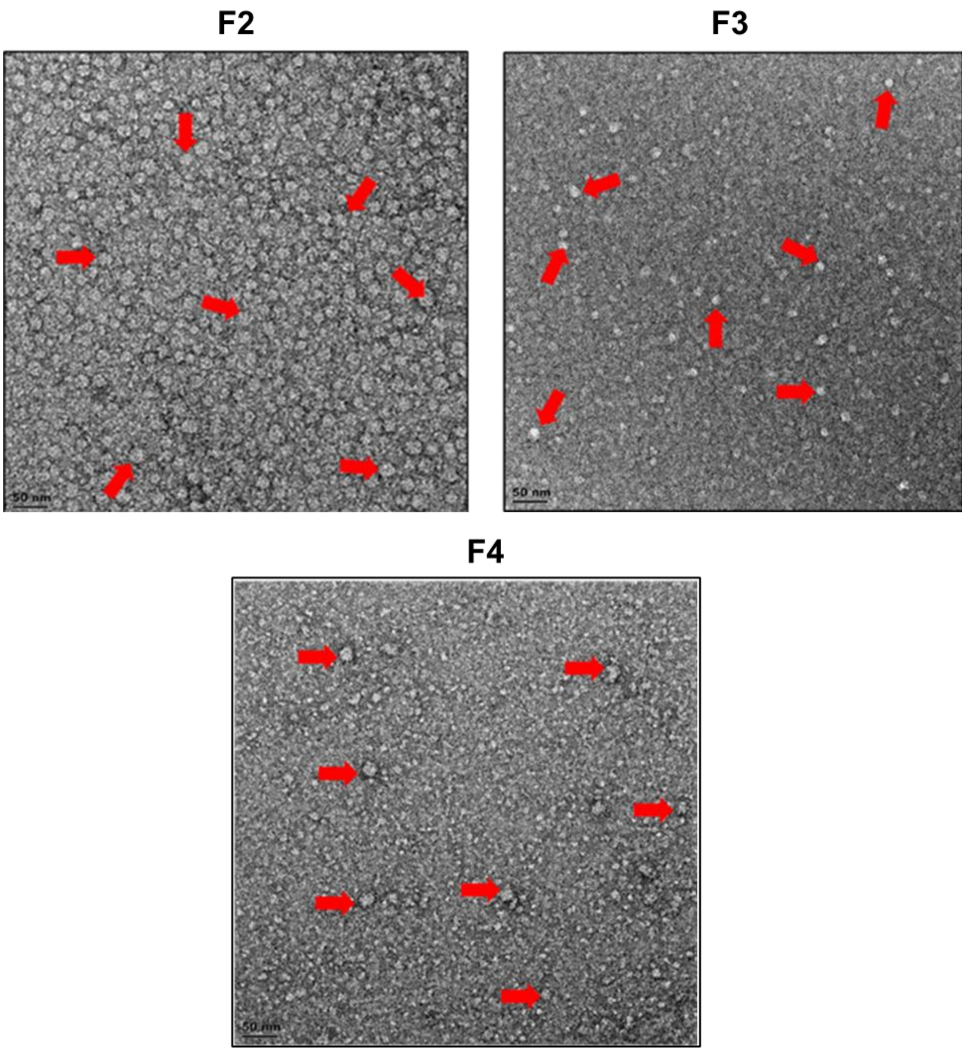

Figure 3.13 Electron micrographs of IEC-purified plant-produced PCV-2 VLPs: Samples were purified by IEC before TEM analysis. The samples observed at the magnification of 40 000 × under EM. Bars are 50 nm in size. Labels: red pointers: VLPs.

Table: 3.2 A summary of the purification methods investigated in this study

<table>
<tr><th></th><th colspan="3">Method used</th><th>Contamination</th><th>VLPs</th></tr>
<tr><td rowspan="2">Method 1</td><td colspan="3">Sucrose gradient ultracentrifugation (pelleting)
Extraction buffer: DB_{150}, Ultracentrifugation speed and duration: 120 000 × <i>g</i> for 4 hours</td><td>Yes</td><td>Yes</td></tr>
<tr><td>Filter sterilising</td><td>Freeze & thaw</td><td>CsCl</td><td>Yes</td><td>No</td></tr>
<tr><td>Method 2</td><td colspan="3">Sucrose gradient ultracentrifugation without pelleting
Extraction buffer: 1× PBS (pH 7.4)
Ultracentrifugation speed and duration: 20 000 × <i>g</i> for 18 hours</td><td>Yes (fraction 3)</td><td>Yes</td></tr>
<tr><td>Method 3</td><td colspan="3">Optiprep™ via sucrose gradient ultracentrifugation
Extraction buffer: DB_{150}
Speed and duration: 120 000 × <i>g</i> for 2 hours</td><td>Yes (fractions 2 & 4)</td><td>Yes</td></tr>
<tr><td>Method 4</td><td colspan="3">IEC</td><td>No</td><td>Yes</td></tr>
</table>

3.3.5.3 Production of PCV-2 VLPs in *E. coli*

The aim of this section was to express the PCV-2 CP in *E. coli* for their trial use in the development of a lateral flow devices while the plant-made PCV-2 VLPs were being optimized. Eventually, *E. coli* – and plant-produced VLPs were assessed in the lateral flow development.

E. coli expressed protein was partially purified using the BugBuster® purification method and the final pellet was washed six times with 1× PBS (pH 7.4) and the final pellet resuspended in the same buffer. The resuspended final pellet obtained after partial purification of *E. coli*-produced PCV-2 CP was analysed on a Coomasie-stained SDS-PAGE gel. A band of approximately 27 kDa was observed in the pPROEX-HTc-PCV-2 construct, indicating the presence of the PCV-2 CP (Figure 3.14, green arrow). No band corresponding to the size of CP was observed in the pPROEX-HTc empty vector which served as a negative control (Figure 3.14).

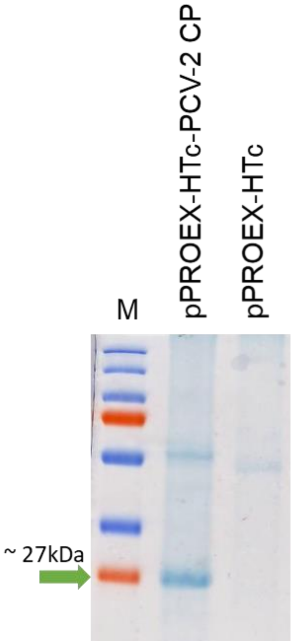

Figure 3.14 Expression of *E. coli*-produced PCV-2 CP. Coomassie-stained SDS-PAGE gel of pPROEX-HTc-PCV-2 and pPROEX-HTc empty vector. A band of approximately 27kDa was present in the pPROEX-HTc-PCV-2 as shown by a green arrow. No band was seen in the empty vector negative control. M: pre-stained protein standard (kDa).

Following the Coomasie blue stain SDS-PAGE analysis, the protein was subjected to quantification and TEM analysis as described in section 2.2.4. *E. coli*-produced PCV-2 CP was quantified relative to known amounts of BSA (58 kDa) using gel densitometry. A BSA standard curve was generated, from which the unknown protein concentrations were calculated (Figure 3.15). The PCV-2 CP band was detected at the expected size of approximately 27 kDa (Figure 3.15 A). A second band of 54 kDa, double the size of the native PCV-2 CP, was also detected and quantified. This band could potentially be a CP dimer. A total CP yield of 0.191 mg/ml and 0.190 mg/ml were obtained for the PCV-2 CP dimer and PCV-2 CP, respectively. The total CP yield was 0.281 mg/ml.

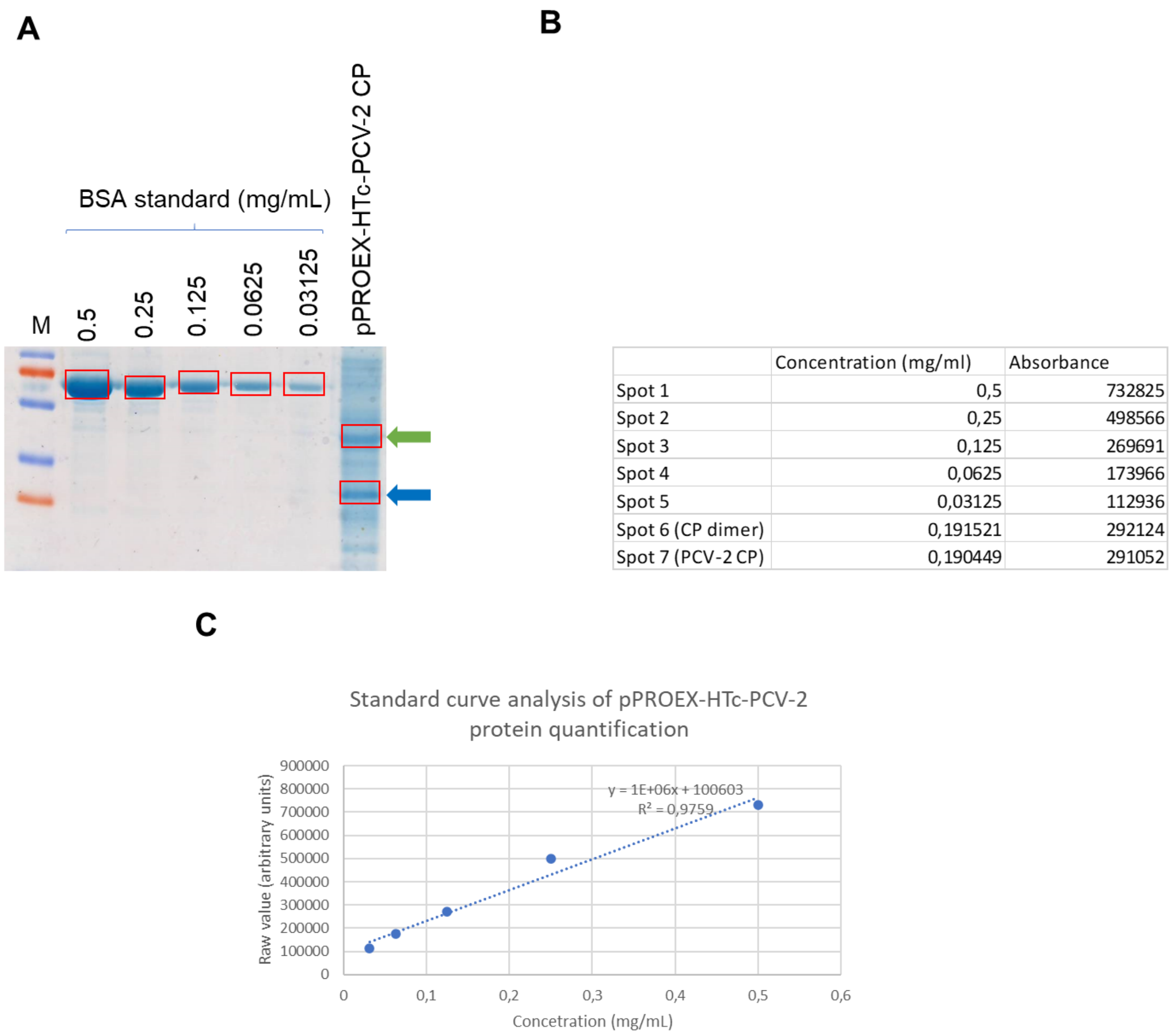

	Concentration (mg/ml)	Absorbance
Spot 1	0,5	732825
Spot 2	0,25	498566
Spot 3	0,125	269691
Spot 4	0,0625	173966
Spot 5	0,03125	112936
Spot 6 (CP dimer)	0,191521	292124
Spot 7 (PCV-2 CP)	0,190449	291052

Figure 3.15 Gel densitometry analysis of PCV-2 CP. Quantification of *E. coli* expressed pPROEX-HTc-PCV-2 (A) assessed through densitometry evaluation of the appropriate bands, the blue arrow shows the PCV-2 CP band of approximately 27 kDa while the green arrow shows the CP dimer of approximately 54 kDa. Each BSA standard concentration is indicated above the lane (A). The absorbance is shown in the table for each standard and CP (B). C shows the BSA standard curve, the equation was used for quantification of both the PCV-2 CP and CP dimer relative to the BSA standard.

The *E. coli*-produced PCV-2 CP was subjected to TEM analysis to evaluate if the *E. coli*-produced protein was able to assemble into VLPs. VLPs of a size range between 12- 20 nm were observed in the pPROEX-HTc-PCV-2 CP (Figure 3.16 A) sample. These VLPs resembled the VLPs purified using IEC. No VLPs were observed in the pPROEX-HTc empty vector negative control (Figure 3.16 B).

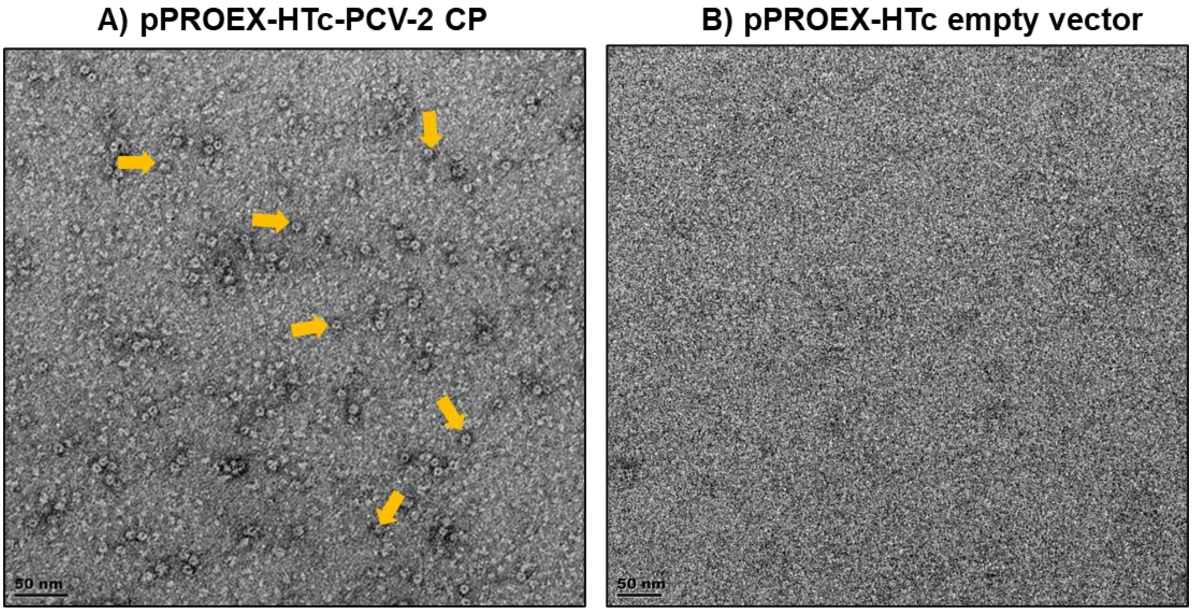

Figure 3.16 TEM analysis of purified *E. coli*-produced PCV-2 CP: A) pPROEX-HTc-PCV-2 and B) pPROEX-HTc empty vector. Samples were purified using the BugBuster® purification protocol and visualised at a magnification of 40 000 ×. Scale bars are 50 nm in size. Labels: yellow arrows: VLPs.

3.3.6 Lateral flow development

This part of the study was conducted by Antrum Biotech (Pty) Ltd and the aim was to assess if *E. coli*- and plant made VLPs and the polyclonal antibodies raised in rabbits against PCV-2 CP (Gunter *et al.*, 2019) could be used as antigen and antibodies in the development of the lateral flow assay.

Initially, polyclonal antibodies were isolated from rabbit sera utilising two methods, protein A purification or ammonium sulphate precipitation. The ability of HRP conjugated antibodies to bind coated PCV-2 VLPs, using a direct ELISA, was investigated in order to determine whether the conjugation was a success. As indicated by their affinity for *E. coli* and/or plant expressed PCV VLPs, both the protein A isolated and precipitated antibodies were successfully conjugated to HRP. Protein A isolated conjugated polyclonal antibody, however, outperformed precipitated conjugated polyclonal antibody because it showed similar affinity for PCV VLPs expressed by plant or *E. coli* at all conjugated antibody concentrations (results not shown). The purity of each of the antibodies was assessed on an SDS-PAGE gel and the presence of a heavy chain was observed in both antibodies. The light chain was not observed in the precipitated IgG (Figure 3.17).

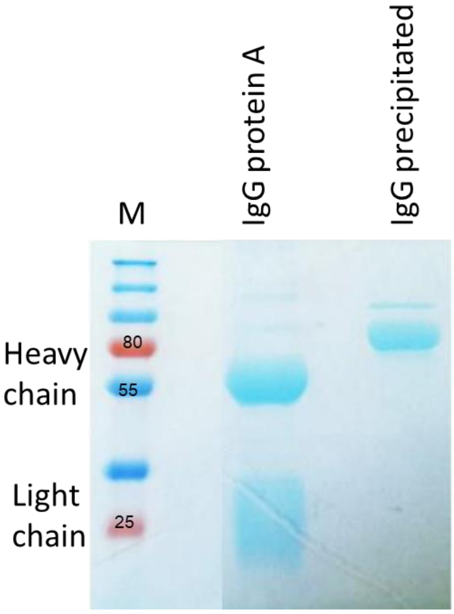

Figure 3.17 Purity of the antibodies. IgG protein A antibody showed the presence of a heavy chain (approximately 60 kDa) and a light chain (25 kDa). IgG precipitated antibody showed the presence of a heavy chain at approximately 80 kDa. No light chain was observed in the precipitated IgG antibody.

The functionality of the antibodies was assessed by direct ELISA using both *E. coli* and plant made VLPs. Based on the ODs of the ELISAs Protein A isolated antibodies were found to be functionally superior (higher ODs) compared to precipitated antibody (Table 3.3). Both antibodies showed higher affinity for *E. coli* expressed VLPs when compared to plant expressed CP.

Table 3.3: The optical densities (ODs at 450nm) for each antibody interaction.

		Optical density readings, highlighting unconjugated antibody affinity for PCV-2 VLPs			
		IgG protein A		IgG precipitated	
Coated *E. coli* PCV-2 VLPs	5 µg/ml	2.259	2.275	0.185	0.203
	0 µg/ml (blank)	0.317	0.205	0.048	0.083
Coated plant PCV-2 VLPs	5 µg/ml	2.391	2.575	0.513	0.489
	0 µg/ml (blank)	0.24	0.236	0.081	0.081

Serological based lateral flow assays involve coating nitrocellulose membranes with VLPs and detecting antibodies against the antigen (VLPs) in the sample. The coating method was optimised by comparing different incubation temperatures (overnight at 4°C, overnight at room temperature and 2 hours at 37°C) of antigen on the nitrocellulose membranes. It was found that incubation of the antigen overnight at room temperature or for 2 hours at 37°C resulted in optimal binding of the VLPs to the nitrocellulose membrane.

In order to optimize the lateral flow, two alternative strategies were developed for detecting antibody; these were: double mix and triple mix. The procedures are outlined in methods Section 3.2.7. Both strategies showed positive outcomes with specific detection of antibody in buffer being observed. The antibody was diluted in buffer before applying to the test strip Initial limit of detection (antibody in buffer) was done in which the concentration of unconjugated precipitated antibody was serially diluted in buffer (to mimic the sample) to determine whether the serological lateral flow assay can detect clinically relevant concentrations of antibody in serum and thus, is fit-for-purpose. Specific antibody detection was observed at concentrations four-fold lower than the original concentration in both double and triple mix lateral flow assay set-ups.

The final phase of the project involved determining the limit of detection and whether the test is fit-for-purpose in a sample matrix of interest. The lateral flow nitrocellulose membrane was coated with VLPs using the IsoFlow™ instrument in order to apply the VLPs to the nitrocellulose membrane in a homogenous line. These IsoFlow™ coated lateral flow strips were subsequently analysed for their ability to detect the anti-PCV-2 antibodies in buffer. The lateral flow assays were analysed using both the double and the triple mix strategies as described in methods under Section 3.2.7. In addition, both the precipitated anti-PCV-2 antibodies and the protein A purified antibodies were used for these experiments. Results from these initial experiments on the lateral flow strips coated with the IsoFlow™ instrument indicated that using either the precipitated or protein A purified anti-PCV-2 antibodies in both a double and a triple mix, produced a positive signal on the test strips. However, using the triple mix strategy with the precipitated anti-PCV-2 antibody resulted in the most pronounced positive signal and therefore this combination was used to determine the initial limit of detection of the antibody in buffer.

To determine the limit of detection of the antibody in buffer, the concentration of the unconjugated precipitated antibody was serially diluted (1 to 1:128) and applied to the lateral flow strips using the triple mix strategy. A positive signal was obtained down to a 1:16 dilution of the unconjugated precipitated antibody within 7 minutes and down to a 1:64 dilution within 12 minutes (Figure 3.18).

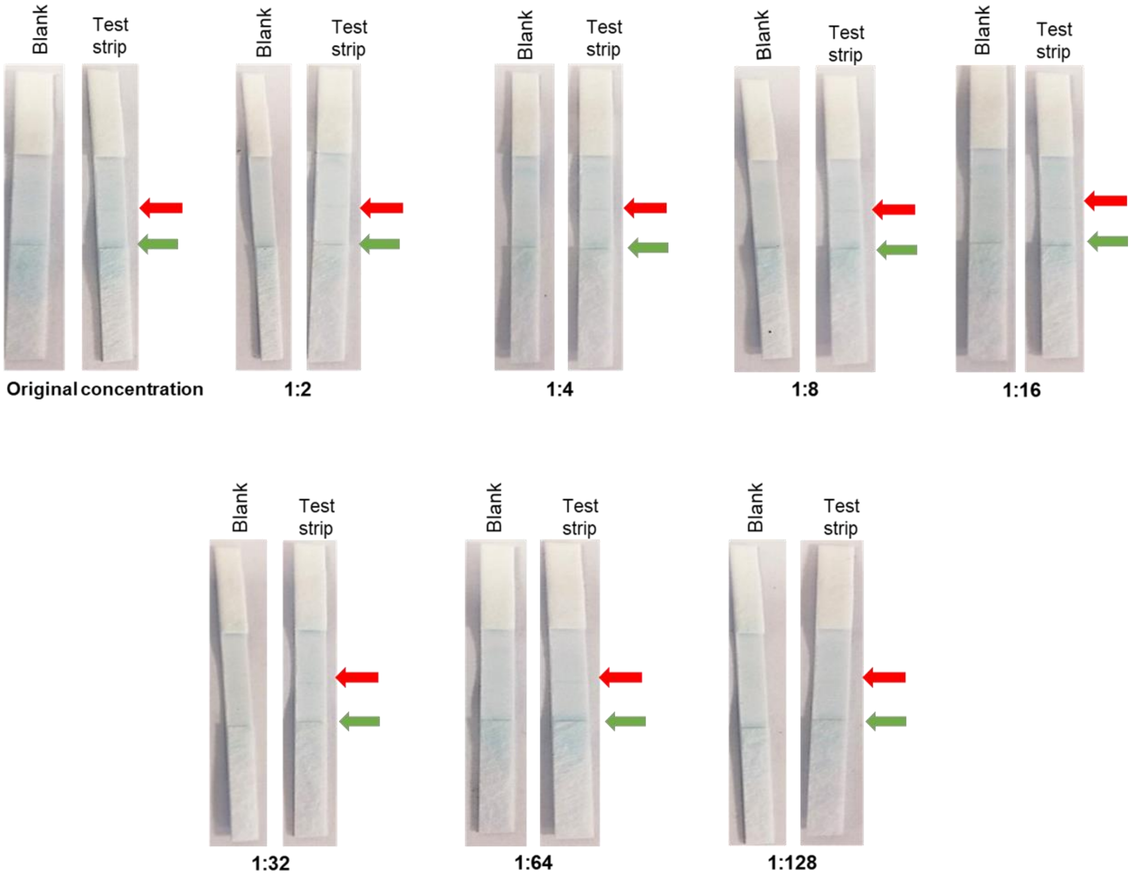

Figure 3.18: Triple mix: Sample (unconjugated precipitated IgG) diluted from 1:2 to 1:128 pre-incubated with the secondary detection antibody and strep-HRP applied to the strips followed by chromogen application. Red arrow shows the test line while the green arrow shows the negative control line.

Lastly, as a proof of concept that the nitrocellulose membrane can be coated with a negative control line and a test line simultaneously (on one test strip) and still result in a valid test, lateral flow strips were coated with the *E. coli*-expressed VLPs (test line) and a negative control line (buffer) using the IsoFlow™ instrument. Each test strip thus included a negative control and a test line. The unconjugated precipitated antibody was subsequently applied to the lateral flow strips in serum at the original concentration, 1:2, 1:4 and 1:8 dilutions using the triple mix strategy (Figure 3.19). The results indicated that the lateral flow strips coated with both a negative control line and a test line still produced a valid signal.

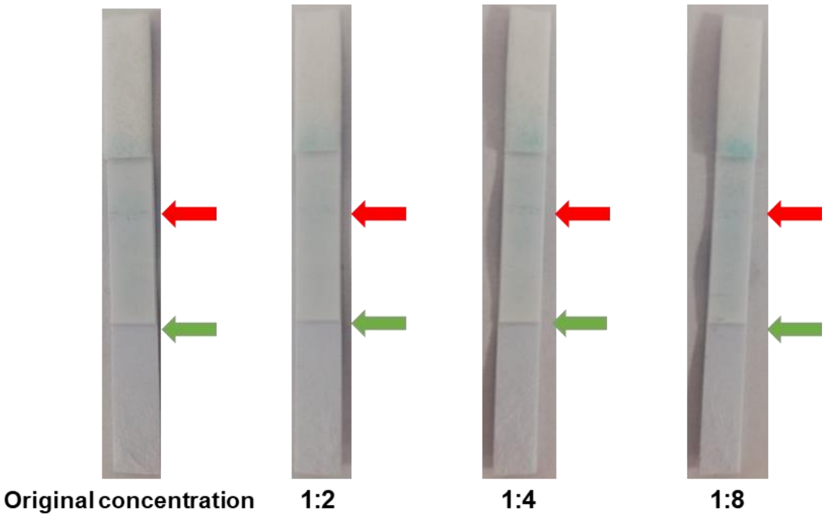

Figure 3.19 Triple mix: Sample (unconjugated precipitated IgG in serum) diluted from 1 to 1:8 pre-incubated with the secondary detection antibody and strep-HRP applied to the strips followed by chromogen application. Red arrow shows the test line and the green arrow shows the negative control line.

3.4 Discussion

The CP of PCV-2 can self-assemble spontaneously into VLPs that are of significant biopharmaceutical use (Duan *et al.*, 2019, Chae, 2012). The transient plant-based expression system is just one of the many systems for production of recombinant proteins and it has been demonstrated to be easily manageable and cost effective (Ma *et al.*, 2003, Kopertekh and Schiemann, 2019).

In this chapter, I focused on investigating if recombinantly expressed PCV-2 CP expressed with the novel pCBP-2 vector was able to assemble into VLPs. VLPs have the ability to serve as strong antigenic component for use in vaccine and diagnostic assay development (Frietze *et al.*, 2016, Wang *et al.*, 2020). VLPs are safe to use and it is possible to produce high-quality, reproducible antigen on a large scale compared to inactivated or live-attenuated antigens (Noad and Roy, 2003, Raghunandan, 2011).

Initially the PCV-2 *cp* was cloned into pCBP-2 that had an LPH signal peptide to direct protein synthesis in the ER. Gunter *et al.* (2019) showed that best expression was obtained with pEAQ-*HT*, which targets protein expression to the cytoplasm; therefore my aim was to improve on his findings to increase expression levels of CP. Based on the intensity of bands observed on a Coomassie-stained gel (Figure 3.4), higher levels of CP was expressed with pCBP-2 compared to expression with pEAQ-*HT*. These results showed that the novel pCBP-2 vector outperformed the pEAQ-*HT* vector for recombinant expression of PCV-2 CP. However, even though it was shown that expression with this vector resulted in higher accumulation of CP compared to expression with pEAQ-*HT*, no VLPs were observed after purification (Figure 3.6). The LPH signal peptide added extra amino acids to the N terminal of the CP which potentially interfered with VLP formation. Therefore, PCV-2 *cp* was cloned into pCBP-2 without the LPH signal peptide, which resulted in protein expression being targeted to the cytoplasm. The removal of this peptide sequence resulted in expression of CP as well as assembly into VLPs in the cytoplasm (Figure 3.7).

Expression time-trials were carried out to assess when CP expressed with pCBP-2 (without a signal peptide) would yield the most VLPs (results not shown). The pCBP-2 yielded higher levels of CP than the pEAQ-*HT* vector. VLPs that were similar to native virions and VLPs produced with other recombinant expression systems ranging between 12-20 nm in size were observed at 6 dpi (Figure 3.7) (Nainys *et al.*, 2014, Masuda *et al.*, 2018). Initially it appeared as though low amounts of VLPs were observed in the resuspended pellet after sucrose gradient purification. This was potentially because the resuspended pellet sample was concentrated and densely populated with proteins, or the presence of sucrose or co-purification of plant proteins made it difficult to observe isolated particles during TEM analysis. After diluting the samples many VLPs were observed in the 1:10 dilution and the amount of the VLPs observed decreased as the sample was further diluted. Furthermore, grid staining was optimised by reducing the staining time from 1 minute to 30 seconds to avoid overstaining.

Purity is crucial when preparing VLPs for use as a diagnostic reagent (Bhat and Rao, 2020). Even though high levels of recombinant proteins are necessary to achieve competitive yield, consideration must also be given to the effective recovery of proteins of purity. Partial purification of the VLPs used in this study involved the use of density gradient ultracentrifugation which is a regularly used method to purify VLPs from various expression systems (Gunter *et al.*, 2019, Wu *et al.*, 2012, Regnard *et al.*, 2017, Rowell, 2019, Khayat *et al.*, 2019). In the current study, plant-made CP was partially purified by concentrating the CP in a pellet which has passed through both a 45% and 65% sucrose cushion. After ultracentrifugation, PCV-2 VLPs were observed with EM in the pelleted samples (Figure 3.7). These results were similar to previous results reporter by (Gunter *et al.*, 2019). Although this method has been often used to purify VLPs produced in various systems, we consistently observed that our samples were contaminated with bacteria. It was possible that concentrating the CP in the pellet, resulted in co-precipitation of bacteria associated with the plants. Therefore, we set about to optimise the purification strategy for obtaining higher purity and sterility of PCV-2 VLPs.

At first attempts were made to remove bacterial contamination from already purified VLPs. VLPs were filter sterilized through 0.22 µm syringe filters. Filtering is an easy and often used method to sterilise media and protein after purification (Nail and Akers, 2012, Fishman and Berg, 2019). After filter-sterilizing the protein was lost on the filters (results not shown). This could have been because the filters had a high protein binding capability, which resulted in the protein binding to the filters instead of passing through.

Freeze–thaw of protein causes strong fluctuations in temperature which can damage or destroy microbial cells present in the protein and disrupt cell aggregates (Zuanazzi *et al.*, 2020, Papanicolas *et al.*, 2019). This method was employed to reduce bacterial load in the samples but led to a significant loss of protein after the 3rd freeze-thaw cycle, indicating that the VLPs were not stable during extreme temperature fluctuations. Moreover, all samples remained contaminated.

Since the VLPs could not be sterilised after partial purification, different purification methods were explored in this study. These methods included ultracentrifugation and IEC. For ultracentrifugation, parameters such as the centrifugation speed and time which affects sedimentation of the VLPs were adjusted to ensure that the VLPs remained in suspension in the gradient fractions, rather than collecting them in the pellet. The first attempt of ultracentrifugation at a lower speed without pelleting used in this study involved extraction in 1× PBS (pH 7.4), here, CP and VLPs were observed in all the fractions with the highest concentration of CP observed in fractions 3-5 (Figure 3.8). The second ultracentrifugation approach involved extracting CP in DB_{150} buffer and load it on the sucrose gradients before pooling the fractions for Optiprep™ gradient. Figure 3.11 shows that the fractions analysed after the Optiprep™ gradient ultracentrifugation had the CP present in fractions 2-6. Although, ultracentrifugation performed in this study was successful at isolating VLPs, bacterial contamination results showed to be inconsistent as some of the fractions were contaminated while others were not. The purification method established in this study had to be reproducible to be able to continuously produce VLPs of high quality and purity for diagnostic assays. With this method, VLP fractions that were contaminated had to be discarded, which is an unnecessary waste of protein rendering the purification method ineffective and expensive.

As the results obtained with ultracentrifugation were variable and not reproducible, we investigated the use of IEC for purification of PCV-2 VLPs. This method has successfully been used by previous researchers for purification of PCV-2 VLPs. We investigated the method reported by Masuda *et al.* (2018) for the purification of plant-produced VLPs. In the present study we investigated two extraction buffers: 1x PBS (pH 7.4) and DB_{150} (pH 6.8), for extraction of proteins from biomass. The DB_{150} buffer contains arginine which stabilize the proteins (Shmueli *et al.*, 2019), extraction of the CP in 1x PBS (pH 7.4) also demonstrated promising results, making it suitable for extraction of the PCV-2 CP. Since extraction in PBS was preferred for IEC purification, CP extracted in 1x PBS (pH 7.4) was clarified and successfully purified using IEC (Figure 3.12). The PCV-2 CP produced in *N. benthamiana* was found to have a high affinity to the anion exchange column, these results were similar to that of the study by Masuda *et al.* (2018) in which the PCV-2 CP was produced in silkworm and purified using the same method. Interestingly, it was shown by Zaveckas *et al.* (2015) , that yeast-produced PCV-2 CP had high affinity to the cation exchange columns. Adjusting the pH of the crude extract from 6.8 to 4 prior to $(NH_4)_2SO_4$ precipitation, significantly reduced the presence of host cell proteins in the sample and aided with greater recovery of PCV-2 CP (Menzel *et al.*, 2016, Martinez *et al.*, 2019, Wu *et al.*, 2014). It was shown previously that lowering the pH results in precipitation of host cell proteins, which results in the removal of the majority of host cell proteins from crude plant extracts and helps with the recovery of highly pure target protein (Martinez *et al.*, 2019); which is why this method was trialled in this study. EM analysis was carried out on fractions eluted off the IEC column and VLPs were observed in fractions 2,3 and 4 which corresponds to 0.3 M, 0.45 M and 0.6 M NaCl respectively. More VLPs were observed in the 0.3 M NaCl eluted fraction and decreased as the concentration of NaCl increased (Figure 3.13). None of the fractions analysed after IEC purification showed the presence of bacterial contamination indicating that we were able to develop a method for the purification of PCV-2 VLPs.

PCV-2 VLPs were made in *E. coli* and tested for their use in lateral flow devices while the optimization of VLP production in plants was underway. The PCV-2 CP was successfully expressed in *E. coli*, and assembled into VLPs ranging between 12-20 nm, similar to those produced by (Marcekova *et al.*, 2009). PCV VLPs which mimic the structure and size of native virions are easily produced in *E. coli* and can be detected by PCV-2 specific antibodies (Zhang *et al.*, 2016). The *E. coli*-based pPROEX-HT expression method offers easy cloning and can efficiently express recombinant proteins (Polayes and Hughes Jr, 1994). The partially purified *E. coli*- produced VLPs were quantified for use in the development of a lateral flow assay and the yield was 0.281 mg/ml (Figure 3.15). The expected band of 27 kDa for CP was observed on the Coomassie blue-stained gel, together with a CP dimer which is double the size of the native CP at approximately 54 kDa (Figure 3.14). Wu *et al.* (2016) reported the same observation for recombinant PCV-2 CP expressed in *E. coli*.

The rabbit-derived polyclonal antibodies that target PCV-2 VLPs were successfully isolated from the serum and were functional in both unconjugated and conjugated (HRP) form. Modification of the polyclonal antibody may occur during precipitation (lack of a light chain in SDS-PAGE image, figure 3.17), which impacts PCV-2 VLP affinity. This has been noted in functionality, modification and lateral flow experiments as protein A isolated IgG outperformed precipitated IgG. The lateral flow assay results showed that the serological lateral flow assay set-up can successfully detect the anti-PCV-2 precipitated antibody in buffer (mimic antibody in serum sample), using nitrocellulose coated with *E. coli* expressed VLPs. Additionally, the results in this part of study show that the initial limit of detection was determined to be 1:16 of the original unconjugated precipitated anti-PCV-2 antibody concentration, indicating the potential of the lateral flow assays to detect the anti-PCV-2 antibodies in serum samples. The lateral flow assays are thus fit-for-purpose, suggesting their use in diagnosing PCV-2 in swine herds. Once the diagnostic kit is ready for use, blood samples will be taken from swine for testing.

In conclusion, fully assembled PCV-2 VLPs were successfully produced in *N. benthamiana* using the novel pCBP-2 plant expression vector. A simple and highly scalable IEC purification method was established to obtain pure VLPs for potential use as an antigen in diagnostics and vaccines. This method can easily be scaled up compared to ultracentrifugation. PCV-2 VLPs were used to develop a lateral flow. Recombinant expression of the CP in plants for use in diagnostic assays has not yet been reported on thus far, therefore the expression of this immunogenic protein in plants for this specific purpose is intrinsically novel.

4 Chapter 4: General conclusions and future work

The aim of this study was to assess expression of PCV-2 CP with the novel pCBP-2 plant expression vector and optimising a purification method that would allow for recovery of CP of high purity. The overall objective was to produce PCV-2 CP of high purity and yields using a reliable expression system that is easily scalable and would permit a fast response in terms of diagnosis and identification of the cause of the disease in the case of PCV-2 pandemic. Development of cheaper diagnostics can be useful in disease surveillance in the swine industry as tests can be carried out regularly. Since it has been reported that PCV-2 continuously undergoes genetic shifts (Burbelo *et al.*, 2019, Franzo *et al.*, 2020), this study is relevant to combat a wide range of PCVAD caused by emerging PCV-2 strains by producing a cheaper diagnostic reagent which may be useful in developing affordable diagnostics. With the new discovery of PCV-3 which was first identified in the United States thorough a metagenomics approach and is associated with various clinical syndromes, including gastrointestinal, reproductive, respiratory and neurological disorders in swine (Saporiti *et al.*, 2020a, Palinski *et al.*, 2017b, Phan *et al.*, 2016a), there is a need for ongoing research which may provide a platform for studies aimed at developing diagnostic tools or vaccines against this newly emerged genotype of PCV. It was proved that plant expression platform can be used to rapidly produce highly immunogenic PCV-2 VLPs (Gunter *et al.*, 2019). The finding of the study by Gunter *et al.* (2019) has led to this study with a focus on exploring the transient expression system, utilizing *N. benthamiana* to improve and produce PCV-2 VLPs with a better yields. In addition, various methods for improving purification of PCV-2 VLPs were investigated with the aim to establish a reliable purification method which allows recovery of VLPs that are of high purity and free of contamination.

The pEAQ-*HT* vector which was previously the best vector for expression was directly compared to the novel pCBP-2 vector. Despite the fact that pCBP-2 vector had the best yield of protein, at first no VLPs were obtained when the vector had a signal peptide which led to further assessment of VLP formation using the same vector lacking a signal peptide. Eventually VLPs were produced and the vector still outperformed the pEAQ-*HT* vector in terms of expression yields. This study is the first to report that the pCBP-2 expression vector can be used to achieve higher yields of PCV-2 CP compared to the previously studied pEAQ-*HT* expression vector. Based on gel densitometry analysis, PCV-2 yields (chapter 2) obtained using the pCBP-2 vector was approximately two-fold higher than that obtained with the pEAQ-*HT* vector. This does not include the observed CP dimer seen on the SDS-PAGE gel which could possibly increase the total protein yield. I further showed that co-expression with an RNA silencing expressor significantly enhance expression which enables achieving higher yield of protein.

Moreover, I have shown that IEC purification method can be a potentially reliable, highly scalable and promising method of achieving pure VLPs. In order for plants to be a powerful system for the production of recombinant proteins, higher protein yields must be achieved, therefore continuous optimisation is crucial. As mentioned earlier, the most hindering factor of this project was time due to Covid-19 global pandemic hence troubleshooting could not be performed to a great extent. This would enable investigations of whether this method compromises the yield of the protein or not compared to sucrose purified protein. In addition, this experiment would require to be repeated with a negative control empty vector to validate the method. Nevertheless, IEC was a proof of concept which is promising as VLPs that were similar to those obtained in other studies were observed as discussed in section 3.4 of the previous chapter.

The overall aim of this project was to express protein which could potentially be used as a reagent in diagnostic tests such as ELISA and lateral flow assays. In this study, plant-made CP and *E. coli*-made VLPs were expressed and used in the development of lateral flow assays using PCV-2 rabbit antisera. This is because it was difficult to get plant- made VLPs at first and by the time the lateral flow work was ongoing, I was still optimizing VLPs production in plants. For this reason, after I successfully produced plant- made VLPs, the lateral flow work was already about to be completed. Even though, the idea was to test the functionality of these CP and VLPs using swine sera obtained from various sources using these tests, due to time constraints that did not happen and would have to be done in future and the limit of detection would be determined. The VLPs/CP were used as a coating reagent in the lateral flow development and their functionality was assessed. Although all VLPs/CP showed satisfactory functionality, the *E. coli* expressed VLPs had higher affinity to both antibodies (IgG protein A and IgG precipitated) compared to plant expressed CP. This, however, does not necessarily means that the *E. coli*-made proteins are more potent than plant-made proteins as this could be explained by the fact that the antibodies were made in rabbits using the *E.coli* produced VLPs. Therefore, the epitope presentation on the *E. coli* produced VLPs might be different than that of the plant-produced CP, thus conformation of epitopes. Therefore, further optimization needs to be done to get a better understanding on this finding.

Since a lateral flow device is a rapid and straightforward testing method which allows faster decision making and requires no expertise to interpret the results it is of paramount importance that plant-made VLPs' functionality is assessed in the lateral flow in comparison to the *E. coli*-made. Since proof of concept was shown for the lateral flow devices using *E.coli* VLPs and that the fundamental groundwork has been laid out, it would be beneficial to test pure, high quality plant-made VLPs produced in this study on diagnostic assays. Furthermore, the sensitivity and specificity of the immunoassays need to be analysed. Also, since the test lines of the lateral flow strips were not easily visible, future considerations would include refinement of the lateral flow assay to obtain clearer and more easily visible test lines on the lateral flow strips. Nonetheless this work successfully demonstrated that the PCV-2 VLPs are fit for use in the development of the lateral flow device for diagnostics purposes.

Even though, the idea was to test the functionality of these CP and VLPs using swine sera obtained from various sources using these tests, due to time constraints (global pandemic) that did not happen and would have to be done in future and the limit of detection would be determined. In this study, all the necessary clearance such as section 20 and animal ethics was obtained for this part of the project which would make it easier to continue.

References

Afghah, Z., Webb, B., Meng, X.-J. & Ramamoorthy, S. 2017. Ten years of PCV2 vaccines and vaccination: is eradication a possibility? *Veterinary microbiology,* 206**,** 21-28.

Afolabi, K. O., Iweriebor, B. C., Okoh, A. I. & Obi, L. C. 2017a. Global Status of Porcine circovirus Type 2 and Its Associated Diseases in Sub-Saharan Africa. *Adv Virol,* 2017**,** 6807964.

Afolabi, K. O., Iweriebor, B. C., Okoh, A. I. & Obi, L. C. 2017b. Global status of porcine circovirus type 2 and its associated diseases in sub-saharan Africa. *Advances in virology,* 2017.

Ahmad, A., O Pereira, E., J Conley, A., S Richman, A. & Menassa, R. 2010. Green biofactories: recombinant protein production in plants. *Recent patents on biotechnology,* 4**,** 242-259.

Alarcon, P., Rushton, J. & Wieland, B. 2013. Cost of post-weaning multi-systemic wasting syndrome and porcine circovirus type-2 subclinical infection in England–an economic disease model. *Preventive veterinary medicine,* 110**,** 88-102.

Alarcon, P., Velasova, M., Mastin, A., Nevel, A., Stärk, K. D. & Wieland, B. 2011. Farm level risk factors associated with severity of post-weaning multi-systemic wasting syndrome. *Preventive veterinary medicine,* 101**,** 182-191.

Allan, G., Kennedy, S., Mcneilly, F., Foster, J., Ellis, J., Krakowka, S., Meehan, B. & Adair, B. 1999a. Experimental reproduction of severe wasting disease by co-infection of pigs with porcine circovirus and porcine parvovirus. *Journal of comparative pathology,* 121**,** 1-11.

Allan, G., Mc Neilly, F., Meehan, B., Kennedy, S., Mackie, D., Ellis, J., Clark, E., Espuna, E., Saubi, N. & Riera, P. 1999b. Isolation and characterisation of circoviruses from pigs with wasting syndromes in Spain, Denmark and Northern Ireland. *Veterinary microbiology,* 66**,** 115-123.

Allan, G., Mcneilly, F., Cassidy, J., Reilly, G., Adair, B., Ellis, W. & Mcnulty, M. 1995. Pathogenesis of porcine circovirus; experimental infections of colostrum deprived piglets and examination of pig foetal material. *Veterinary microbiology,* 44**,** 49-64.

Allan, G., Mcneilly, F., Kennedy, S., Daft, B., Ellis, J., Haines, D., Meehan, B. & Adair, B. 1998. Isolation of porcine circovirus-like viruses from pigs with a wasting disease in the USA and Europe. *Journal of Veterinary Diagnostic Investigation,* 10**,** 3-10.

Aravindaram, K., Kuo, T. Y., Lan, C. W., Yu, H. H., Wang, P. H., Chen, Y. S., Chen, G. H. C. & Yang, N. S. 2009. Protective immunity against porcine circovirus 2 in mice induced by a gene-based combination vaccination. *The Journal of Gene Medicine: A cross-disciplinary journal for research on the science of gene transfer and its clinical applications,* 11**,** 288-301.

Arnau, J., Lauritzen, C., Petersen, G. E. & Pedersen, J. 2006. Current strategies for the use of affinity tags and tag removal for the purification of recombinant proteins. *Protein expression and purification,* 48**,** 1-13.

Barta, A., Sommergruber, K., Thompson, D., Hartmuth, K., Matzke, M. A. & Matzke, A. J. 1986. The expression of a nopaline synthase—human growth hormone chimaeric gene in transformed tobacco and sunflower callus tissue. *Plant molecular biology,* 6**,** 347-357.

Beach, N. M. & Meng, X.-J. 2012. Efficacy and future prospects of commercially available and experimental vaccines against porcine circovirus type 2 (PCV2). *Virus research,* 164**,** 33-42.

Beach, N. M., Ramamoorthy, S., Opriessnig, T., Wu, S. Q. & Meng, X.-J. 2010. Novel chimeric porcine circovirus (PCV) with the capsid gene of the emerging PCV2b subtype cloned in the genomic backbone of the non-pathogenic PCV1 is attenuated in vivo and induces protective and cross-protective immunity against PCV2b and PCV2a subtypes in pigs. *Vaccine,* 29**,** 221-232.

Benchabane, M., Goulet, C., Rivard, D., Faye, L., Gomord, V. & Michaud, D. 2008. Preventing unintended proteolysis in plant protein biofactories. *Plant biotechnology journal,* 6**,** 633-648.

Bhat, A. I. & Rao, G. P. 2020. In Vitro Expression of Viral Coat Protein in Prokaryotic System and Its Purification. *Characterization of Plant Viruses.* Springer.

Blanchard, P., Mahé, D., Cariolet, R., Keranflec'h, A., Baudouard, M., Cordioli, P., Albina, E. & Jestin, A. 2003a. Protection of swine against post-weaning multisystemic wasting syndrome (PMWS) by porcine circovirus type 2 (PCV2) proteins. *Vaccine,* 21**,** 4565-4575.

Blanchard, P., Mahé, D., Cariolet, R., Truong, C., Le Dimna, M., Arnauld, C., Rose, N., Eveno, E., Albina, E. & Madec, F. 2003b. An ORF2 protein-based ELISA for porcine circovirus type 2 antibodies in post-weaning multisystemic wasting syndrome. *Veterinary microbiology,* 94**,** 183-194.

Blunt, R., Mcorist, S., Mckillen, J., Mcnair, I., Jiang, T. & Mellits, K. 2011. House fly vector for porcine circovirus 2b on commercial pig farms. *Veterinary microbiology,* 149**,** 452-455.

Bogdan, J., West, K., Clark, E., Konoby, C., Haines, D., Allan, G., Mcneilly, F., Meehan, B., Krakowka, S. & Ellis, J. A. 2001. Association of porcine circovirus 2 with reproductive failure in pigs: a retrospective study, 1995-1998. *The Canadian Veterinary Journal,* 42**,** 548.

Boivin, G., Mazzulli, T. & Petric, M. 2016. Diagnosis of viral infections. *Clinical Virology***,** 291-319.

Bolin, S. R., Stoffregen, W. C., Nayar, G. P. & Hamel, A. L. 2001. Postweaning multisystemic wasting syndrome induced after experimental inoculation of cesarean-derived, colostrum-deprived piglets with type 2 porcine circovirus. *Journal of Veterinary Diagnostic Investigation,* 13**,** 185-194.

Bucarey, S. A., Noriega, J., Reyes, P., Tapia, C., Sáenz, L., Zuñiga, A. & Tobar, J. A. 2009. The optimized capsid gene of porcine circovirus type 2 expressed in yeast forms virus-like particles and elicits antibody responses in mice fed with recombinant yeast extracts. *Vaccine,* 27**,** 5781-5790.

Burbelo, P. D., Iadarola, M. J. & Chaturvedi, A. 2019. Emerging technologies for the detection of viral infections. *Future virology,* 14**,** 39-49.

Burgyán, J. 2008. Role of silencing suppressor proteins. *Plant Virology Protocols.* Springer.

Carman, S., Mcewen, B., Delay, J., Van Dreumel, T., Lusis, P., Cai, H. & Fairles, J. 2006. Porcine circovirus-2 associated disease in swine in Ontario (2004 to 2005): ONTARIO. *The Canadian Veterinary Journal,* 47**,** 761.

Chae, C. 2004. Postweaning multisystemic wasting syndrome: a review of aetiology, diagnosis and pathology. *The Veterinary Journal,* 168**,** 41-49.

Chae, C. 2005. A review of porcine circovirus 2-associated syndromes and diseases. *The Veterinary Journal,* 169**,** 326-336.

Chae, C. 2012. Commercial porcine circovirus type 2 vaccines: Efficacy and clinical application. *The Veterinary Journal,* 194**,** 151-157.

Chae, C. 2016. Porcine respiratory disease complex: Interaction of vaccination and porcine circovirus type 2, porcine reproductive and respiratory syndrome virus, and Mycoplasma hyopneumoniae. *The veterinary journal,* 212**,** 1-6.

Chan, S. K., Du, P., Ignacio, C., Mehta, S., Newton, I. G. & Steinmetz, N. F. 2020. Biomimetic Virus-Like Particles as Severe Acute Respiratory Syndrome Coronavirus 2 Diagnostic Tools. *ACS nano*.

Chen, G., Mai, K., Zhou, L., Wu, R., Tang, X., Wu, J., He, L., Lan, T., Xie, Q. & Sun, Y. 2017. Detection and genome sequencing of porcine circovirus 3 in neonatal pigs with congenital tremors in South China. *Transboundary and emerging diseases,* 64**,** 1650-1654.

Chen, P., Zhang, L., Chang, N., Shi, P., Gao, T., Zhang, L. & Huang, J. 2018. Preparation of virus-like particles for porcine circovirus type 2 by YeastFab Assembly. *Virus genes,* 54**,** 246-255.

Chen, Q. 2008. Expression and purification of pharmaceutical proteins in plants. *Biological Engineering Transactions,* 1**,** 291-321.

Chen, Q. & Davis, K. R. 2016. The potential of plants as a system for the development and production of human biologics. *F1000Research,* 5.

Chen, R. 2012. Bacterial expression systems for recombinant protein production: E. coli and beyond. *Biotechnology advances,* 30**,** 1102-1107.

Chiou, M.-T., Yang, C.-Y., Chang, T.-C., Chen, C., Lin, C.-F. & Ye, L.-J. 2010. Shedding pattern and serological profile of porcine circovirus type 2 infection in cesarean-derived, colostrum-deprived and farm-raised pigs. *Journal of Veterinary Medical Science***,** 1011290394-1011290394.

Conley, A. J., Joensuu, J. J., Jevnikar, A. M., Menassa, R. & Brandle, J. E. 2009a. Optimization of elastin-like polypeptide fusions for expression and purification of recombinant proteins in plants. *Biotechnology and bioengineering,* 103**,** 562-573.

Conley, A. J., Joensuu, J. J., Menassa, R. & Brandle, J. E. 2009b. Induction of protein body formation in plant leaves by elastin-like polypeptide fusions. *BMC biology,* 7**,** 1-18.

Curtis, R. & Cardineau, C. 1990. Oral immunization by transgenic plants. World Patent Application, WO 90/02484. *Patent record available from the World Intellectual Property Organization (WIPO)*.

Daff. 2018. *A profile of the South African pork market value chain* [Online]. Available: https://www.daff.gov.za/daffweb3/Branches/Economic-Development-Trade-Marketing/Marketing/Annual-Publications [Accessed].

De Almeida, M. R., Junior, A. S., Fietto, J. L. R., Bressan, G. C., Salgado, R. L., Onofre, T. S., Fausto, M. C., Vidigal, P. M. P., Kalks, S. P. & Crispim, J. S. 2017. Recombinant antigens of porcine circovirus 2 (PCV-2) for vaccine formulations, diagnostic kit and use thereof. Google Patents.

Deng, J., Li, X., Zheng, D., Wang, Y., Chen, L., Song, H., Wang, T., Huang, Y., Pang, W. & Tian, K. 2018. Establishment and application of an indirect ELISA for porcine circovirus 3. *Archives of virology,* 163**,** 479-482.

Depicker, A., Stachel, S., Dhaese, P., Zambryski, P. & Goodman, H. 1982. Nopaline synthase: transcript mapping and DNA sequence. *Journal of molecular and applied genetics,* 1**,** 561-573.

Diamos, A. G., Rosenthal, S. H. & Mason, H. S. 2016. 5′ and 3′ untranslated regions strongly enhance performance of geminiviral replicons in Nicotiana benthamiana leaves. *Frontiers in plant science,* 7**,** 200.

Drew, T., Grierson, S., King, D., Hicks, D., Done, S., Banks, M., Neser, J., Evans, D. & Grimbeek, P. 2004. Genetic similarity between porcine circovirus type 2 isolated from the first reported case of PMWS in South Africa and North American isolates. British Medical Journal Publishing Group.

Duan, J., Yang, D., Chen, L., Yu, Y., Zhou, J. & Lu, H. 2019. Efficient production of porcine circovirus virus-like particles using the nonconventional yeast Kluyveromyces marxianus. *Applied microbiology and biotechnology,* 103**,** 833-842.

Dupont, K., Nielsen, E., Baekbo, P. & Larsen, L. 2008. Genomic analysis of PCV2 isolates from Danish archives and a current PMWS case–control study supports a shift in genotypes with time. *Veterinary microbiology,* 128**,** 56-64.

Fahad, S., Khan, F. A., Pandupuspitasari, N. S., Ahmed, M. M., Liao, Y. C., Waheed, M. T., Sameeullah, M., Hussain, S., Saud, S. & Hassan, S. 2015. Recent developments in therapeutic protein expression technologies in plants. *Biotechnology letters,* 37**,** 265-279.

Fan, H., Chen, H., Tong, T., Ju, C., Lu, J. & Huang, H. 2005. The expression of porcine circovirus type 2 ORF2 gene in insect cells and its character. *Sheng wu gong cheng xue bao= Chinese journal of biotechnology,* 21**,** 975-978.

Fan, H., Ju, C., Tong, T., Huang, H., Lv, J. & Chen, H. 2007. Immunogenicity of empty capsids of porcine circovius type 2 produced in insect cells. *Veterinary research communications,* 31**,** 487-496.

Fan, H., Pan, Y., Fang, L., Wang, D., Wang, S., Jiang, Y., Chen, H. & Xiao, S. 2008. Construction and immunogenicity of recombinant pseudotype baculovirus expressing the capsid protein of porcine circovirus type 2 in mice. *Journal of virological methods,* 150**,** 21-26.

Fan, S., Ku, X., Chen, F., Wang, Y., Yu, X. & He, Q. 2017. Complete genome sequence of a novel porcine circovirus type 3 strain, PCV3/CN/Hubei-618/2016, isolated from China. *Genome Announc.,* 5**,** e00100-17.

Fauquet, C. M., Mayo, M. A., Maniloff, J., Desselberger, U. & Ball, L. A. 2005. *Virus taxonomy: VIIIth report of the International Committee on Taxonomy of Viruses*, Academic Press.

Fenaux, M., Opriessnig, T., Halbur, P., Elvinger, F. & Meng, X. 2004a. A chimeric porcine circovirus (PCV) with the immunogenic capsid gene of the pathogenic PCV type 2 (PCV2) cloned into the genomic backbone of the nonpathogenic PCV1 induces protective immunity against PCV2 infection in pigs. *Journal of virology,* 78**,** 6297-6303.

Fenaux, M., Opriessnig, T., Halbur, P., Elvinger, F. & Meng, X. 2004b. Two amino acid mutations in the capsid protein of type 2 porcine circovirus (PCV2) enhanced PCV2 replication in vitro and attenuated the virus in vivo. *Journal of virology,* 78**,** 13440-13446.

Feng, H., Blanco, G., Segalés, J. & Sibila, M. 2014. Can Porcine circovirus type 2 (PCV2) infection be eradicated by mass vaccination? *Veterinary microbiology,* 172**,** 92-99.

Finsterbusch, T. & Mankertz, A. 2009. Porcine circoviruses—small but powerful. *Virus research,* 143**,** 177-183.

Fishman, J. B. & Berg, E. A. 2019. Protein A and protein G purification of antibodies. *Cold Spring Harbor Protocols,* 2019**,** pdb. prot099143.

Floss, D. M., Sack, M., Arcalis, E., Stadlmann, J., Quendler, H., Rademacher, T., Stoger, E., Scheller, J., Fischer, R. & Conrad, U. 2009. Influence of elastin-like peptide fusions on the quantity and quality of a tobacco-derived human immunodeficiency virus-neutralizing antibody. *Plant biotechnology journal,* 7**,** 899-913.

Fort, M., Sibila, M., Nofrarías, M., Pérez-Martín, E., Olvera, A., Mateu, E. & Segalés, J. 2012. Evaluation of cell-mediated immune responses against porcine circovirus type 2 (PCV2) Cap and Rep proteins after vaccination with a commercial PCV2 sub-unit vaccine. *Veterinary immunology and immunopathology,* 150**,** 128-132.

Fort, M., Sibila, M., Pérez-Martín, E., Nofrarías, M., Mateu, E. & Segalés, J. 2009. One dose of a porcine circovirus 2 (PCV2) sub-unit vaccine administered to 3-week-old conventional piglets elicits cell-mediated immunity and significantly reduces PCV2 viremia in an experimental model. *Vaccine,* 27**,** 4031-4037.

Fox, J. L. 2012. First plant-made biologic approved. Nature Publishing Group.

Franzo, G., Delwart, E., Fux, R., Hause, B., Su, S., Zhou, J. & Segalés, J. 2020. Genotyping Porcine Circovirus 3 (PCV-3) Nowadays: Does It Make Sense? *Viruses,* 12**,** 265.

Franzo, G. & Segales, J. 2018. Porcine circovirus 2 (PCV-2) genotype update and proposal of a new genotyping methodology. *PLoS One,* 13**,** e0208585.

Franzo, G. & Segalés, J. 2018. Porcine circovirus 2 (PCV-2) genotype update and proposal of a new genotyping methodology. *PloS one,* 13**,** e0208585.

Frietze, K. M., Peabody, D. S. & Chackerian, B. 2016. Engineering virus-like particles as vaccine platforms. *Current opinion in virology,* 18**,** 44-49.

Gallie, D. R. 2001. Cap-independent translation conferred by the 5′ leader of tobacco etch virus is eukaryotic initiation factor 4G dependent. *Journal of virology,* 75**,** 12141-12152.

Gallie, D. R., Tanguay, R. L. & Leathers, V. 1995. The tobacco etch viral 5′ leader and poly (A) tail are functionally synergistic regulators of translation. *Gene,* 165**,** 233-238.

Gao, Z., Dong, Q., Jiang, Y., Opriessnig, T., Wang, J., Quan, Y. & Yang, Z. 2014. ORF4-protein deficient PCV2 mutants enhance virus-induced apoptosis and show differential expression of mRNAs in vitro. *Virus research,* 183**,** 56-62.

Gleba, Y., Klimyuk, V. & Marillonnet, S. 2005. Magnifection—a new platform for expressing recombinant vaccines in plants. *Vaccine,* 23**,** 2042-2048.

Gómez, E., Zoth, S. C. & Berinstein, A. 2009. Plant-based vaccines for potential human application. *Human vaccines,* 5**,** 738-744.

Goodin, M. M., Zaitlin, D., Naidu, R. A. & Lommel, S. A. 2008. Nicotiana benthamiana: its history and future as a model for plant–pathogen interactions. *Molecular plant-microbe interactions,* 21**,** 1015-1026.

Grau-Roma, L., Crisci, E., Sibila, M., Lopez-Soria, S., Nofrarias, M., Cortey, M., Fraile, L., Olvera, A. & Segalés, J. 2008. A proposal on porcine circovirus type 2 (PCV2) genotype definition and their relation with postweaning multisystemic wasting syndrome (PMWS) occurrence. *Veterinary microbiology,* 128**,** 23-35.

Grgacic, E. V. & Anderson, D. A. 2006. Virus-like particles: passport to immune recognition. *Methods,* 40**,** 60-65.

Gunter, C. J. 2017. Production of particle-based porcine circovirus candidate vaccines in plants. University of Cape Town.

Gunter, C. J., Regnard, G. L., Rybicki, E. P. & Hitzeroth, I. I. 2019. Immunogenicity of plant-produced porcine circovirus-like particles in mice. *Plant biotechnology journal*.

Guo, L., Fu, Y., Wang, Y., Lu, Y., Wei, Y., Tang, Q., Fan, P., Liu, J., Zhang, L. & Zhang, F. 2012. A porcine circovirus type 2 (PCV2) mutant with 234 amino acids in capsid protein showed more virulence in vivo, compared with classical PCV2a/b strain. *PLoS One,* 7**,** e41463.

Guo, X. Q., Wang, L. Q., Qiao, H., Yang, X. W., Yang, M. F. & Chen, H. Y. 2015. Enhancement of the immunogenicity of a porcine circovirus type 2 DNA vaccine by a recombinant plasmid coexpressing capsid protein and porcine interleukin-6 in mice. *Microbiology and immunology,* 59**,** 174-180.

Han, H. H., Karkada, N., Jayadeva, G. & Dubin, G. 2017. Serologic response to porcine circovirus type 1 (PCV1) in infants vaccinated with the human rotavirus vaccine, Rotarix™: a retrospective laboratory analysis. *Human vaccines & immunotherapeutics,* 13**,** 237-244.

Harding, J. C. 1998. Postweaning multisystemic wasting syndrome: epidemiology and clinical presentation. *Journal of Swine Health and Production,* 6**,** 249-254.

Harding, J. C. & Clark, E. G. 1997. Recognizing and diagnosing postweaning multisystemic wasting syndrome (PMWS). *Journal of Swine Health and Production,* 5**,** 201-203.

He, J., Cao, J., Zhou, N., Jin, Y., Wu, J. & Zhou, J. 2013. Identification and functional analysis of the novel ORF4 protein encoded by porcine circovirus type 2. *Journal of virology,* 87**,** 1420-1429.

Hedil, M., Sterken, M. G., De Ronde, D., Lohuis, D. & Kormelink, R. 2015. Analysis of tospovirus NSs proteins in suppression of systemic silencing. *PLoS One,* 10**,** e0134517.

Hefferon, K. 2014. Plant virus expression vector development: new perspectives. *BioMed research international,* 2014.

Hemann, M., Beach, N. M., Meng, X.-J., Wang, C., Halbur, P. G. & Opriessnig, T. 2014. A live-attenuated and an inactivated chimeric porcine circovirus (PCV) 1-2 vaccine are both effective at inducing a humoral immune response and reducing PCV2 viremia and intrauterine infection in female swine of breeding age. *Canadian journal of veterinary research,* 78**,** 8-16.

Hiatt, A., Caffferkey, R. & Bowdish, K. 1989. Production of antibodies in transgenic plants. *Nature,* 342**,** 76-78.

Hinnebusch, A. G., Ivanov, I. P. & Sonenberg, N. 2016. Translational control by 5′-untranslated regions of eukaryotic mRNAs. *Science,* 352**,** 1413-1416.

Hu, G., Wang, N., Yu, W., Wang, Z., Zou, Y., Zhang, Y., Wang, A., Deng, Z. & Yang, Y. 2016. Generation and immunogenicity of porcine circovirus type 2 chimeric virus-like particles displaying porcine reproductive and respiratory syndrome virus GP5 epitope B. *Vaccine,* 34**,** 1896-1903.

Huddy, S. M., Hitzeroth, I. I., Meyers, A. E., Weber, B. & Rybicki, E. P. 2018. Transient Expression and Purification of Horseradish Peroxidase C in Nicotiana benthamiana. *International journal of molecular sciences,* 19**,** 115.

Ilha, M., Nara, P. & Ramamoorthy, S. 2020. Early antibody responses map to non-protective, PCV2 capsid protein epitopes. *Virology,* 540**,** 23-29.

Islam, M. R., Kwak, J. W., Lee, J. S., Hong, S. W., Khan, M. R. I., Lee, Y., Lee, Y., Lee, S. W. & Hwang, I. 2019. Cost-effective production of tag-less recombinant protein in Nicotiana benthamiana. *Plant biotechnology journal,* 17**,** 1094-1105.

Jacobsen, B., Krueger, L., Seeliger, F., Bruegmann, M., Segalés, J. & Baumgaertner, W. 2009. Retrospective study on the occurrence of porcine circovirus 2 infection and associated entities in Northern Germany. *Veterinary microbiology,* 138**,** 27-33.

Johnson, C. S., Joo, H. S., Direksin, K., Yoon, K.-J. & Choi, Y. K. 2002. Experimental in utero inoculation of late-term swine fetuses with porcine circovirus type 2. *Journal of Veterinary Diagnostic Investigation,* 14**,** 507-512.

Jonsson, L. 2013. Emerging infectious diseases: using PCV2 as a model of disease transmission dynamics at the livestock-wildlife interface in Uganda [Dissertation]. Fakulteten för Veterinärmedicin och Husdjursvetenskap, Institutionen för ….

Juhan, N., Leroith, T., Opriessnig, T. & Meng, X. 2010. The open reading frame 3 (ORF3) of porcine circovirus type 2 (PCV2) is dispensable for virus infection but evidence of reduced pathogenicity is limited in pigs infected by an ORF3-null PCV2 mutant. *Virus research,* 147**,** 60-66.

Júnior, A. S., De Carvalho, O. V., Bulos, L. H. S., Fietto, J. L. R., Moraes, M. P. & De Almeida, M. R. 2012. Porcine Circovirus 2: immunopathogenesis and recent developments in vaccines. *World Journal of Vaccines,* 2**,** 96.

Kant, R. & Dasgupta, I. 2019. Gene silencing approaches through virus-based vectors: speeding up functional genomics in monocots. *Plant molecular biology,* 100**,** 3-18.

Karuppannan, A. & Opriessnig, T. 2017a. Porcine circovirus type 2 (PCV2) vaccines in the context of current molecular epidemiology. *Viruses,* 9**,** 99.

Karuppannan, A. K. & Opriessnig, T. 2017b. Porcine circovirus type 2 (PCV2) vaccines in the context of current molecular epidemiology. *Viruses,* 9**,** 99.

Kekarainen, T., Gonzalez, A., Llorens, A. & Segales, J. 2014. Genetic variability of porcine circovirus 2 in vaccinating and non-vaccinating commercial farms. *Journal of General Virology,* 95**,** 1734-1742.

Kekarainen, T., Mccullough, K., Fort, M., Fossum, C., Segalés, J. & Allan, G. 2010. Immune responses and vaccine-induced immunity against Porcine circovirus type 2. *Veterinary immunology and immunopathology,* 136**,** 185-193.

Kennedy, S., Moffett, D., Mcneilly, F., Meehan, B., Ellis, J., Krakowka, S. & Allan, G. 2000. Reproduction of lesions of postweaning multisystemic wasting syndrome by infection of conventional pigs with porcine circovirus type 2 alone or in combination with porcine parvovirus. *Journal of comparative pathology,* 122**,** 9-24.

Khayat, R., Brunn, N., Speir, J. A., Hardham, J. M., Ankenbauer, R. G., Schneemann, A. & Johnson, J. E. 2011. The 2.3-angstrom structure of porcine circovirus 2. *Journal of virology,* 85**,** 7856-7862.

Khayat, R., Wen, K., Alimova, A., Gavrilov, B., Katz, A., Galarza, J. M. & Gottlieb, P. 2019. Structural characterization of the PCV2d virus-like particle at 3.3 Å resolution reveals differences to PCV2a and PCV2b capsids, a tetranucleotide, and an N-terminus near the icosahedral 3-fold axes. *Virology,* 537**,** 186-197.

Kim, S.-C., Nazki, S., Kwon, S., Juhng, J.-H., Mun, K.-H., Jeon, D.-Y., Jeong, C.-G., Khatun, A., Kang, S.-J. & Kim, W.-I. 2018. The prevalence and genetic characteristics of porcine circovirus type 2 and 3 in Korea. *BMC veterinary research,* 14**,** 294.

Klaumann, F., Correa-Fiz, F., Franzo, G., Sibila, M., Núñez, J. I. & Segalés, J. 2018. Current knowledge on porcine circovirus 3 (pcv-3): A novel virus with a yet unknown impact on the swine industry. *Frontiers in veterinary science,* 5.

Koczula, K. M. & Gallotta, A. 2016. Lateral flow assays. *Essays in biochemistry,* 60**,** 111-120.

Kong, D., Xie, Z., Liu, L., Song, S., Kuang, H., Cui, G. & Xu, C. 2017. Development of indirect competitive ELISA and lateral-flow immunochromatographic assay strip for the detection of sterigmatocystin in cereal products. *Food and Agricultural Immunology,* 28**,** 260-273.

Kopertekh, L. & Schiemann, J. 2019. Transient production of recombinant pharmaceutical proteins in plants: evolution and perspectives. *Current Medicinal Chemistry,* 26**,** 365-380.

Krakowka, S., Ellis, J., Meehan, B., Kennedy, S., Mcneilly, F. & Allan, G. 2000. Viral wasting syndrome of swine: experimental reproduction of postweaning multisystemic wasting syndrome in gnotobiotic swine by coinfection with porcine circovirus 2 and porcine parvovirus. *Veterinary Pathology,* 37**,** 254-263.

Krenek, P., Samajova, O., Luptovciak, I., Doskocilova, A., Komis, G. & Samaj, J. 2015. Transient plant transformation mediated by Agrobacterium tumefaciens: Principles, methods and applications. *Biotechnology Advances,* 33**,** 1024-1042.

Krishnan, B. R. 2000. Current status of DNA vaccines in veterinary medicine. *Advanced drug delivery reviews,* 43**,** 3-11.

Ladekjaer-Mikkelsen, A., Nielsen, J., Storgaard, T., Bøtner, A., Allan, G. & Mcneilly, F. 2001. Transplacental infection with PCV-2 associated with reproductive failure in a gilt. *Veterinary Record,* 148**,** 759-760.

Lai, H. & Chen, Q. 2012. Bioprocessing of plant-derived virus-like particles of Norwalk virus capsid protein under current Good Manufacture Practice regulations. *Plant Cell Reports,* 31**,** 573-584.

Leite, M. L., Sampaio, K. B., Costa, F. F., Franco, O. L., Dias, S. C. & Cunha, N. B. 2019. Molecular farming of antimicrobial peptides: available platforms and strategies for improving protein biosynthesis using modified virus vectors. *Anais da Academia Brasileira de Ciências,* 91.

Li, J., Shi, J.-L., Wu, X.-Y., Fu, F., Yu, J., Yuan, X.-Y., Peng, Z., Cong, X.-Y., Xu, S.-J. & Sun, W.-B. 2015. Improvement of the immunogenicity of porcine circovirus type 2 DNA vaccine by recombinant ORF2 gene and CpG motifs. *Viral immunology,* 28**,** 290-296.

Lico, C., Chen, Q. & Santi, L. 2008. Viral vectors for production of recombinant proteins in plants. *Journal of cellular physiology,* 216**,** 366-377.

Lin, J.-H., Zeng-Weng, C., Jyh-Perng, W., Peng, T.-T., Huei-Yu, L., Huang, W.-Z., Shih-Rong, W. & Cheng-Yao, Y. 2019. Method of preparing porcine circovirus type 2 capsid protein and pharmaceutical composition comprising same. Google Patents.

Liu, F., Ge, S., Li, L., Wu, X., Liu, Z. & Wang, Z. 2012. Virus-like particles: potential veterinary vaccine immunogens. *Research in veterinary science,* 93**,** 553-559.

Liu, X., Liu, Y., Zhang, Y., Zhang, F. & Du, E. 2020. Incorporation of a truncated form of flagellin (TFlg) into porcine circovirus type 2 virus-like particles enhances immune responses in mice. *BMC veterinary research,* 16**,** 1-10.

Liu, Y.-F., Guo, Q.-H., Chen, L., Zhao, J., Chang, H.-T., Wang, X.-W., Yang, X. & Wang, C.-Q. 2013. Induction of mucosal immunity by intranasal immunization with recombinant adenovirus expressing major epitopes of Porcine circovirus-2 capsid protein. *Veterinary immunology and immunopathology,* 154**,** 48-53.

Liu, Z., Guo, F., Wang, F., Li, T.-C. & Jiang, W. 2016. 2.9 Å resolution cryo-EM 3D reconstruction of close-packed virus particles. *Structure,* 24**,** 319-328.

Lomonossoff, G. P. & D’aoust, M.-A. 2016. Plant-produced biopharmaceuticals: a case of technical developments driving clinical deployment. *Science,* 353**,** 1237-1240.

Lőrincz, M., Cságola, A., Biksi, I., Szeredi, L., Dán, Á. & Tuboly, T. 2010. Detection of porcine circovirus in rodents. *Acta Veterinaria Hungarica,* 58**,** 265-268.

Lv, Q.-Z., Guo, K.-K. & Zhang, Y.-M. 2014. Current understanding of genomic DNA of porcine circovirus type 2. *Virus genes,* 49**,** 1-10.

Ma, J. K., Drake, P. M. & Christou, P. 2003. The production of recombinant pharmaceutical proteins in plants. *Nature Reviews Genetics,* 4**,** 794-805.

Maclean, J., Koekemoer, M., Olivier, A., Stewart, D., Hitzeroth, I., Rademacher, T., Fischer, R., Williamson, A.-L. & Rybicki, E. 2007. Optimization of human papillomavirus type 16 (HPV-16) L1 expression in plants: comparison of the suitability of different HPV-16 L1 gene variants and different cell-compartment localization. *Journal of General Virology,* 88**,** 1460-1469.

Madson, D., Patterson, A., Ramamoorthy, S., Pal, N., Meng, X. & Opriessnig, T. 2009a. Reproductive failure experimentally induced in sows via artificial insemination with semen spiked with porcine circovirus type 2. *Veterinary pathology,* 46**,** 707-716.

Madson, D. M., Ramamoorthy, S., Kuster, C., Pal, N., Meng, X.-J., Halbur, P. G. & Opriessnig, T. 2008. Characterization of shedding patterns of porcine circovirus types 2a and 2b in experimentally inoculated mature boars. *Journal of veterinary diagnostic investigation,* 20**,** 725-734.

Madson, D. M., Ramamoorthy, S., Kuster, C., Pal, N., Meng, X.-J., Halbur, P. G. & Opriessnig, T. 2009b. Infectivity of porcine circovirus type 2 DNA in semen from experimentally-infected boars. *Veterinary research,* 40**,** 1.

Mahmoodi, S., Pourhassan-Moghaddam, M., Wood, D. W., Majdi, H. & Zarghami, N. 2019. Current affinity approaches for purification of recombinant proteins. *Cogent Biology,* 5**,** 1665406.

Mankertz, A., Çaliskan, R., Hattermann, K., Hillenbrand, B., Kurzendoerfer, P., Mueller, B., Schmitt, C., Steinfeldt, T. & Finsterbusch, T. 2004. Molecular biology of Porcine circovirus: analyses of gene expression and viral replication. *Veterinary microbiology,* 98**,** 81-88.

Mankertz, A., Domingo, M., Folch, J. M., Lecann, P., Jestin, A., Segalés, J., Chmielewicz, B., Plana-Durán, J. & Soike, D. 2000. Characterisation of PCV-2 isolates from Spain, Germany and France. *Virus research,* 66**,** 65-77.

Marcekova, Z., Psikal, I., Kosinova, E., Benada, O., Sebo, P. & Bumba, L. 2009. Heterologous expression of full-length capsid protein of porcine circovirus 2 in Escherichia coli and its potential use for detection of antibodies. *Journal of virological methods,* 162**,** 133-141.

Margaria, P., Miozzi, L., Rosa, C., Axtell, M. J., Pappu, H. R. & Turina, M. 2015. Small RNA profiles of wild-type and silencing suppressor-deficient tomato spotted wilt virus infected Nicotiana benthamiana. *Virus research,* 208**,** 30-38.

Marillonnet, S., Thoeringer, C., Kandzia, R., Klimyuk, V. & Gleba, Y. 2005. Systemic Agrobacterium tumefaciens–mediated transfection of viral replicons for efficient transient expression in plants. *Nature biotechnology,* 23**,** 718-723.

Marques, L. É. C., Silva, B. B., Dutra, R. a. F., Florean, E. O. P. T., Menassa, R. & Guedes, M. I. F. 2019. Transient expression of dengue virus NS1 antigen in Nicotiana benthamiana for use as a diagnostic antigen. *Frontiers in Plant Science,* 10**,** 1674.

Marsian, J. & Lomonossoff, G. P. 2016. Molecular pharming—VLPs made in plants. *Current opinion in biotechnology,* 37**,** 201-206.

Martínez, C. A., Topal, E., Giulietti, A. M., Talou, J. R. & Mason, H. 2010. Exploring different strategies to express Dengue virus envelope protein in a plant system. *Biotechnology letters,* 32**,** 867-875.

Martinez, M., Spitali, M., Norrant, E. L. & Bracewell, D. G. 2019. Precipitation as an enabling technology for the intensification of biopharmaceutical manufacture. *Trends in biotechnology,* 37**,** 237-241.

Mason, H. S., Lam, D. & Arntzen, C. J. 1992. Expression of hepatitis B surface antigen in transgenic plants. *Proceedings of the National Academy of Sciences,* 89**,** 11745-11749.

Masuda, A., Lee, J. M., Miyata, T., Sato, T., Hayashi, S., Hino, M., Morokuma, D., Karasaki, N., Mon, H. & Kusakabe, T. 2018. Purification and characterization of immunogenic recombinant virus-like particles of porcine circovirus type 2 expressed in silkworm pupae. *Journal of General Virology,* 99**,** 917-926.

Meehan, B. M., Mcneilly, F., Todd, D., Kennedy, S., Jewhurst, V. A., Ellis, J. A., Hassard, L. E., Clark, E. G., Haines, D. M. & Allan, G. M. 1998. Characterization of novel circovirus DNAs associated with wasting syndromes in pigs. *Journal of General Virology,* 79**,** 2171-2179.

Melanie, S., Witvliet, M. H. & Fachinger, V. 2019. A vaccine for intradermal application against pcv2 and prrs virus infection. Google Patents.

Menzel, S., Holland, T., Boes, A., Spiegel, H., Bolzenius, J., Fischer, R. & Buyel, J. F. 2016. Optimized blanching reduces the host cell protein content and substantially enhances the recovery and stability of two plant-derived malaria vaccine candidates. *Frontiers in plant science,* 7**,** 159.

Meroni, P. L., Chan, E. K., Damoiseaux, J., Andrade, L. E. C., Bossuyt, X., Conrad, K., Mariette, X., Sheldon, J., Rönnelid, J. & Fritzler, M. J. 2019. Unending story of the indirect immunofluorescence assay on HEp-2 cells: old problems and new solutions? *Annals of the rheumatic diseases,* 78**,** e46-e46.

Messenger, S. & Rupprecht, C. E. 2015. An indirect fluorescent antibody test for the serological detection of rabies virus immunoglobulin g and immunoglobulin m antibodies. *Current Laboratory Techniques in Rabies Diagnosis, Research and Prevention, Volume 2.* Elsevier.

Miletic, S., Simpson, D. J., Szymanski, C. M., Deyholos, M. K. & Menassa, R. 2016. A plant-produced bacteriophage tailspike protein for the control of Salmonella. *Frontiers in plant science,* 6**,** 1221.

Mo, X., Li, X., Yin, B., Deng, J., Tian, K. & Yuan, A. 2019. Structural roles of PCV2 capsid protein N-terminus in PCV2 particle assembly and identification of PCV2 type-specific neutralizing epitope. *PLoS pathogens,* 15**,** e1007562.

Nail, S. L. & Akers, M. J. 2012. *Development and manufacture of protein pharmaceuticals*, Springer Science & Business Media.

Nainys, J., Lasickiene, R., Petraityte-Burneikiene, R., Dabrisius, J., Lelesius, R., Sereika, V., Zvirbliene, A., Sasnauskas, K. & Gedvilaite, A. 2014. Generation in yeast of recombinant virus-like particles of porcine circovirus type 2 capsid protein and their use for a serologic assay and development of monoclonal antibodies. *BMC biotechnology,* 14**,** 100.

Nauwynck, H., Sanchez, R., Meerts, P., Lefebvre, D., Saha, D., Huang, L. & Misinzo, G. 2012. Cell tropism and entry of porcine circovirus 2. *Virus research,* 164**,** 43-45.

Nawagitgul, P., Harms, P. A., Morozov, I., Thacker, B. J., Sorden, S. D., Lekcharoensuk, C. & Paul, P. S. 2002. Modified indirect porcine circovirus (PCV) type 2-based and recombinant capsid protein (ORF2)-based enzyme-linked immunosorbent assays for detection of antibodies to PCV. *Clin. Diagn. Lab. Immunol.,* 9**,** 33-40.

Nawagitgul, P., Morozov, I., Bolin, S. R., Harms, P. A., Sorden, S. D. & Paul, P. S. 2000. Open reading frame 2 of porcine circovirus type 2 encodes a major capsid protein. *Journal of General Virology,* 81**,** 2281-2287.

Nayar, G., Hamel, A. & Lin, L. 1997. Detection and characterization of porcine circovirus associated with postweaning multisystemic wasting syndrome in pigs. *The Canadian Veterinary Journal,* 38**,** 385.

Noad, R. & Roy, P. 2003. Virus-like particles as immunogens. *Trends in microbiology,* 11**,** 438-444.

O'connor, B., Gauvreau, H., West, K., Bogdan, J., Ayroud, M., Clark, E. G., Konoby, C., Allan, G. & Ellis, J. A. 2001. Multiple porcine circovirus 2-associated abortions and reproductive failure in a multisite swine production unit. *The Canadian Veterinary Journal,* 42**,** 551.

Ojok, L., Okuni, J. B., Hohloch, C., Hecht, W. & Reinacher, M. 2013. Detection and characterisation of porcine circovirus 2 from Ugandan pigs. *Indian Journal of Veterinary Pathology,* 37**,** 77-80.

Olvera, A., Cortey, M. & Segales, J. 2007. Molecular evolution of porcine circovirus type 2 genomes: phylogeny and clonality. *Virology,* 357**,** 175-185.

Opriessnig, T., Meng, X.-J. & Halbur, P. G. 2007. Porcine circovirus type 2–associated disease: update on current terminology, clinical manifestations, pathogenesis, diagnosis, and intervention strategies. *Journal of Veterinary Diagnostic Investigation,* 19**,** 591-615.

Opriessnig, T., Xiao, C.-T., Gerber, P. F. & Halbur, P. G. 2013. Emergence of a novel mutant PCV2b variant associated with clinical PCVAD in two vaccinated pig farms in the US concurrently infected with PPV2. *Veterinary microbiology,* 163**,** 177-183.

Ouardani, M., Wilson, L., Jette, R., Montpetit, C. & Dea, S. 1999. Multiplex PCR for detection and typing of porcine circoviruses. *Journal of clinical microbiology,* 37**,** 3917-3924.

Palinski, R., Piñeyro, P., Shang, P., Yuan, F., Guo, R., Fang, Y., Byers, E. & Hause, B. M. 2017a. A novel porcine circovirus distantly related to known circoviruses is associated with porcine dermatitis and nephropathy syndrome and reproductive failure. *Journal of virology,* 91**,** e01879-16.

Palinski, R., Piñeyro, P., Shang, P., Yuan, F., Guo, R., Fang, Y., Byers, E. & Hause, B. M. 2017b. A novel porcine circovirus distantly related to known circoviruses is associated with porcine dermatitis and nephropathy syndrome and reproductive failure. *Journal of virology,* 91.

Papanicolas, L. E., Choo, J. M., Wang, Y., Leong, L. E., Costello, S. P., Gordon, D. L., Wesselingh, S. L. & Rogers, G. B. 2019. Bacterial viability in faecal transplants: which bacteria survive? *EBioMedicine,* 41**,** 509-516.

Patterson, A., Madson, D., Halbur, P. & Opriessnig, T. 2011a. Shedding and infection dynamics of porcine circovirus type 2 (PCV2) after natural exposure. *Veterinary microbiology,* 149**,** 225-229.

Patterson, A., Ramamoorthy, S., Madson, D., Meng, X., Halbur, P. & Opriessnig, T. 2011b. Shedding and infection dynamics of porcine circovirus type 2 (PCV2) after experimental infection. *Veterinary microbiology,* 149**,** 91-98.

Patterson, A. R., Johnson, J. K., Ramamoorthy, S., Hesse, R. A., Murtaugh, M. P., Puvanendiran, S., Pogranichniy, R. M., Erickson, G. A., Carman, S. & Hause, B. 2011c. Interlaboratory comparison of porcine circovirus-2 indirect immunofluorescent antibody test and enzyme-linked immunosorbent assay results on experimentally infected pigs. *Journal of Veterinary Diagnostic Investigation,* 23**,** 206-212.

Peng, Z., Ma, T., Pang, D., Su, D., Chen, F., Chen, X., Guo, N., Ouyang, T., Ouyang, H. & Ren, L. 2016. Expression, purification and antibody preparation of PCV2 Rep and ORF3 proteins. *International journal of biological macromolecules,* 86**,** 277-281.

Pêra, F. F., Mutepfa, D. L., Khan, A. M., Els, J. H., Mbewana, S., Van Dijk, A. A., Rybicki, E. P. & Hitzeroth, I. I. 2015. Engineering and expression of a human rotavirus candidate vaccine in Nicotiana benthamiana. *Virology journal,* 12**,** 1-11.

Pereira, E. O., Kolotilin, I., Conley, A. J. & Menassa, R. 2014. Production and characterization of in planta transiently produced polygalacturanase from Aspergillus niger and its fusions with hydrophobin or ELP tags. *BMC biotechnology,* 14**,** 1-11.

Peyret, H., Brown, J. K. & Lomonossoff, G. P. 2019. Improving plant transient expression through the rational design of synthetic 5′ and 3′ untranslated regions. *Plant methods,* 15**,** 108.

Peyret, H. & Lomonossoff, G. P. 2013. The pEAQ vector series: the easy and quick way to produce recombinant proteins in plants. *Plant molecular biology,* 83**,** 51-58.

Phan, T. G., Giannitti, F., Rossow, S., Marthaler, D., Knutson, T. P., Li, L., Deng, X., Resende, T., Vannucci, F. & Delwart, E. 2016a. Detection of a novel circovirus PCV3 in pigs with cardiac and multi-systemic inflammation. *Virology journal,* 13**,** 1-8.

Phan, T. G., Giannitti, F., Rossow, S., Marthaler, D., Knutson, T. P., Li, L., Deng, X., Resende, T., Vannucci, F. & Delwart, E. 2016b. Detection of a novel circovirus PCV3 in pigs with cardiac and multi-systemic inflammation. *Virology journal,* 13**,** 184.

Pillay, P., Schlüter, U., Van Wyk, S., Kunert, K. J. & Vorster, B. J. 2014. Proteolysis of recombinant proteins in bioengineered plant cells. *Bioengineered,* 5**,** 15-20.

Pillet, S., Couillard, J., Trepanier, S., Poulin, J.-F., Yassine-Diab, B., Guy, B., Ward, B. J. & Landry, N. 2019. Immunogenicity and safety of a quadrivalent plant-derived virus like particle influenza vaccine candidate—Two randomized Phase II clinical trials in 18 to 49 and≥ 50 years old adults. *PloS one,* 14.

Pogranichnyyp, R. M., Yoon, K.-J., Harms, P. A., Swenson, S. L., Zimmerman, J. J. & Sorden, S. D. 2000. Characterization of immune response of young pigs to porcine circovirus type 2 infection. *Viral immunology,* 13**,** 143-153.

Pogue, G. P. & Holzberg, S. 2012. Transient virus expression systems for recombinant protein expression in dicot-and monocotyledonous plants. *Plant Science***,** 191-216.

Polayes, D. & Hughes Jr, A. 1994. Efficient protein expression and simple purification using the pPROEX-1 super (TM) system. *Focus,* 16**,** 81-84.

Porta, C. & Lomonossoff, G. P. 2002. Viruses as vectors for the expression of foreign sequences in plants. *Biotechnology and Genetic Engineering Reviews,* 19**,** 245-292.

Qiu, X., Wong, G., Audet, J., Bello, A., Fernando, L., Alimonti, J. B., Fausther-Bovendo, H., Wei, H., Aviles, J. & Hiatt, E. 2014. Reversion of advanced Ebola virus disease in nonhuman primates with ZMapp. *Nature,* 514**,** 47-53.

Racine, S., Kheyar, A., Gagnon, C. A., Charbonneau, B. & Dea, S. 2004. Eucaryotic expression of the nucleocapsid protein gene of porcine circovirus type 2 and use of the protein in an indirect immunofluorescence assay for serological diagnosis of postweaning multisystemic wasting syndrome in pigs. *Clin. Diagn. Lab. Immunol.,* 11**,** 736-741.

Raghunandan, R. 2011. Virus-like particles: innate immune stimulators. *Expert review of vaccines,* 10**,** 409-411.

Regnard, G. L., Rybicki, E. P. & Hitzeroth, I. I. 2017. Recombinant expression of beak and feather disease virus capsid protein and assembly of virus-like particles in Nicotiana benthamiana. *Virology journal,* 14**,** 174.

Ren, L., Chen, X. & Ouyang, H. 2016. Interactions of porcine circovirus 2 with its hosts. *Virus genes,* 52**,** 437-444.

Rodriguez-Cariñg, C. & Segales, J. 2009. Ultrastructural findings in lymph nodes from pigs suffering from naturally occurring postweaning multisystemic wasting syndrome. *Veterinary pathology,* 46**,** 729-735.

Rose, N., Opriessnig, T., Grasland, B. & Jestin, A. 2012. Epidemiology and transmission of porcine circovirus type 2 (PCV2). *Virus research,* 164**,** 78-89.

Rowell, J. S. 2019. *Porcine Circovirus Cap-Induced Apoptosis of Non-Infected PK15 Cells.* Cumming School of Medicine.

Rybicki, E. P. 2009. Plant-produced vaccines: promise and reality. *Drug discovery today,* 14**,** 16-24.

Rybicki, E. P. 2010. Plant-made vaccines for humans and animals. *Plant biotechnology journal,* 8**,** 620-637.

Rybicki, E. P. 2014. Plant-based vaccines against viruses. *Virology journal,* 11**,** 205.

Sack, M., Hofbauer, A., Fischer, R. & Stoger, E. 2015. The increasing value of plant-made proteins. *Current opinion in biotechnology,* 32**,** 163-170.

Sainsbury, F., Thuenemann, E. C. & Lomonossoff, G. P. 2009. pEAQ: versatile expression vectors for easy and quick transient expression of heterologous proteins in plants. *Plant biotechnology journal,* 7**,** 682-693.

Sala, F., Rigano, M. M., Barbante, A., Basso, B., Walmsley, A. M. & Castiglione, S. 2003. Vaccine antigen production in transgenic plants: strategies, gene constructs and perspectives. *Vaccine,* 21**,** 803-808.

Sambrook, J., Fritsch, E. F. & Maniatis, T. 1989. *Molecular cloning: a laboratory manual*, Cold spring harbor laboratory press.

Santos, M. R., Assao, V. S., Santos, F. D. a. A., Salgado, R. L., Carneiro, A. P., Fietto, J. L. R., Bressan, G. C., De Almeida, M. R., Lobato, Z. I. P. & Ueira-Veira, C. 2018. Utilization of phage display to identify antigenic regions in the PCV2 capsid protein for the evaluation of serological responses in mice and pigs. *Archives of virology,* 163**,** 1877-1887.

Saporiti, V., Cruz, T. F., Correa-Fiz, F., Núñez, J. I., Sibila, M. & Segalés, J. 2020a. Similar frequency of Porcine circovirus 3 (PCV-3) detection in serum samples of pigs affected by digestive or respiratory disorders and age-matched clinically healthy pigs. *Transboundary and Emerging Diseases,* 67**,** 199-205.

Saporiti, V., Huerta, E., Correa-Fiz, F., Grosse Liesner, B., Duran, O., Segalés, J. & Sibila, M. 2020b. Detection and genotyping of Porcine circovirus 2 (PCV-2) and detection of Porcine circovirus 3 (PCV-3) in sera from fattening pigs of different European countries. *Transboundary and Emerging Diseases*.

Schillberg, S., Twyman, R. M. & Fischer, R. 2005. Opportunities for recombinant antigen and antibody expression in transgenic plants—technology assessment. *Vaccine,* 23**,** 1764-1769.

Schwarz, D. S. & Blower, M. D. 2016. The endoplasmic reticulum: structure, function and response to cellular signaling. *Cellular and Molecular Life Sciences,* 73**,** 79-94.

Scotti, N. & Rybicki, E. P. 2013. Virus-like particles produced in plants as potential vaccines. *Expert review of vaccines,* 12**,** 211-224.

Segalés, J., Allan, G. M. & Domingo, M. 2005. Porcine circovirus diseases. *Animal Health Research Reviews,* 6**,** 119-142.

Segales, J. & Domingo, M. 2002. Postweaning mulstisystemic wasting syndrome (PMWS) in pigs. A review. *Veterinary Quarterly,* 24**,** 109-124.

Segalés, J., Kekarainen, T. & Cortey, M. 2013. The natural history of porcine circovirus type 2: from an inoffensive virus to a devastating swine disease? *Veterinary microbiology,* 165**,** 13-20.

Shaaltiel, Y., Bartfeld, D., Hashmueli, S., Baum, G., Brill-Almon, E., Galili, G., Dym, O., Boldin-Adamsky, S. A., Silman, I. & Sussman, J. L. 2007. Production of glucocerebrosidase with terminal mannose glycans for enzyme replacement therapy of Gaucher's disease using a plant cell system. *Plant biotechnology journal,* 5**,** 579-590.

Shen, W.-J. & Forde, B. G. 1989. Efficient transformation of Agrobacterium spp. by high voltage electroporation. *Nucleic acids research,* 17**,** 8385.

Shmueli, M. D., Levy-Kanfo, L., Haj, E., Schoenfeld, A. R., Gazit, E. & Segal, D. 2019. Arginine refolds, stabilizes, and restores function of mutant pVHL proteins in animal model of the VHL cancer syndrome. *Oncogene,* 38**,** 1038-1049.

Shopan, J., Lv, X., Hu, Z., Zhang, M. & Yang, J. 2020. Eukaryotic Translation Initiation Factors Shape RNA Viruses Resistance in Plants. *Horticultural Plant Journal*.

Sigmund, I. K., Yermak, K., Perka, C., Trampuz, A. & Renz, N. 2018. Is the enzyme-linked immunosorbent assay more accurate than the lateral flow alpha defensin test for diagnosing periprosthetic joint infection? *Clinical orthopaedics and related research,* 476**,** 1645.

Sinha, A., Shen, H., Schalk, S., Beach, N., Huang, Y., Halbur, P., Meng, X. & Opriessnig, T. 2010. Porcine reproductive and respiratory syndrome virus infection at the time of porcine circovirus type 2 vaccination has no impact on vaccine efficacy. *Clin. Vaccine Immunol.,* 17**,** 1940-1945.

Soh, J. H., Chan, H.-M. & Ying, J. Y. 2020. Strategies for developing sensitive and specific nanoparticle-based lateral flow assays as point-of-care diagnostic device. *Nano Today,* 30**,** 100831.

Song, Y., Jin, M., Zhang, S., Xu, X., Xiao, S., Cao, S. & Chen, H. 2007. Generation and immunogenicity of a recombinant pseudorabies virus expressing cap protein of porcine circovirus type 2. *Veterinary microbiology,* 119**,** 97-104.

Sorden, S. D. 2000. Update on porcine circovirus and postweaning multisystemic wasting syndrome (PMWS). *Journal of swine Health and Production,* 8**,** 133-136.

Streatfield, S. J. 2007. Approaches to achieve high-level heterologous protein production in plants. *Plant biotechnology journal,* 5**,** 2-15.

Sun, N., Sun, P., Lv, H., Sun, Y., Guo, J., Wang, Z., Luo, T., Wang, S. & Li, H. 2016. Matrine displayed antiviral activity in porcine alveolar macrophages co-infected by porcine reproductive and respiratory syndrome virus and porcine circovirus type 2. *Scientific reports,* 6**,** 24401.

Takeda, A., Sugiyama, K., Nagano, H., Mori, M., Kaido, M., Mise, K., Tsuda, S. & Okuno, T. 2002. Identification of a novel RNA silencing suppressor, NSs protein of Tomato spotted wilt virus. *FEBS letters,* 532**,** 75-79.

Tischer, I., Gelderblom, H., Vettermann, W. & Koch, M. 1982. A very small porcine virus with circular single-stranded DNA. *Nature,* 295**,** 64.

Tischer, I., Rasch, R. & Tochtermann, G. 1974. Characterization of papovavirus and picornavirus-like particles in permanent pig kidney cell lines. *Zenibl. Bukt.,* 226**,** 153-67.

Tiwari, S., Verma, P. C., Singh, P. K. & Tuli, R. 2009. Plants as bioreactors for the production of vaccine antigens. *Biotechnology advances,* 27**,** 449-467.

Todd, D. 2005. Circoviridae. *Virus Taxonomy, 8th Report of the International Committee on Taxonomy of Viruses***,** 327-334.

Tremblay, R., Wang, D., Jevnikar, A. M. & Ma, S. 2010. Tobacco, a highly efficient green bioreactor for production of therapeutic proteins. *Biotechnology Advances,* 28**,** 214-221.

Trundova, M. & Celer, V. 2007. Expression of porcine circovirus 2 ORF2 gene requires codon optimized E. coli cells. *Virus genes,* 34**,** 199-204.

Tschofen, M., Knopp, D., Hood, E. & Stöger, E. 2016. Plant molecular farming: much more than medicines.

Tsekoa, T. L., Singh, A. A. & Buthelezi, S. G. 2020. Molecular farming for therapies and vaccines in Africa. *Current Opinion in Biotechnology,* 61**,** 89-95.

Tu, Y., Wang, Y., Wang, G., Wu, J., Liu, Y., Wang, S., Jiang, C. & Cai, X. 2013. High-level expression and immunogenicity of a porcine circovirus type 2 capsid protein through codon optimization in Pichia pastoris. *Applied microbiology and biotechnology,* 97**,** 2867-2875.

Turpen, T. H., Reinl, S. J., Charoenvit, Y., Hoffman, S. L., Fallarme, V. & Grill, L. K. 1995. Malaria epitopes expressed on the surface of recombinant tobacco mosaic virus. *Bio/technology,* 13**,** 53-57.

Van Den Berg, A. & Dowdy, S. F. 2011. Protein transduction domain delivery of therapeutic macromolecules. *Current opinion in biotechnology,* 22**,** 888-893.

Verreault, D., Létourneau, V., Gendron, L., Massé, D., Gagnon, C. A. & Duchaine, C. 2010. Airborne porcine circovirus in Canadian swine confinement buildings. *Veterinary microbiology,* 141**,** 224-230.

Vitale, A. & Pedrazzini, E. 2005. Recombinant pharmaceuticals from plants: the plant endomembrane system as bioreactor. *Molecular Interventions,* 5**,** 216.

Voinnet, O., Rivas, S., Mestre, P. & Baulcombe, D. 2003. Retracted: An enhanced transient expression system in plants based on suppression of gene silencing by the p19 protein of tomato bushy stunt virus. *The Plant Journal,* 33**,** 949-956.

Wang, K., Huang, L., Kong, J. & Zhang, X. 2008. Expression of the capsid protein of porcine circovirus type 2 in Lactococcus lactis for oral vaccination. *Journal of virological methods,* 150**,** 1-6.

Wang, N., Zhan, Y., Wang, A., Zhang, L., Khayat, R. & Yang, Y. 2016. In silico analysis of surface structure variation of PCV2 capsid resulting from loop mutations of its capsid protein (Cap). *The Journal of general virology,* 97**,** 3331.

Wang, X., Jiang, P., Li, Y., Jiang, W. & Dong, X. 2007. Protection of pigs against post-weaning multisystemic wasting syndrome by a recombinant adenovirus expressing the capsid protein of porcine circovirus type 2. *Veterinary microbiology,* 121**,** 215-224.

Wang, Y., Wang, G., Duan, W.-T., Sun, M.-X., Wang, M.-H., Wang, S.-H., Cai, X.-H. & Tu, Y.-B. 2020. Self-assembly into virus–like particles of the recombinant capsid protein of porcine circovirus type 3 and its application on antibodies detection. *AMB Express,* 10**,** 3.

Waterhouse, P. M., Wang, M.-B. & Finnegan, E. J. 2001a. Role of short RNAs in gene silencing. *Trends in plant science,* 6**,** 297-301.

Waterhouse, P. M., Wang, M.-B. & Lough, T. 2001b. Gene silencing as an adaptive defence against viruses. *Nature,* 411**,** 834-842.

Wei, Y.-W., Zhu, H.-Z., Huang, L.-P., Xia, D.-L., Wu, H.-L., Bian, H.-Q., Feng, L. & Liu, C.-M. 2020. Efficacy in pigs of a new inactivated vaccine combining porcine circovirus type 2 and Mycoplasma hyorhinis. *Veterinary Microbiology***,** 108588.

Wen, S., Sun, W., Li, Z., Zhuang, X., Zhao, G., Xie, C., Zheng, M., Jing, J., Xiao, P. & Wang, M. 2018. The detection of porcine circovirus 3 in Guangxi, China. *Transboundary and emerging diseases,* 65**,** 27-31.

West, K. H., Bystrom, J. M., Wojnarowicz, C., Shantz, N., Jacobson, M., Allan, G. M., Haines, D. M., Clark, E. G., Krakowka, S. & Mcneilly, F. 1999. Myocarditis and abortion associated with intrauterine infection of sows with porcine circovirus 2. *Journal of Veterinary Diagnostic Investigation,* 11**,** 530-532.

Wozniak, A., Milek, D., Matyba, P. & Stadejek, T. 2019. Real-Time PCR Detection Patterns of Porcine Circovirus Type 2 (PCV2) in Polish Farms with Different Statuses of Vaccination against PCV2. *VIRUSES-BASEL,* 11.

Wroblewski, T., Tomczak, A. & Michelmore, R. 2005. Optimization of Agrobacterium-mediated transient assays of gene expression in lettuce, tomato and Arabidopsis. *Plant Biotechnology Journal,* 3**,** 259-273.

Wu, P.-C., Chen, T.-Y., Chi, J.-N., Chien, M.-S. & Huang, C. 2016. Efficient expression and purification of porcine circovirus type 2 virus-like particles in Escherichia coli. *Journal of biotechnology,* 220**,** 78-85.

Wu, P.-C., Lin, W.-L., Wu, C.-M., Chi, J.-N., Chien, M.-S. & Huang, C. 2012. Characterization of porcine circovirus type 2 (PCV2) capsid particle assembly and its application to virus-like particle vaccine development. *Applied microbiology and biotechnology,* 95**,** 1501-1507.

Wu, X., Gong, F. & Wang, W. 2014. Protein extraction from plant tissues for 2DE and its application in proteomic analysis. *Proteomics,* 14**,** 645-658.

Xi, X., Mo, X., Xiao, Y., Yin, B., Lv, C., Wang, Y., Sun, Z., Yang, Q., Yao, Y. & Xuan, Y. 2016. Production of Escherichia coli-based virus-like particle vaccine against porcine circovirus type 2 challenge in piglets: Structure characterization and protective efficacy validation. *Journal of biotechnology,* 223**,** 8-12.

Xiao, C.-T., Halbur, P. G. & Opriessnig, T. 2015. Global molecular genetic analysis of porcine circovirus type 2 (PCV2) sequences confirms the presence of four main PCV2 genotypes and reveals a rapid increase of PCV2d. *Journal of General Virology,* 96**,** 1830-1841.

Xiao, C.-T., Harmon, K. M., Halbur, P. G. & Opriessnig, T. 2016. PCV2d-2 is the predominant type of PCV2 DNA in pig samples collected in the US during 2014–2016. *Veterinary microbiology,* 197**,** 72-77.

Yang, R., Tao, Y., Li, G., Chen, J., Shu, J. & He, Y. 2019. Immunoenhancement of Recombinant Neisseria meningitides PorB Protein on Porcine Circovirus Type 2 and Mycoplasma hyopneumoniae Genetically Engineered Vaccines. *Protein and peptide letters,* 26**,** 776-784.

Yang, X., Hou, L., Ye, J., He, Q. & Cao, S. 2012. Detection of porcine circovirus type 2 (PCV2) in mosquitoes from pig farms by PCR. *Pak Vet J,* 32**,** 134-135.

Yin, S., Sun, S., Yang, S., Shang, Y., Cai, X. & Liu, X. 2010. Self-assembly of virus-like particles of porcine circovirus type 2 capsid protein expressed from Escherichia coli. *Virology journal,* 7**,** 166.

Young, M. G., Cunningham, G. L. & Sanford, S. E. 2011. Circovirus vaccination in pigs with subclinical porcine circovirus type 2 infection complicated by ileitis. *Journal of swine health and production,* 19**,** 175-180.

Yusibov, V., Streatfield, S. J. & Kushnir, N. 2011. Clinical development of plant-produced recombinant pharmaceuticals: vaccines, antibodies and beyond. *Human vaccines,* 7**,** 313-321.

Zaveckas, M., Snipaitis, S., Pesliakas, H., Nainys, J. & Gedvilaite, A. 2015. Purification of recombinant virus-like particles of porcine circovirus type 2 capsid protein using ion-exchange monolith chromatography. *Journal of Chromatography B,* 991**,** 21-28.

Zhai, S.-L., Chen, S.-N., Xu, Z.-H., Tang, M.-H., Wang, F.-G., Li, X.-J., Sun, B.-B., Deng, S.-F., Hu, J. & Lv, D.-H. 2014a. Porcine circovirus type 2 in China: an update on and insights to its prevalence and control. *Virology journal,* 11**,** 88.

Zhai, S.-L., Chen, S.-N., Xu, Z.-H., Tang, M.-H., Wang, F.-G., Li, X.-J., Sun, B.-B., Deng, S.-F., Hu, J. & Lv, D.-H. 2014b. Porcine circovirus type 2 in China: an update on and insights to its prevalence and control. *Virology journal,* 11**,** 1-13.

Zhang, H. H., Hu, W. Q., Li, J. Y., Liu, T. N., Zhou, J. Y., Opriessnig, T. & Xiao, C. T. 2020a. Novel circovirus species identified in farmed pigs designated as Porcine circovirus 4, Hunan province, China. *Transboundary and emerging diseases,* 67**,** 1057-1061.

Zhang, J., Liu, W., Chen, W., Li, C., Xie, M. & Bu, Z. 2016. Development of an immunoperoxidase monolayer assay for the detection of antibodies against peste des petits ruminants virus based on BHK-21 cell line stably expressing the goat signaling lymphocyte activation molecule. *PloS one,* 11**,** e0165088.

Zhang, S., Mou, C., Cao, Y., Zhang, E. & Yang, Q. 2020b. Immune response in piglets orally immunized with recombinant Bacillus subtilis expressing the capsid protein of porcine circovirus type 2. *Cell Communication and Signaling,* 18**,** 23.

Zhang, Z., Cui, L., Wang, L., Yang, Z., Cui, Z. & Chang, W. 2014. Generation and evaluation of avian leukosis virus subgroup J envelope glycoprotein recombinant pseudovirions. *Journal of virological methods,* 202**,** 1-7.

Zuanazzi, J. S. G., Goes, E. S. D. R., Almeida, F. L. a. D., Goes, M. D., Lara, J. a. F. D. & Ribeiro, R. P. 2020. Effects of freezing and thawing cycles on the quality of Nile tilapia fillets. *Food Science and Technology,* 40**,** 300-304.

Zupan, J., Muth, T. R., Draper, O. & Zambryski, P. 2000. The transfer of DNA from Agrobacterium tumefaciens into plants: a feast of fundamental insights. *The Plant Journal,* 23**,** 11-28.